UNIVERSITÀ DEGLI STUDI DELLA TUSCIA DI VITERBO

DIPARTIMENTO DI AGROBIOLOGIA ED AGROCHIMICA

CORSO DI DOTTORATO DI RICERCA

In "**GENETICA E BIOLOGIA CELLULARE**"

-XXII Ciclo-

DISSEZIONE GENETICA DELLA SPERMATOGENESI IN *DROSOPHILA MELANOGASTER*: CARATTERIZZAZIONE GENETICA, CITOLOGICA E MOLECOLARE DI UN GRUPPO DI MUTANTI MASCHIO-STERILI COINVOLTI NEL CICLO CELLULARE MEIOTICO

BIO/18

Coordinatore: Prof. GIORGIO PRANTERA

Firma ……..

Tutor: Prof. GIORGIO PRANTERA

Firma……

Dottoranda: SILVIA VOLPI

Firma ……..

INDEX

ABSTRACT

My research was focused on a set of ethyl methanesulfonate (EMS)-induced male sterile recessive mutations mapping to chromosomes 2 and 3 in *Drosophila melanogaster*. The fruitfly is an amenable system to study spermatogenesis process for several reasons: ease of cytological analysis; availability of mutations at any step; and highly improved methods of genetic and molecular investigation. My study consisted in the genetic, molecular and cytological dissection of two groups of *Drosophila* male sterile mutants: *twine*-noncomplementing and *twine*-complementing mutants. *Twine* is a gene mapping on the left arm of chromosome 2 and encoding for a phosphatase responsible for the triggering of the Cdc2-CyclinB complex, underlying meiotic entry. twe^{HB5} loss of function mutation causes the primary spermatocytes to fail both meiotic divisions, yet allowing some further spermatid differentiation. However, the ensuing phenotype is sterile, since the sperms are not mobile. The set of EMS-induced male sterile mutations I've been handling showed a mutant phenotype resembling that of twe^{HB5}, thus, implying the possibility that the *twine*-noncomplementing mutations were allelic to *twine*. Mapping of such mutations by meiotic recombination together with sequencing of *twine* region in the genome of these flies suggested that *12-228, 60-40* and *54-23* mutations had two mutations on chromosome 2 selected for male sterility: one accounting for male sterility and the other one on *twine* gene, underlying the meiotic phenotype. The just mentioned results were also supported by the "cleaning" of the chromosome 2, carried out in these mutants by meiotic recombination. Different were the outcomes from *50-38* stock, another *twine*-noncomplementing mutation. In this case, recombination mapping and *twine* sequencing as well as chromosome "cleaning" suggested the presence of a single mutation on chromosome 2 of these mutants, close to *twine* gene, underlying both male sterility and meiotic phenotype. A detailed cytological analysis of this mutant by antibodies against some basic effectors of meiotic cell cycle, like α-tubulin to detect meiotic spindle, lamin for nuclear envelope and Spd2 for centrosomes, proved the failure of nuclear envelope breakdown and spindle assembly besides defects in number and localization of centrosomes in primary spermatocytes. Such anomalies underlie the failure of meiosis in *50-38* male mutants. Cytological characterization also revealed defects during the later stages of spermatogenesis, consisting into mislocalization of basal body that prevented a proper cyst polarization.

Among the *twine*-complementing mutations, one, named *71-43*, resulted extremely interesting because of the following features. Mapping data by recombination and deficiency, and chromosome "cleaning" placed it on the distal portion of the right arm of the chromosome 2 as the only mutation present on this chromosome, responsible for meiotic and sterile phenotype. Cytological dissection of the spermatogenesis process in these mutants by means of antibodies provided the evidence of a

panoply of anomalies, starting from young primary spermatocytes until to spermatids. In particular, defects of nuclear envelope, centrosomes and meiotic spindle were detected by immunofluorescence experiments in the early stages of male germ line development as well as impairment of nucleus-basal body docking, cyst polarization and spermatid individualization processes in the later stages. The failure of assembly of a canonical meiotic cell cycle machinery accounted for the execution of only one, as well defective, meiotic division in *71-43* male mutants. *71-43* homozygous mutant females showed reduced fertility, thus indicating that the function performed by this gene in oogenesis is likely redundant. A lower mitotic index in mutant larval brains in comparison with wildtype, pointed out that *71-43* acts also in mitosis, even though its action should be dispensable since no delayed development nor lethality are apparent. Towards the molecular identification of the gene mutated in *71-43* stock, different approaches were followed, both via forward and reverse genetics. Complementation analysis of males heterozygous for *71-43* mutation and a mutated allele of most of the genes embedded into the region where *71-43* was identified to lie, allowed to rule out all the genes so far tested as candidates for *71-43* locus. Proteomics approach, consisted in a comparative study of protein profiles of *71-43* homozygote *vs* *71-43* heterozygote testes, underlined the presence of some proteins misregulated in *71-43* mutants, whose genes however map outside the *71-43* genetic interval. Such an analysis, however, provided intriguing clues about the putative pathways where *71-43* may act and, therefore, new roads to pursue.

RIASSUNTO

La mia ricerca nel corso del dottorato si è concentrata su un gruppo di mutazioni recessive maschio-sterili, indotte da etil metansulfonato (EMS), localizzate sui cromosomi 2 e 3 in *Drosophila melanogaster*. Il moscerino della frutta è un sistema modello per lo studio del processo della spermatogenesi per varie ragioni: la facilità di indagine citologica, la disponibilità di mutazioni ad ogni stadio e di metodi di indagine molecolare e genetica altamente sviluppati. La mia analisi è consistita nella dissezione genetica, molecolare e citologica di due gruppi di mutanti maschio-sterili di *Drosophila*: quelli che non complementano *twine* e quelli che, invece, lo complementano. *Twine* è un gene che risiede sul braccio sinistro del cromosoma 2 e codifica per una fosfatasi responsabile dell'attivazione del complesso Cdc2-CiclinaB, alla base dell'entrata in meiosi. La mutazione a perdita di funzione twe^{HB5} rende gli spermatociti primari incapaci di eseguire entrambe le divisioni meiotiche, permettendo tuttavia un certo differenziamento degli spermatidi. Il fenotipo che ne risulta è, comunque, sterile in quanto gli spermatozoi prodotti non sono mobili. Il gruppo di mutazioni recessive maschio-sterili, indotte da EMS, sul quale ho concentrato la mia ricerca, mostrava un fenotipo simile a quello dei mutanti twe^{HB5}, suggerendo, quindi, la possibilità che tali mutazioni fossero alleli del gene *twine*. Esperimenti di mappatura per ricombinazione meiotica insieme al sequenziamento della regione *twine* nel genoma dei mutanti *12-228*, *60-40* e *54-23*, hanno suggerito la presenza di due mutazioni sul cromosoma 2 di questi mutanti, selezionate per il fenotipo maschio sterile: una responsabile della sterilità maschile e l'altra a carico della sequenza genica di *twine*, alla quale si deve il fenotipo meiotico. I risultati appena menzionati erano anche supportati dai dati di "ripulitura" del cromosoma 2 eseguita in questi mutanti mediante ricombinazione meiotica. Diversi erano i risultati ottenuti dallo stock *50-38*, ovvero un'altra mutazione che non complementa *twine*. In questo caso, i dati di mappatura per ricombinazione e del sequenziamento di *twine*, insieme a quelli ottenuti dalla "ripulitura" del cromosoma, indicavano la presenza di una singola mutazione sul cromosoma 2 di questi mutanti, molto vicina al gene *twine*, che determina sia il fenotipo maschio-sterile che meiotico. Una dettagliata analisi citologica di questo mutante attraverso anticorpi in grado di rilevare alcuni componenti chiave del ciclo cellulare meiotico, quali la α-tubulina per il fuso meiotico, la lamina per la membrana nucleare ed Spd2 per i centrosomi, evidenziava l'incapacità, da un lato, di disassemblaggio della membrana nucleare e, dall'altro, di assemblaggio del fuso meiotico, oltre a difetti nel numero e nella localizzazione dei centrosomi negli spermatociti primari. Tali anomalie sono alla base della mancata esecuzione di entrambe le divisioni meiotiche nei maschi mutanti *50-38*. La caratterizzazione citologica mostrava anche difetti durante gli stadi tardivi della spermatogenesi, consistenti nella errata localizzazione del corpo basale, che impedisce di eseguire una corretta polarizzazione della cisti.

Tra le mutazioni che complementano *twine*, una, chiamata *71-43*, risultava estremamente interessante per via delle seguenti caratteristiche. I risultati della mappatura genica, effettuata sia tramite ricombinazione meiotica che attraverso l'uso di deficienze, e della "ripulitura" del cromosoma, posizionavano la mutazione *71-43* sulla porzione distale del braccio destro del cromosoma 2 come unica mutazione presente su tale cromosoma, a cui si deve il fenotipo meiotico e maschio-sterile. La dissezione citologica del processo della spermatogenesi, eseguita per mezzo di anticorpi, ha permesso di riscontrare la presenza, in questi mutanti, di anomalie a partire dai primi stadi della spermatogenesi fino a quelli più tardivi. In particolare, gli esperimenti di immunofluorescenza hanno evidenziato dei difetti di membrana nucleare, di centrosomi e di fuso meiotico nelle prime fasi dello sviluppo delle cellule germinali maschili così come aberrazioni nei processi che caratterizzano le fasi finali del differenziamento degli spermatidi, quali l'ancoraggio nucleo-corpo basale, la polarizzazione delle cisti e l'individualizzazione degli spermatozoi. L'incapacità di assemblaggio di un canonico macchinario del ciclo cellulare meiotico giustificava l'esecuzione di una sola divisione meiotica, peraltro non corretta, nei mutanti *71-43*. Femmine mutanti *71-43* mostravano ridotta fertilità, indicando quindi che la funzione espletata da questo gene nell'oogenesi è probabilmente ridondante. Un indice mitotico inferiore nei cervelli larvali dei mutanti rispetto a quello dei selvatici ha suggerito, inoltre, che *71-43* agisce anche in mitosi, sebbene la sua azione sembrerebbe essere dispensabile, in quanto né ritardato sviluppo né letalità sono visibili. Differenti approcci, basati sia su metodi genetici classici che innovativi, sono stati seguiti verso l'identificazione molecolare del gene mutato nel ceppo *71-43*. L'analisi per complementazione di maschi eterozigoti per la mutazione *71-43* ed un allele mutato della maggior parte dei geni che risiedono nella regione in cui il locus *71-43* mappa, ha permesso di scartare tutti quelli finora testati come potenziali candidati per tale locus. L'approccio proteomico, fondato sullo studio comparativo dei profili di espressione proteica dei testicoli degli omozigoti *71-43 vs* gli eterozigoti, ha mostrato l'esistenza di alcune proteine misregolate nei mutanti *71-43*, i cui geni, comunque, risiedono al di fuori dell'intervallo genico di *71-43*. Tale analisi ha fornito, tuttavia, intriganti indizi riguardo ai putativi processi in cui il gene *71-43* può agire e, quindi, nuove strade da percorrere.

1. INTRODUCTION

1.1 *DROSOPHILA MELANOGASTER* SPERMATOGENESIS

The *Drosophila* testis is a long tube with a straight apical and a coiled basal end (Fig.1). The different stages are laid out in chronological order from its apical tip to its basis, making it easy to discern distinct stages of germ cell development. Male germ line stem cells reside in the germinal proliferation center, at the tip of the testis (white arrow, Fig.1). Following an asymmetrical division, each of them generates another stem cell and a primary spermatogonium, encysted by two-somatically derived cyst cells. The spermatogonium undertakes four rounds of mitotic division to generate 16 interconnected cells, that then enter into a so called "growth period" (brackets, Fig1 and Scheme 1). Upon this premeiotic G_2 phase, spermatogonia display a 25-fold increase in their nuclear volume, due to the transcription of many genes required in the subsequent meiotic stages. In *Drosophila* most transcription is shut off upon entry into the meiotic divisions, differently from mammals, where transcription is readily detected, by ^{3}H-Uridine incorporation, in early spermatids and continues until chromatin compaction (Monesi, 1965). Until very recently, there was only data from experiments by Olivieri and Olivieri in 1965, where no radiographic labelling of nascent transcripts was revealed in *Drosophila* spermatids. Hence, transcription of genes required for spermatid differentiation occurs in primary spermatocytes, and the transcripts are stored in the cytoplasm for later use. Last year, White-Cooper's group provided some evidence about the transcription of 24 genes, named "comets" and "cups", in the mid-elongation spermatids, just before histone to protamine chromatin transition, also showing a curious localization of these transcripts at the extreme distal ends of the elongating cells (Barreau et al., 2008).

There is no meiotic recombination in male *Drosophila*, so after homologous chromosome pairing, most of the classic stages of meiotic prophase are not apparent in these cells. As the spermatogonial cells exit from the growth phase they develop into primary spermatocytes which undergo two meiotic divisions (large arrowhead, Fig.1 and Scheme 1), resulting in 64 haploid onion-stage spermatids. Cysts of haploid early round spermatids at the 'onion stage' are identified easily by their regular array of phase-light, spherical nuclei paired with phase-dark, nucleus similar size, mitochondrial derivatives or Nebenkernes, containing multiple layers of mitochondrial membranes (black arrow, Fig.1 and Scheme 1). Such a stage is an excellent indicator of any lack of fidelity in the meiotic divisions, as far as both chromosomal segregation and cytokinesis anomalies. The former by the nucleus size, since it's directly proportional to DNA content; the latter by the evenly mitochondria partition between the daughter cells, since each cell after meiotic division is

characterized by the same mitochondria amount, visible as a same-sized spherical Nebenkern per spermatid.

The final stage of spermatogenesis consists in the elongation of spermatids, with dramatic morphological changes to transform themselves into fully elongated cells of 1.8 mm in length (small arrowheads, Fig.1 and Scheme 1). Besides tail formation, consisting into mitochondrial derivative and axoneme elongation, sperm maturation also involves nucleus conformational change from round to needle shape, through the switch from a nucleosome- to a protamine-based chromatin structure, determining a high chromatin condensation and compaction (Rathke C. et al., 2007). Their heads are oriented towards the basal end of the tube, with the sperm tails pushing up the testis towards the apical tip. Since cytokinesis is incomplete during gonial and meiotic divisions, the 64 haploid spermatids are connected among each other by cytoplasmic bridges, and they need to individualize in order to become functional. The individualization process involves a coordinated movement of actin-based 'investment cones' from the nuclei along the tails, expelling waste cytoplasm into a 'waste bag' (Fabrizio et al., 1998). Mature sperms coil and pass into the seminal vesicle where they acquire motility. On mating they move into the ejaculatory duct, where they are mixed with seminal fluid produced by the accessory glands, and then transferred into the female (Fuller, 1993).

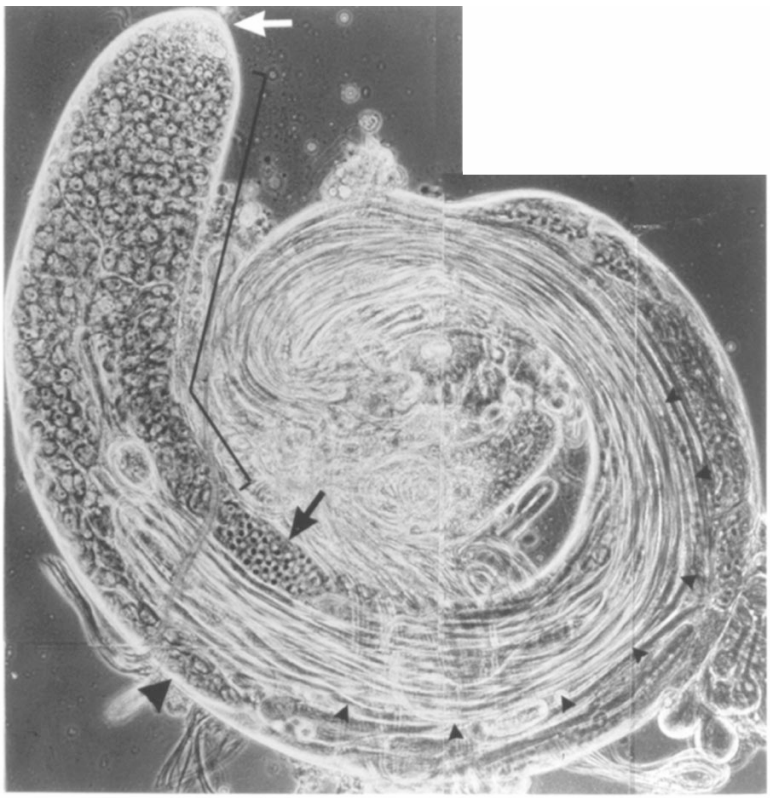

Fig.1 wildtype *Drosophila melanogaster* testis viewed by phase contrast microscopy (by Fuller M.T., 1998)

White arrow at the apical tip of the testis points out the germinal proliferation center where male germ line cells reside. The region of the testis included into the brackets contains gonial cells executing mitotic divisions and primary

spermatocytes at the growth phase. The large arrowhead near the start of the coiled part of the testis shows cells entering meiotic divisions, whereas the black arrow to the opposite side points out cysts of haploid early round spermatids at the "onion stage". Small arrowheads along the testis indicate bundles containing 64 elongating spermatids, filling the testis up the lumen.

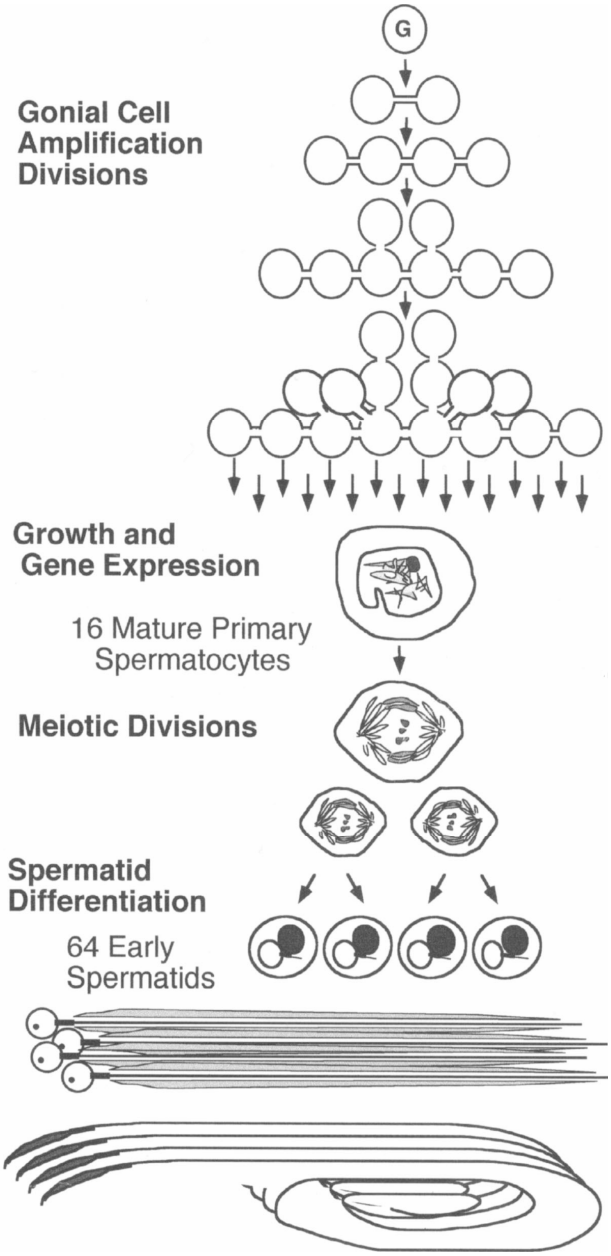

Scheme 1. wildtype spermatogenesis in *Drosophila melanogaster* (by Fuller M.T., 1998).
A spermatogonium undergoes four rounds of mitotic amplification divisions with incomplete cytokinesis. The resulting 16 interconnected cells enter the primary spermatocyte period of growth and gene expression. For simplicity, only one of the 16 primary spermatocytes in a cyst is shown. All 16 primary spermatocytes exit the cell growth and transcription program and enter meiotic divisions, resulting in a cyst of 64 interconnected, onion-stage, haploid, round spermatids. Each spermatid in an onion-stage cyst has the same sized nucleus (white sphere) and the same sized mitochondrial derivative (black sphere). The haploid spermatids remain interconnected and proceed through the dramatic morphological changes of spermiogenesis, eventually, with the production of fully elongated individualized sperms.

1.2 *DROSOPHILA* AS MODEL SYSTEM FOR STUDYING SPERMATOGENESIS PROCESS

Drosophila is a particularly suitable organism to undertake the genetic dissection of the complex process of germ cell meiosis and differentiation that culminates in mature sperm formation. The reasons are several:

1. the ease to cytologically analyse such a process and discern distinct stages of germ cell development, since each different stage is laid out in chronological order from the apical tip of the testis to the basis.
2. The presence or absence of a germ line, the number and quality of mitotic and meiotic divisions, and the production of motile sperm can all be scored simply using phase contrast optics.
3. Sterile mutations can be easily generated at any step, identified and investigated, providing the starting point for molecular biological studies. To date, a number of genome-wide genetic screens for male sterile mutations have been carried out, making available a lot of mutations affecting different stages.
4. The availability of the complete DNA sequence of the *Drosophila* genome (from 1998) has been enormously improved the identification of genes required for spermatogenesis.
5. Spermatogenesis process has shown a remarkable degree of evolutionary conservation, so that the data obtained in *Drosophila* may have a broad applicability to other systems, including humans.

1.3 MALE MEIOTIC PROPHASE AND PROMETAPHASE: HOW PRIMARY SPERMATOCYTES GET READY TO ENTER MEIOSIS

As soon as a spermatogonial cell comes out from gonial division program, switches to a growth and gene expression program, entering a very long G2 interphase (it approximately lasts 3.5 days in *D.melanogaster*) (Lindsley and Tokuyasu, 1980), that can be considered a meiotic prophase. During this period, the cell transcribes most of the genes required for the further meiotic and post-meiotic stages (see above) and starts to get ready for cellular division. Chromatin appears as three masses or clumps, closely apposed to the inner nuclear envelope. The two larger masses represent the two somatically-paired autosomes of *Drosophila* genome (2 and 3 chromosomes), whereas the less dense chromatin mass corresponds to the X and Y chromosomes and the tiny fourth chromosomes (generally visible as dots) (Cenci et al., 1994). At this time are also apparent the Y chromosomes loops. In 1916 Bridges demonstrated that Y chromosome is not basic for vitality since flies with X/0 karyotype are vital, phenotipically male but completely sterile individuals. This means that Y chromosome carries genes required only for male fertility. Three of the six “fertility factors” (kl-5, kl-3 and ks-1) present in Y chromosome form lampbrush-like loops in *Drosophila melanogaster* primary spermatocytes, representing the cytological manifestation of their activity (Bonaccorsi et al., 1998). One major characteristic for all loops is that they are bound by several proteins, coded by autosomal genes, whose mutations alter loops morphology and provoke sterility. Some of them also have pleiotropic effects on meiosis and post-meiotic development (Ceprani et al., 2008). Y loops disintegrate during meiotic prophase pointing out the end of the growth phase and the beginning of the first meiotic division. While chromatin is organized into three clumps, representing an analogous state of interphase chromatin, the centrosomes, by now duplicated and consequently each formed by a pair of centrioles, migrate from plasma membrane to nuclear membrane where they start to nucleate astral microtubules and move towards the opposite poles of the nucleus. Cells enter prometaphase during which, concomitantly to spindle formation, there is a progressive chromatin condensation and the nuclear envelope breakdown, necessary to allow microtubules to make contact with chromosome kynetochores. Nuclear membrane is constituted by an inner envelope, made of lamins, which contact bivalents, located underneath nuclear envelope. As the bivalents start to congregate to metaphase plate, nuclear envelope disaggregates probably subsequently lamina phosphorylation that brings about nuclear lamina depolymerisation with consequent nuclear envelope breakdown. Lamin polymerisation will take place at telophase when nuclear envelope again forms around each of the two separated nuclei. In 1998, it was hypothesized a functional role for nuclear lamina in maintaining and alterating the three-dimensional genome structure (Gigliotti et

al., 1998). An important contribute in such a function is given by nuclear pore complex too, as proved by looking at the effects of mutations on the gene *Nup154*, homologous to rat *Nup155* and yeast *Nup170* and *Nup157* nucleoporins. *Nup154* male mutants are sterile and show meiotic arrest at the transition from prophase to prometaphase with alterated nuclear envelope structure in proximity to nuclear pores. Nuclear membrane of primary spermatocytes formed small evaginations near nuclear pores, that presumably detached in the surrounding cytoplasm as distinct vesicles, a phenotype reminiscent of the herniations described in nuclear envelopes of some nucleoporin yeast mutants. Meiotic arrest and further abnormalities in *Nup154* mutants are justified by the authors as consequence of a misregulated nuclear import and export of factors underlying meiosis and spermatid development (Gigliotti et al., 1998). In support of this theory there is very recent data about *Drosophila* mutants of *Dα1* gene, encoding Importin α, a protein which functions as an adapter to link cargoes to import across nuclear pores from cytoplasm to nucleus through importin α/β1 heterodimer. In *Drosophila* there are three importin α–genes, *Dα1, Dα2, Dα3*. The last one required for general viability, whereas *Dα1* and *Dα2* required almost exclusively for gametogenesis: *Dα1* affects more severely spermatogenesis than *Dα2*, exhibiting completely sterility of Dα1 null mutants. These sterile males have numerous large round spermatid cysts, only partially elongated and not organized into bundles, also showing abnormal large round shape nuclei instead of needle-shape. Such a phenotype suggests a direct or indirect role for Dα1 in chromatin condensation, by means of nuclear import of chromatin remodelling factors (Ratan et al., 2008). The importance of a regulated nucleocytoplasmic trafficking for driving a correct male germ cell differentiation is highlighted in mammals as well. The mammalian testis-specific nucleoporin BS-63 has, as binding partner in a yeast 2-hybrid assay, an AT-hook domain chromatin remodelling factor, aF10, suggesting that factors like aF10 may access the nucleus through direct interaction with nucleoporins. It's definitely evident that regulation of nucleocytoplasmic shuttling and, thereby, of the access of critical factors to the nucleus is a fundamental means of driving male germ line differentiation together with regulation of gene transcription (Hogarth et al., 2005).

1.4 HOMOLOGOUS CHROMOSOMES PAIRING DURING MALE MEIOSIS IN *DROSOPHILA*

In sexual reproduction, the accurate segregation of homologous chromosomes during meiosis is a crucial step. Meiotic pairing of homologs is essential for their proper orientation along the metaphase plate and their subsequent disjunction during anaphase I. In *Drosophila* females, there are two systems ensuring segregation: a chiasmata system and the so-called "distributive system" (Day and Grell, 1976) that guarantee the segregation of achiasmata homologous chromosomes. The former is based on the formation of chiasmata, physical structures assembled at sites of reciprocal exchange. These structures are the last remaining sites of physical attachment between homologs at meiosis I metaphase, providing the strategy used by recombination-proficient organisms to ensure the maintenance of homolog associations until that stage.

The latter system is presumably necessary for the small fourth chromosome that never recombines in *Drosophila* females. According to Grell, the choice of partners in the distributive system is not determined by homology but rather by the availability, size and shape of these chromosomes.

Different is the situation in *Drosophila* males, where meiosis occurs in the absence of recombination and of a recognizable synaptonemal complex (SC) (Baker and Hall, 1976). Moreover, mutations affecting distributive segregation in females have no effect on meiosis I in males, thus suggesting the existence of a distinct pathway for homolog segregation in males (Moore et al., 1994). The isolation of mutants that alter the segregation of specific chromosomes has revealed the presence of different segregation systems in males. One example may be represented by *teflon* mutants where pairing, specifically between autosomal bivalents, is defective with subsequent failure of unpaired autosomes to orient to opposite poles resulting in nondisjunction phenomenon. Conversely, *tef* mutation doesn't affect sex chromosomes segregation (Tomkiel et al., 2001). Accordingly, there is a distinction between sex chromosomes and autosomes pairing and segregation. Pairing of sex chromosomes requires specific sequences from the rDNA gene repeats present in the heterochromatin of the X and Y chromosomes (McKee and Karpen, 1990), as proved by the failure to pair and the high degree of nondisjunction of sex chromosomes deleted for the rDNA locus. Pairing of autosomes, on the other hand, requires multiple regions of homology in the euchromatin, at least for the initiation of meiotic pairing, originally suggested by Metz to take place during the last gonial mitotic division (Metz, 1926). Upon this stage, the heterochromatic regions would be associated non-specifically. According to the model proposed by Vazquez and collaborators in 2002, heterochromatic associations would be responsible for the maintenance of

homolog pairing during late G2. Separation of chromosomes into distinct territories, each corresponding to a set of paired homologs, underneath the nuclear envelope in mid-G2, would disrupt non-specific heterochromatic interactions between nonhomologous chromosomes while preserving interactions between heterochromatic regions on homologous chromosomes. Separation of homologs and sister chromatids along the euchromatic chromosome arms also occurs together with separation of homologous centromeres while sister centromeres remain tightly paired until the second meiotic division. Therefore, despite the associations along the euchromatic autosomal arms and at the centromeres are loosen, homologous chromosomes remain in close physical proximity within each territory during late spermatocyte development, through heterochromatic associations and probably the contribute of some internal nuclear structure of the envelope into attaching and ensuring correct meiotic pairing (Vazquez et al., 2002). This theory still seems to be confirmed, since the latest data showed by Tsai and McKee at the *Drosophila* Conference 2009 would not prove the pairing of 9, tested by FISH, autosomal heterochromatic sequences, during mid and late G2.

Although control of meiosis I appears to be quite different between males and females, processes that ensure sister chromatid adhesion and segregation at meiosis II, instead, seem to be under common control in the two sexes. This is exemplified by the *mei-S332* and *ord* mutations which affect the control of sister chromatid separation in both sexes (Lee and Orr-Weaver, 2001).

1.5 GENETIC CONTROL OF MALE MEIOSIS IN *DROSOPHILA*

The genetic control of spermatogenesis in *Drosophila* can be divided in three main programmatic switches. The first checkpoint occurs when a stem cell has to decide if maintaining the stem cell fate or switching into the spermatogenesis program. Upon the growth phase there is the second regulatory point, when the spermatogonial cells shift from a program of active mitotic divisions into one of growth and gene expression. The third checkpoint is when the primary spermatocyte exits the extended G_2 phase to enter the first meiotic division. At this stage, two classes of genes have been shown by previous works to be required for meiotic entry - the so-called "Spermatocyte arrest class" and the "Twine class"-.

Spermatocyte Arrest genes coordinately control meiosis and spermiogenesis. In meiotic-arrest mutant testes, primary spermatocytes fail to initiate transcription of many genes whose products are required after meiosis as well as fail to express some meiotic gene products. Thus, mutant testes contain morphologically normal spermatogenic cells up to mature primary spermatocytes, which then arrest and fail to initiate either the meiotic divisions or spermatid differentiation, filling testes with primary spermatocytes arrested at the end of growth phase, without the presence of any meiotic and post-meiotic cells. Hence, it's evident that the meiotic cell cycle progression and the onset of spermatid differentiation both require the action of this class of genes. Arrest Class genes have been, currently, subdivided, according to their molecular targets and specific role in promoting transcription, into two classes: *always early* (*aly*)-class and *cannonball* (*can*)-class (Lin et al., 1996; White-Cooper et al., 1998). The former is constituted by 5 genes: *aly*, encoding one of the two *Drosophila* homologues of the *C.elegans* gene *lin*-9; *cookie monster* (*comr*); *achinthya/vismay* (*achi/vis*) and *matotopetli* (*topi*), both encoding sequence-specific DNA-binding proteins; *tombola* (*tomb*), encoding a chromatin-associated protein. Tomb, Achi/Vis and Topi presumably enter the nucleus independently and localize to chromatin by means of sequence-specific DNA-binding activity, while Aly and Comr become or remain nuclear as a complex. Nuclear Aly and Comr bind to and stabilise Tomb, then interact with Topi and Achi/Vis by forming a *Drosophila* testis-specific meiotic arrest complex (tMAC) (Beall et al., 2007) to facilitate cooperative DNA binding. Since the *aly*-class gene products accumulate on chromatin in transcriptionally active regions of primary spermatocytes, their function strictly depends on the chromatin localisation where they act alterating chromatin structure, in order to permit the high levels of transcription necessary for spermatocytes. *aly* class is required for transcription of meiotic control genes like *boule*, *twine* and *cyclin B* (see below), as well as spermatid differentiation genes such as *fuzzy onions* and *don juan*.

On the other hand, *can*-class is constituted by genes codifying testis-specific TBP-associated factors (tTAFs), paralogs of generally expressed TAF subunits of transcription factor IID (TFIID). Recruitment of TFIID to sequences near the transcriptional start site is thought to, in turn, recruit and/or stabilise PolII binding in the preinitiation complex. The multisubunit TFIID complex contains the TATA-binding protein (TBP) and 12-14 TBP-associated factors (TAFs). Recently, alternative forms of TBP and tissue-specific TAfs have been described in a number of organisms, *Drosophila* as well, and proposed to play a role in selective activation of cell-type specific gene expression programs during cellular differentiation. In *Drosophila melanogaster,* 5 tTAFs have been so far described: *cannonball* (*can*), encoding a paralog of dTAF5, expressed only in male germ cells; *meiosis I arrest* (*mia*), paralog of dTAF6; *spermatocyte arrest* (*sa*), paralog of dTAF8; *no hitter* (*nht*), paralog of dTAF4; *ryan express* (*rye*), paralog of dTAF12. These genes are required either to allow translation of the meiotic gene *twine* or to stabilise *twine* protein in mature primary spermatocytes, apart from allowing the transcription of spermatid differentiation genes. Several evidences support the existence of a testis-specific TFIID, an alternative TAF-containing protein complex, proposed to regulate a testis-specific gene expression program in primary spermatocytes, required for terminal differentiation of male germ cells. The action mechanism hypothesized for the *can*-class meiotic-arrest genes is the following: they activate transcription in two ways, globally by sequestering the PRC1 complex, (Polycomb Repression Complex) away from active chromatin by means of a re-localisation of this repressor to the nucleolus in spermatocytes, thus, implicating subnuclear architecture in the regulation of terminal differentiation, and locally by the exclusion of PRC1 at target promoters. tTAFs binding to target promoters reduces Polycomb binding and promotes the recruitment of Trithorax (Trx) complex, an activator complex, with consequent accumulation of H3K4me3, a mark of transcriptional active chromatin (Hiller et al., 2001; Hiller et al., 2004; Perezgasga et al., 2004; Chen et al., 2005; Wright et al., 2006; Jiang et al., 2007; Metcalf and Wassarman, 2007; Kolthur-Seetharam et al., 2008). Similarly to tTAFs, *TRF2* or *TLF* (TBP-like factor) may be the major transcription-initiating factor of the testis-specific TFIID complex in primary spermatocytes, since its high-level expression during the growth phase in mature spermatocytes is coincident with a decrease of TBP expression. Moreover, *trf2* mutants show pre-meiotic chromatin condensation defects together with abnormal chromosome congregation, implying an essential role for TRF2 to allow primary spermatocytes to enter the first meiotic division (Kopytova et al., 2006). Some russian researchers also found a protein, Modulo, the *Drosophila* homologue of nucleolin, that presumably cooperates with testis-specific TFIID to induce expression of spermatid differentiation genes, such as *β2-tubulin*, and whose itself expression is under control of meiotic-arrest genes and requires Boule, the protein that also controls

the G2/M meiotic transition through post-transcriptional regulation of Cdc25/Twine (see below). Thus, Modulo plays an important role in integration of meiosis and spermatid differentiation in *Drosophila* spermatogenesis, providing a mechanistic link between these two pathways (Mikhaylova et al., 2006). A strongly reminiscent phenotype of spermatocyte-arrest mutants is observed in *off-schedule* (*ofs*) mutants testes even if with some differences. *ofs* mutants exhibit the lack of meiosis and of any significant differentiation together with a significant cell size defect. However, there are some differences with arrest-class, for example in Cyclin A accumulation. Indeed, Cyclin A in spermatocyte-arrest class persists in the cytoplasm without translocating to the nucleus, whereas in *ofs* mutants the nuclear translocation of Cyclin A is precocious and then its degradation is delayed. Differently from Cyclin A, nuclear Boule accumulation is delayed in G2 with consequent delay in Twine accumulation. Several key meiotic regulators show advanced or delayed patterns in these mutants, hence the name *off-schedule*. This gene is homologous to eukaryotic translation initiation factor eIF4G. Because translation is primarily regulated at initiation, eIF4G is instrumental in determining the translational capacity of a cell and thus its ability to accumulate mass. Therefore, *ofs* mutant phenotype suggests that sufficient cell mass must accumulate before spermatocytes execute meiosis and differentiation as if mass accumulation were used to time the G2/M transition. Spermatocytes monitor growth during G2 as one way to ensure that execution of the meiotic divisions is timed co-ordinately with spermatid differentiation (Franklin-Dumont et al., 2007; Baker and Fuller, 2007). A similar system exists during the mitotic cell cycle in yeast: for cells to maintain the same average size overall several divisions, there are control points acting during G1 predominantly in budding yeast and G2 in fission yeast, to allow cell cycle progression only when the cell reached a threshold size (Rupes, 2002).

Mutations that result in a uniform block of the progression of spermatogenesis are rare among male-sterile mutants in *D.melanogaster*. For the most male sterile mutants, spermatogenesis proceeds despite defects in one or even several morphogenetic events, leading to the production of aberrant spermatids, suggesting that the majority of events in spermatogenesis proceed by independent pathways. Twine-class mutations, which I introduced before, belong to this context, since mutant spermatocytes skip several crucial events of meiotic divisions, however they initiate and enact spermatid differentiation. Both flagellar elongation and condensation and shaping of spermatid nuclei proceed despite failure to execute previous meiotic divisions, with the final production of immotile sperm bundles, unable to fecundate. Genes so far identified belonging to *twine*-class are: *Dmcdc2*, *twine* (*twe*), *pelota* (*pelo*) and *boule* (*bol*). *Dmcdc2* is required for mitosis; mutations result in developmental defects and larval lethality (Stern et al., 1993). To investigate its role in meiosis, a temperature-sensitive *Dmcdc2* allele has been engineered making possible to study the meiotic

function in *Dmcdc2*^{ts} mutants (Sigrist et al., 1995). *Dmcdc2* codifies for the cdc2 protein kinase, well known to form the Cdc2-Cyclin B complex, underlying the G2/M transition. Indeed, entry into mitosis is triggered by the activation of M cyclin/cdc2 kinase complexes. The activity of these complexes is controlled by a cycle of phosphorylation and dephosphorylation of the cdc2 kinase (reviewed by Nurse, 1990). Phoshorylation is mediated by Wee1 (on tyrosine 15 in *S.pombe* and threonine 14 in higher eukaryotes) and inhibits cdc2 activity (Gould et al., 1990; Krek and Nigg, 1991a.b), while the removal of these inhibitory phosphates by cdc25 phosphatase, activates the M-cyclin/ cdc2 kinase complex (Dumphy and Newport, 1989; Gautier et al., 1989; Labbe et al., 1989). Inactivation of this complex is required for exit from mitosis and needs the M cyclin destruction by a mechanism of ubiquitin-dependent proteolysis during metaphase (Glotzer et al., 1991). Studies in a variety of distantly related organisms have emphasized the similarities in the regulation of mitotic and meiotic M-phase. According to this, the entry into meiosis in *Drosophila* is regulated by the same mechanism based on the activation by de-phosphorylation of cdc2-Cyclin B complex. The phosphatase responsible to remove inhibitory phosphates on cdc2 kinase in male and female meiosis is codified by *twine/cdc25* gene. The *cdc25* gene was initially identified in *Schizosaccharomyces pombe* (Russel and Nurse, 1986) and later its *Drosophila* homolog was found at the *string* locus (Edgar and O'Farrell, 1989). Mutations in the *cdc25* and in *string* block the cell cycle at G2-phase; moreover in *Drosophila* the timing of the embryonic cell divisions is also affected (Edgar and O'Farrell, 1990). In *Drosophila*, a second *cdc25* homolog was identified in 1992 (Courtot et al., 1992). This gene was *twine*, which, differently from *string*, is required in meiosis but not in mitosis. The *twine* gene is transcribed relatively early during the long G2 phase, but *twine* mRNA accumulation is not sufficient to promote entry into the meiotic divisions, differently from that observed in early embryos where the transcription of *string*/*cdc25* gene is both necessary and sufficient to drive the G2/M transition (Edgar and O'Farrell, 1989, 1990). TWINE is activated by POLO kinase thus triggering cdc2-Cyclin B complex. This complex itself, once activated, phosphorylates and activates its same activator (TWINE) and inhibits its repressor (Wee1), by a positive feedback loop. Mutations in *twine* result in male and female sterility but do not affect the embryonic development or viability of the fly (Alphey et al., 1992; White-Cooper et al., 1993). Surprisingly in female mutants entry into the first meiotic division occurs at the correct stage of oogenesis. The defect starts after entry into meiosis, in mature stage-14 oocytes, when oogenesis should arrest at metaphase of meiosis I, to then normally re-start after egg-activation, which occurs during egg laying. In *twine* females, mutant oocytes don't arrest at metaphase I but continue to progress through aberrant cell cycles during which chromosomes are replicated and segregated irregularly. This phenotype suggests that *twine* function in females is required to

maintain the arrest of oocyte at metaphase I by keeping Dmcdc2 protein de-phosphorylated and thereby active (White-Cooper et al., 1993).

The *pelota* gene encodes a RNA-binding protein, *S.cerevisiae* DOM34 homolog, required not only for male gametogenesis but also for eye development, thereby for mitosis (Eberhart and Wasserman, 1995). In contrast *boule* is expressed only in the testis and *boule* mutations affect only meiosis. Boule protein has a conserved RNA-binding domain that has been shown to directly bind *twine* mRNA. By means of this interaction, Boule exerts a translational control of Twine, as supported by a markedly reduced Twine protein expression in a genetic background deficient in *boule*. Also, although the male sterile phenotype produced by mutation of the *pelota* gene closely resembles that produced in *twine* or *boule* mutants, the *β2-twine* transgene does not restore meiotic entry in a *pelota* male, whereas it does in *boule* mutants (Maines and Wasserman, 1999). Boule belongs to the *DAZ* (Deleted in Azoospermia) gene family and one member of this family in humans- human BOULE- was shown having a very similar function as the *Drosophila* homolog as a regulator of meiosis, because spermatogenesis was rescued in *boule* mutant flies made transgenic for the human BOULE gene (Luetjens et al., 2004).

The loss-of-function phenotype of *twe, pelo, Dmcdc2* and *bol* alleles is characterized by failure into execution of both meiotic divisions, however they are still able to undergo some spermatid differentiation. In all these null mutants, spermatogenesis is normal until late meiotic prophase, at which point the cell cycle arrests. Chromosomes are partially condensed but never move away from the nuclear periphery of primary spermatocytes towards the center of nucleus. Nucleolus regularly breaks down. In contrast, while in a wildtype scenary the nuclear envelope breaks down during prophase and nuclear lamins disperse, forming diffuse clouds around the chromatin to then associate again with the reformed nuclear envelope after meiosis, in *twine*-class mutants the nuclear envelope does not breakdown (Eberhart and Wasserman, 1995). It's, however, noteworthy to say that White-Cooper and colleagues reported in 1993 contrasting data, showing that nuclear envelope breakdown still occurs in twe^{HB5} (null allele) male mutants (White-Cooper et al., 1993). Another crucial event of meiotic cell division, lacking in *twine*-class mutants, is the spindle formation. Normally, during the late meiotic prophase, the centrosomes separate and move towards the opposite poles of the cell; after they reach the poles, the cytoplasmic tubulin network, previously formed, breaks down and a spindle is formed. In these mutants, centrosomes separate but don't complete their migration and they nucleate no significant asters. Thereby, a spindle is never observed (White-Cooper et al., 1993; Eberhart and Wasserman, 1995). Despite the meiotic defects just mentioned, some post-meiotic differentiation occurs, such as nebenkern and tail elongation and nuclear shaping of spermatid heads. Two lines of evidence prove that spermatocyte-arrest mutants

arrest at a precocious point of cell cycle in comparison with *twine*-class mutants. As mentioned before, nucleolus breaks down in *twine*-class mutants, whereas a distinct nucleolus is still visible in primary spermatocytes of meiotic arrest mutants. Another hint is represented by the nuclear presence of Cyclin A in *twine*-class mutants where it remains until degradation at onion-stage spermatid, conversely to a still cytoplasmic localization in primary spermatocytes of arrest-class mutants. Furthermore, the phenotype of *twine; sa* and *twine; can* double mutants is similar to *sa/Df* and *can/can* phenotype, indicating that *can* and *sa* are epistatic to *twine* (Lin et al., 1996).

From the literature, hypomorphic *twine* (*twe*^{ZO758}) and *pelota* (*pelota*^{weak}) alleles are known. *twe*^{ZO758} homozygotes execute a single division, the first meiotic division, resulting in cysts of 32 cells, in contrast with 16 cell-cysts of *twe*^{HB5} null mutants. Spermatocytes from *twe*^{ZO758} / *twe*^{ZO758} males with only a single wildt-ype copy of *boule* fail to enter meiosis, resembling phenotype of flies homozygous for loss-of-function *twine* alleles (Maines and Wasserman, 1999). *pelota*^{weak} homozygote mutants show some meioses, albeit aberrant. Mutant spermatids contain two or four nuclei in a single cell, indicating a failure of cytokinesis in one or both meiotic divisions. In some cells, the nuclei are of different sizes, a sign of uneven chromosome complements, thus reflecting defects in chromosome segregation. Defects within a cyst are usually heterogeneous, with some cells displaying meiotic defects while others appear wild-type or are arrested before meiosis I. The presence of such anomalies during meiotic cell divisions in weak *pelota* alleles is explained by Eberhart and Wasserman as direct consequence of aberrant regulation and initiation of meiotic divisions rather than the possibility that *pelota* plays separate roles in the meiotic entry and in specific meiotic processes such as spindle formation and cytokinesis (Eberhart and Wasserman, 1995).

The regulation of second meiotic division is still not well understood. No genes have been identified for which loss-of-function mutations specifically block MII. There is evidence, however, that *Dmcdc2*, *twine* and *roughex* (*rux*) play a critical role in control of MII.

Dmcdc2 mutant males that carry two copies of the *Dmcdc2*^{ts} transgene are sterile at all temperatures, with defects in meiosis. At 18°C -permissive temperature- they execute MI but fail in MII, producing 32-cell spermatid cysts. When shifted as adults to 27°C –nonpermissive temperature- they fail to execute either meiotic division (Sigrist et al., 1995).

As far as the role of *twine* in the regulation of MII, in *twine* mutants, background expression of *string* from a heat-shock promoter in late primary spermatocytes, is sufficient to rescue entry into MI, but not MII (Sigrist et al., 1995). Moreover, in females, *twine* mutants execute MI but not MII, suggesting that *twine* play a unique role in MII (Courtot et al., 1992; White-Cooper et al., 1993). Since flies with two copies of the *Dmcdc2*^{ts} transgene execute MI but fail in MII, the level of kinase

activity may be of particular importance for entry into MII and Twine phosphatase would play a basic task for maintaining this level of cdc2 kinase activity.

Roughex gene acts as negative regulator of MII (Gonczy et al., 1994). An increase in *roughex* gene dosage blocks MII while allowing normal execution of MI. Reciprocally, germ cells from *rux* mutants attempt to execute an extra MII-like division. Thereby, these data strongly suggest that *rux* negatively regulates MII, with excess *rux* preventing MII and insufficient *rux* permitting an additional MII. In *rux* mutants there is an increase in Cyclin A levels prior to MI. Since lowering the dose of either *twine* or *cyclin A* suppresses the extra division, consistent with the hypothesis that the excess cdc2 activity is responsible for the extra meiotic division in the *rux* mutants, presumably *rux* acts by limiting the amount of cdc2 activity available for MII.

1.6 SPINDLE FORMATION AND FUNCTION DURING MALE MEIOTIC DIVISIONS IN *DROSOPHILA*

During spermatocyte growth phase, centrosomes dissociate from the nuclear membrane and become associated with the spermatocyte cell membrane. As the cell enters meiotic prophase, centrosomes migrate back to the nuclear membrane and nucleate two asters while the network of microtubules, previously formed around the nucleus, disappears. In late prophase, the asters, initially located on the same side of the nucleus, migrate to the opposite poles where they radiate spindle fibers that reach the bivalents. Nuclei become irregularly shaped and are surrounded by structures corresponding to a system of parafusorial and astral membranes that surround the spindle and the poles during male meiosis. By the following prometaphase, the bivalents are connected to the spindle poles by kinetochore microtubules and start to congress to a metaphase plate. In addition to pole-to-chromosome microtubules, meiotic spindle shows bundles of microtubules that do not encounter the chromosomes, instead they originate from the poles, run outside the metaphase plate, ending either in the opposite pole or distally to the metaphase plate. As spermatocyte enter anaphase, the spindle organization changes: the density of microtubules in the region between the segregating sets of chromosomes –central spindle- (for more details see below) progressively increases, whereas the microtubules located in proximity of chromosomes decrease in number. Centrosome separation occurs early and two distinct centrosomes are already visible in late anaphase. At telophase, the dense bundle of microtubules in the central spindle is squeezed, eventually attaining an hourglass shape. The spindle organization is similar in meiotic second

division. The only difference concerns centrosome composition. At the first meiotic division each centrosome is composed by a pair of centrioles, whereas the second meiotic spindle is built with centrosomes which contain each a single centriole, since there is no centrosome duplication before meiosis-II (Cenci et al., 1994).

There is an open debate about the role of centrosomes in spindle assembly. While some evidence from several systems supports the need for centrosomes, other reports suggest that they are dispensable (commentary by Gonzalez et al., 1998). *Drosophila* female meiosis, for example, is a case in which, under natural conditions, the spindle is built in the absence of centrosomes, thereby, in female meiotic spindle, microtubules originate from around the chromatin and its poles are anastral and not contain centrioles (Huettner, 1933; Theurkauf and Hawley, 1992). The phenotypes of several mutants which alter the centrosome cycle have revealed different mechanisms of spindle assembly. As an example, there is the testis-specific isoform of centrosomin (cnn), expressed during spermatogenesis and closely associated with the centrioles. Mutations on *cnn* gene result in karyokinesis as well as cytokinesis defects deriving from abnormal spindles. Furthermore, the cytokinesis damage is more severe than karyokinesis, suggesting a more susceptibility of cytokinesis to reduced centrosomin function. This result is consistent with the finding that centrosomes are not absolutely required for chromosome segregation, as supported by *Drosophila* female meiosis and studies of micromanipulation by Church et al. (1986), who demonstrated that chromosome pairs relocated from the nucleus to the spermatocyte cytoplasm are capable of organizing minispindles around themselves with no centrosomes at the poles. Similar experiments have been conducted by Rebollo et al. (2004) to study the contribution of centrosomes in spindle organization in *Drosophila* spermatocytes. They took advantage of two experimental conditions that inhibit the natural process of centriole migration from the plasma membrane to the interior of the cell that takes place at the onset of meiosis. Under such conditions, the centrosomes organize asters but these are kept at the plasma membrane, away from the nuclear region. In these cells, microtubules can be seen grow from the remnants of the fenestrated nuclear envelope (NE) and to assemble into anastral bipolar spindles in a centrosome-independent manner. However, these anastral spindles could sustain only some degree of chromosome segregation. The model of spindle assembly during meiosis I in *Drosophila* spermatocytes proposed by the researchers is that, at the beginning, microtubule bundles of centrosomal origin, connecting centrosomes to chromosomes, develop. Immediately after, noncentrosomal microtubules start to polymerise in association with the remnants of the NE. The fully mature spindle would contain a spindle-shaped structure made of microtubules of noncentrosomal origin embedded in another spindle-shape array made of two overlapping asters. Thus, according to this theory, acentrosomal microtubules are nucleated on the

inner side of the remnants of the NE and not around the chromosomes. This is, on a side, in contrast with what seen in *asterless* mutants, where, despite the absence of asters, spermatocytes assemble a peculiar anastral spindle by means of meiotic chromosomes that act as microtubule-organizing centers, thus promoting formation of bipolar minispindles associated with individual bivalents (Bonaccorsi et al., 1998). On the other side, the Rebollo's model is consistent with the phenotype of *fusolo* and *solofuso* mutants, where secondary spermatocytes are produced, devoid of chromosomes, yet able to give rise to bipolar spindles that undergo all the morphological transformations required for a correct cell division, such as central spindle formation. This strongly argues that in *Drosophila* spermatocytes, spindle formation and dynamics are controlled by chromosome-independent factors (Bucciarelli et al., 2003).

Failure in centrosome segregation may result in different phenotypes as evidenced by some mutants. In *ms(1)516* mutants, for example, failure in centrosome segregation gives rise to a monoastral bipolar spindle (Lifschytz and Meyer, 1977), whereas in *polo* (Llamazares et al., 1991) and *aurora* (Glover et al., 1995) (serine-threonine kinases) mutants, the impairment of centrosome segregation determines the formation of monopolar spindles, where microtubules radiate from the single pole which contains the two unsegregated centrosomes.

Centrosomes or MTOC (microtubule organising centers) consist of a pair of centrioles surrounded by a cloud of pericentriolar material, whose components change according to cell-type and development in *Drosophila* (Gonzalez et al., 1998). Centrioles are not essential for microtubule nucleation; rather they appear to organize pericentriolar components into a cohesive focus at spindle poles. Microtubules are nucleated within the pericentriolar cloud, their minus ends within or near the pericentriolar material and their plus ends extending into the cytoplasm (Wilson et al., 1997). γ-tubulin is one of the pericentriolar components. Antibodies against γ-tubulin recognise two orthogonal rods located near the surface of the cell in mature primary spermatocytes. During meiosis the same antibody recognises a dot-like centrosome at the poles of the meiotic spindle and the rod-like structures are no longer present (Wilson et al., 1997). Twine function seems to be required for γ-tub23C reorganization and/or recruitment to centriole pairs specifically at the G2/M transition, when γ-tubulin is visible as a dot at each spindle pole (Wilson et al., 1997). Mutations in γ-tub23C (germ-line specific isoform) impair the assembly of meiotic bipolar spindles. Centrosomes associate with a large number of astral microtubules that later get organized into a conical structure never observed in wildtype cells. Both meiotic divisions fail to be accomplished, as evidenced by the presence of spermatid cysts containing only 16 cells, with each spermatid having a single large nebenkern associated with several nuclei of different sizes. By observing the

behaviour of these mutants, it seems like the depletion of γ-tubulin does not prevent microtubule polymerization or stabilization (Sampaio et a., 2001).

Like other *Drosophila* mutants that disrupt spindle assembly during male meiosis, *γ-tub23C* does not result in meiotic arrest. On the contrary, besides the absence of a bipolar spindle, the chromosome cycle proceeds until abnormal spermatids are formed but prometaphase lasts about 50% longer than in wildtype cells. Same case as it's seen in wildtype spermatocytes following microtubule depolymerisation with colchicine. Both examples, as well as the delay of the onset of anaphase resulting from a relatively high number of misaligned chromosomes, provide evidence substantiating the activity of a feeble meiotic spindle checkpoint in *Drosophila* male meiosis (Rebollo and Gonzalez, 2000).

DSpd2 is another centrosomal protein, recently shown to be enriched at both the centrioles and the pericentriolar material (PCM). Its function is to maintain the cohesion between the two centrioles and to mediate the recruitment of additional PCM components, such as γ-tubulin, DGrip91 and D-TACC. Null mutations in *DSpd2* don't affect vitality of the flies but, instead, provoke sterility in both sexes. Astral microtubule nucleation is suppressed in both neuroblasts and spermatocytes even if a more severe phenotype is seen in the testis (Giansanti et al., 2008). DGrip 91, just mentioned, is a gamma-ring protein (Grip) forming, together with DGrip 84 and γ-tubulin, the γ-tubulin small complex (γ-TuSC) that, in turn, is a component of the larger γ-TuRC (γ-tubulin ring complex), present in the pericentriolar material in *Drosophila*. γ-TuSC displays an open ring-like structure, resembling a lock washer, capped on a side by other Grips, like Grip71, Grip75, Grip128 and Grip163. The activity of γ-TuRC is to nucleate the microtubule assembly within the centrosome and to keep the microtubule minus ends capped by cap components, preventing depolymerisation of the microtubules. Also, the γ-TuRC cap structure is dispensable for microtubule function, as cap Grip mutants provide γTuRC functionality sufficient for the viability. However, they are required for anchoring the γTuRC at specialized MTOCs, (in the germline, for example) allowing microtubules to tightly associate with specific MTOCs, as suggested by the failure of alignment of the nuclei at one end of the sperm bundle, (a phenomenon due to the interaction between nuclei and axoneme microtubules), owing to the loss of γ-tubulin association with spermatid nuclei, in *Grip128* and *Grip75* mutants (Vogt et al., 2006).

1.7 CENTRAL SPINDLE ASSEMBLY AND ITS IMPLICATIONS IN CYTOKINESIS PROCESS

During late anaphase, a dense body of overlapping antiparallel microtubules (MTs), that forms in the region between the two daughter nuclei migrating to the opposite poles, gets evident. This bundle of microtubules has been termed as "central spindle" or "midbody" and its middle part as "central spindle midzone". The midzone, in particular, is associated with a proteinaceous matrix, the so-called "Flemming body" (Zeitlin and Sullivan, 2001), which prevents tubulin immunostaining, thus forming a dark band. About the origin of the central spindle microtubules, there are controversial theories. One of these relies on the presence of transient microtubule organizing centers between the two daughter nuclei, that would de novo nucleate new microtubules which then will be part of central spindle (Vogt et al., 2006). Studies on γ-tubulin localization have provided support for this possibility, since this protein has been found at the minus ends of central spindle MTs (Julian et al., 1993). On the other side, there is the hypothesis according to which the central spindle would consist of MTs dissociated from the spindle poles, with the plus ends in the midzone and the minus ends terminated near the chromosomes migrating to the opposite cell poles. Thereby, these microtubules would be the remnants of the interpolar MTs nucleated by the centrosomes. This is consistent with the presence of Asp (Abnormal Spindle) protein on the borders of the central spindle region, that correspond to the minus ends of microtubules released from the spindle poles, where Asp previously was localized. To strengthen this theory there are the central spindle defects evident in *asp* mutant spermatocytes (Riparbelli et al., 2002). On the contrary, data by *asterless* mutants, previously showed, argue for a self-organization of the central spindle since it regularly assembles in the absence of the asters (Bonaccorsi et al., 1998). Furthermore, there is one more model for the central spindle microtubule composition proposed by Inoue et al. (2004), where the central spindle would consist of two distinct set of MTs, "peripheral" astral MTs and "interior" MTs. The former corresponds to the peripheral MTs of the asters, which dynamically probe the cytoplasm as they extend along the cell periphery and are thought contact the cortex and bundle at the location of the future cleavage site. These MTs translocate toward the spindle equator and form a series of overlapping bundles, a structure termed "peripheral central spindle". The latter, instead, is confined within the "spindle envelope", the highly fenestrated remains of the nuclear membrane that persists in *Drosophila* cells. These interior MTs are proposed to elongate and then to be released from the spindle poles to form the overlapping bundles of the "interior central spindle". The two MT populations are biochemically distinct, as the Orbit/Mast protein (a MT-associated protein) strongly accumulates in the region of interior MTs, the reason why *orbit* mutants fail to

form stable interior central spindles, whereas peripheral MTs normally contact the cortex, generating the signal for cleavage furrow. Although cleavage furrow initiates, it ultimately regresses in these mutants, allowing to postulate a role for peripheral MTs in initiating furrow formation where they contact the equatorial cortex and bundle, and a second function for the interior MTs into stabilizing and propagating the furrow (Inoue et al., 2004). The fact that MTs of central spindle are implicated into furrow positioning and, thus, cytokinesis, introduces another strongly debated issue: the relationship between the central spindle and the cytokinesis structures.

Some results from micromanipulation experiments by Rappaport (Rappaport, 1961) support a role for the asters into stimulating cytokinesis according to a model where an organizing factor is directed along astral microtubules to concentrate at the point at which the plus ends of the microtubules contact the cell cortex. Furthermore, experiments where asters are kept in the cytoplasm and anastral spindle form, the orientation of the cleavage furrow correlates tightly with the position of the two asters and not at all with the orientation of the spindle. Hence, the asters seem to contribute to specify the place of furrow (Rebollo et al., 2004). Contrasting data come from Bonaccorsi et al., (1998), who show normal cell contraction in *asterless* mutants as well as in *DSpd2* mutants where nonetheless the defects in asters nucleation, a regular furrow ingression is visible (Giansanti et al., 2008).

Metaphase chromosomes has been implicated in signalling cytokinesis as well, but the behaviour of the *Drosophila* secondary spermatocytes in *fusolo* mutants argue against the need of chromosomes for cytokinesis to take place. Indeed, these mutant spermatocytes II, even in the absence of chromosomes, assemble a regular contractile apparatus and undergo cytokinesis (Bucciarelli et al., 2003). The other structure suggested to be required for cytokinesis is the central spindle. Both results from *asl* and *fsl* mutants suggest that central spindle is necessary and sufficient to stimulate the cytokinetic process, ruling out the involvement of either astral microtubules or chromosomes. A possible explanation to justify the different results obtained about the presumed factor underlying cytokinesis signalling is that these difference may depend on the cell type. Hence, in large cells, such as those used in the micromanipulation experiments by Rappaport, where the central spindle is far from the cell cortex, astral microtubules may play a role into inducing furrow. Conversely, in *D.melanogaster* spermatocytes it may be the central spindle having this role (Saint and Somers, 2003. The analysis of mutations that impair both central spindle formation and cytokinesis processes reveals a cooperative interaction between central spindle and cytokinetic apparatus components. The impairment of either of these structures prevents the formation of the other, thus displaying an interdependence with each other (Gatti et al., 2000). This the case, for example, of *KLP3A, Pav, Polo, Feo* genes codifying for central spindle components. *KLP3A* gene encodes a

kinesin-like protein that accumulates in the midbody of spermatocytes (Williams et al., 1995). *Pavarotti* (*pav*) locus also encodes a plus-end-directed kinesin-like motor protein. It's related to the mammalian CHO1/MKLP1 and to the *C.elegans* ZEN-4 (Adams et al., 1998) and is mutually dependent with POLO kinase (Carmena et al., 1998), which forms a complex with, for the correct localization in the midbody. Pav interacts with *Drosophila* RacGAP50C, a Rho-family GTPase-activating protein (GAP), forming an evolutionarily conserved complex called "centralspindlin" that has MT bundling activity (Mishima et al., 2002). Microtubule bundling is a feature of the anaphase/telophase microtubule network and appears to play an important role in generating the midzone microtubule network. *Fascetto* (*feo*) gene, homologous to the mammalian PRC1, encodes a conserved microtubule-associated protein (MAP) enriched at the midbody, whose disruption by RNA interference results into aberrant central spindle and failure in cytokinesis (Vernì et al., 2004).

Cytokinetic process may be subdivided into the following steps: the interactions between the spindle and the cortex determine the site of cleavage furrow formation; an actomyosin-based contractile ring assembles at this cortical site, then constricts, leading to furrow ingression. New membrane has to be added, during both furrow ingression and the completion of cytokinesis (see below), for the separation of the daughter cells to allow. The end point of constriction in the cytokinesis of a spermatocyte is the formation of the ring canal, the stabilised residue of the contractile ring that does not close, leading to a persistent cytoplasmic connection between cells. Known contractile-ring associated proteins, apart from actin and myosin II, are, for example, anillin, an actin-binding protein thought to mediate interactions between the contractile ring and the plasma membrane (Giansanti et al., 1999), septins like Peanut; Diaphanous (Dia), a formin homology family protein, Spaghetti squash (sqh), the profilin Chickadee (Chic) (Giansanti et al., 1998), Rho, Rho GEF, a protein encoded by *pebble* gene, discovered to bind to RacGAP50C, thus mediating the interaction between the centralspindlin complex and the contractile ring (Somers and Saint, 2003). Mutations in all these genes similarly disrupt the assembly of both the contractile ring and the central spindle, again suggesting a mutually dependence between these two structures (reviewed by Giansanti et al., 2001).

Moreover, mutations in *twinstar* (*tsr*), *bird nest soup* (*bns*) and *Drosophila citron kinase* (*dck*) specifically affect the final stages of cytokinesis, that include the stabilization of the intercellular bridges (*dck*) and contractile rings disassembly (*tsr*) (Naim et al., 2004).

The later stages of cytokinesis are also characterized by the add of new membrane to the equator of the cell, necessary to accomplish a remodelling of the plasma membrane concomitant with the advancing of cleavage furrow. *Giotto* (*gio*) (Giansanti et al., 2006), *four wheel drive* (*fwd*) (Brill et al., 2000), *vibrator* (Gatt and Glover, 2006) and *four way stop* (*fws*) genes participate to a common

pathway required for the completion of cytokinesis, in terms of contraction of the actin ring, progression of cleavage furrow and maintenance of the attachment between membrane and constriction ring. *Gio* encodes a phosphatidylinositol (PtIns) transfer protein (PITP), proposed to mediate the transfer of lipids from the ER (endoplasmic reticulum) to the furrow membrane, causing a local enrichment in PtIns molecules. An high concentration of these lipids, their phosphorylation by the PtIns 4-kinase, codified by *fwd* gene, and a further phosphorylation that generates PtIns(4,5)P2, all together contribute to mediate membrane-vesicle fusion at the cleavage furrow, allowing formation of new membrane and/or vesicle-mediated targeted delivery of proteins required for cytokinesis.

The involvement of Golgi and Golgi-derived vesicles in membrane trafficking during cytokinesis is sustained by cytokinesis defects evident in mutants of Golgi-associated proteins, like Rab11, Fws and Syntaxin5. Rab11 is a small GTPase, whose localization in *Drosophila* spermatocytes overlaps the distribution of the ER membranes (astral and parafusorial membranes of the spindle envelope). In telophase, instead, it's concentrated in some Golgi-derived vesicles that accumulate at the cleavage furrow, where it's supposed to mediate vesicles fusion necessary for completion of cytokinesis (Giansanti et al., 2007). Syntaxin5, a Golgi-localized SNARE protein (Xu et al., 2002) and Fws, a Golgi-associated protein, both are implicated in Golgi proper architecture and efficient function, necessary to support rapid and extensive increases in cell surface area during the steps leading to the completion of spermatocyte cytokinesis (Farkas et al., 2003).

This idea of a re-organization of the furrow membrane, resulting into the enrichment of phosphoinositides, is not only supported by the phenotype of *gio*, *vibrator* (encoding another PITP) and *fwd* mutants, but also by recent evidence of the importance of very-long-chain fatty acids present in phosphoinositides for the stability of high membrane curvature. Plasma membrane lipids influence membrane biophysical properties such as membrane curvature and elasticity, peculiar characteristics of cytokinesis process. Mutations in *bond* gene, encoding a member of Elovl family of enzymes involved into elongation of very-long-chain fatty acids, block or dramatically slow cleavage furrow ingression in spermatocytes, also showing a detach of contractile ring from the cell cortex. Such findings implicate a role for very-long-chain phosphoinositides in modulating membrane deformability and providing a stable connection of cortical contractile components to the plasma membrane (Szafer-Glusman et al., 2008). New findings have also revealed essential roles for phosphoinositides in basal body docking to the nuclear envelope and in the axoneme architecture and integrity of the developing flagellar axoneme and axial sheath (Wei et al., 2008).

Among the proteins whose loss of function disrupts both central spindle organization and cytokinesis, the chromosomal passenger complex (CPC) is particularly noteworthy. In *Drosophila*

spermatocytes, it is composed of Aurora B serine-threonine kinase, INCENP, inner centromere protein, survivin and Australin (Aust), paralogue of Borealin-related (Borr). CPC shows a very dynamic localization: on the chromatin during interphase, on the kinetochores of chromosome arms during prometaphase and finally on the central spindle midzone and the equatorial plasma membrane, where it assists in the recruitment of the conserved centralspindlin complex, during cytokinesis. This localization correlates with the diverse functions of CPC: modifying the histones at the chromatin, by phosphorylating Ser10 of H3, a modification that accounts for the displacement of heterochromatin protein-1 (HP1) from chromosomes, thus inducing chromosome condensation; correcting erroneous MT-kinetochore attachments, due to an incorrect chromosome alignment on the metaphase plate; and regulating cytokinesis at the central spindle and later the midbody. Given the correlation between localization and function, it's evident that timely and proper localization of the CPC is basic for this complex to exert its diverse functions. A proposed mechanism by which the CPC is targeted to the chromosome arms is via interaction with HP1, as INCENP has been described to interact with this chromatin-associated protein. HP1 displacement from the chromosome arms is mediated by Aurora B. In *Drosophila* the loss of Aurora B or INCENP has been shown to result in a decrease in histone H3 phosphorylation and concomitant defects in chromosome condensation (Adams et al., 2001; Giet and Glover, 2001). Translocation from the centromeres to the central spindle at the metaphase-anaphase transition, could depend on the orchestrated action of some factors, such as microtubules and Cdc14 phosphatase. In *S.cerevisiae*, INCENP is phosphorylated by Cyclin B/Cdk1 until metaphase. Afterwards, Cdc14 dephosphorylates INCENP triggering translocation of the CPC to the central spindle (McCollum, 2004). Centromere localization of the CPC is not a prerequisite for central spindle localization, as evidenced by *Drosophila fusolo* mutants that undergo meiosis without chromosomes but, however, regularly localize Aurora B to the central spindle and execute cytokinesis (Bucciarelli et al., 2003). Relocalization of the CPC from centromeres to the central spindle also requires dynamic microtubules, as treatment of anaphase cells with the microtubule-stabilizing drug taxol impairs central spindle targeting (Vader et al., 2006). Differently from Aurora B and INCENP, Australin is not required for histone H3 phosphorylation in *Drosophila*, but more specifically for sister chromatid cohesion during prometaphase and metaphase, chromosome alignment and segregation. Furthermore, Australin is essential for both anillin accumulation, a very early event of cytokinesis, and centralspindlin recruitment at the cleavage site, as evidenced by the failure of central spindle formation and contractile ring assembly in *aust* mutant spermatocytes (Gao et al., 2008).

1.8 INHERITANCE OF MITOCHONDRIA IN *DROSOPHILA* MALE MEIOSIS

Regulated mitochondrial distribution within cells enables efficient delivery of ATP to energy-requiring structures and promotes equal mitochondrial segregation during cell division. Spermatogenesis in *Drosophila*, as well as in many organisms, involves dramatic and specialized mitochondrial morphogenesis, including aggregation, fusion, membrane wrapping, unfurling and elongation. Mitochondria in *Drosophila* spermatocytes are small and numerous, aggregating on one side of the cell (polar spermatocytes) before dispersing and multiplying as the spermatocyte enlarges prior to meiosis. During meiosis, the mitochondria associate with the central portion of the spindle. By this way, initially it had been believed that the inheritance of mitochondria was achieved passively as a consequence of equal cytokinesis. Then, Basu and Li (1998) proposed an active mechanism to explain mitochondria inheritance. On the light of the intimate association of Des-1 protein with mitochondria aligned along the central spindle, they suggested Des-1 as potential anchor to link mitochondria to the microtubule cytoskeleton during meiosis, thus ensuring equal partitioning of mitochondria to the daughter spermatocytes/spermatids. Later, Ichihara et al. (2007) enforced this idea of an active process underlying mitochondria inheritance, providing further evidence that it is strictly linked with microtubules during male meiotic divisions in *Drosophila*, just such as was documented in *S.pombe* (Yaffe et al., 2003). They showed that at the beginning of prophase I, mitochondria are homogenously distributed throughout the cytoplasm including the areas occupied by asters. Then mitochondria are assembled toward the plus ends of aster microtubules and at metaphase are clustered at the equator of the peripheral cytoplasmic region between two facing asters. Finally, at anaphase, mitochondria are translocated to the interior region of the cells, distributed along central spindle. This distribution suggests that mitochondria inheritance is closely associated with astral and central spindle microtubules and dLarp, a La-related protein co-localizing with mitochondria, would play an essential role in this process, working in concert with plus-ended motors to allow the transport of mitochondria along aster microtubules in plus-ended direction (Ichihara et al., 2007).

Just after meiosis is completed, the mitochondria of the spermatid collect on one side of the haploid nucleus and fuse together into two giant aggregates. These aggregated mitochondria then wrap around one another to produce the spherical Nebenkern. When viewed in cross-section under the transmission electron microscope, the Nebenkern resembles an onion slice, and this early stage of spermatogenesis is called the "onion stage." From results obtained by Liebrich in 1982 in the experiments where the presence of colchicine inhibited mitochondria aggregation in *Drosophila*

hydei spermatids while cytochalasin B did not interfere with mitochondria aggregation, it gathers that microtubules, known to be inhibited by colchicine, are involved in the aggregation process of mitochondria, whereas microfilaments, which are sensitive to cytochalasin B, do not play a detectable role in the aggregation of mitochondria (Liebrich, 1982). When the flagellum elongates, the two mitochondrial regions of the Nebenkern (major and minor) unfold and elongate down the side of the axoneme. Mitochondrial derivatives do not contact the micro-tubules of the axoneme, which is enclosed by a membraneous sheath. Instead, a different population of singlet "cytoplasmic" microtubules, parallel to the axoneme, surrounds each elongating mitochondrial derivative. Such a dramatic developmentally-regulated mitochondrial morphology change is allowed by a dynamic balance between the opposing action of mitochondrial fusion, controlled by *Mitofusin* (*mfn*) and mitochondrial fission, controlled by *drp1*.

Fuzzy onion (*fzo*), the *Drosophila* testis-specific *mfn* homologue, encodes a GTPase associated with mitochondria during the narrow period of spermatogenesis corresponding to the time of mitochondrial fusion. Indeed, it appears on the mitochondria just prior to fusion (during the last stages of meiosis II) and disappears soon afterward (after mitochondrial elongation). Male flies with mutations of the *fuzzy onion* are sterile. They have defective Nebenkern due to the fact that the mitochondria have failed to fuse into the two giant mitochondria. Rather, the unfused mitochondria wrap around each other and elongate. So the defect appears to be that of fusion, since the aggregation, wrapping, and elongation steps are all accomplished (Hales and Fuller, 1997).

Drp1 encodes the Dynamin-related protein 1 (Drp1), which is also a GTPase, mediating mitochondrial division in pre-meiotic cells, necessary for the proper mitochondrial distribution during male meiosis, as well as post-meiotic unfurling of the two mitochondrial derivatives (either directly or indirectly) (Aldridge et al., 2007).

The phenotypes of *Drp1* and *fzo* mutant primary spermatocytes are consistent with a role for *Drp1* in mitochondrial fission and a role for *Fzo* in mitochondrial fusion, suggesting that mitochondrial fission and fusion are normally active and counterbalanced in primary spermatocytes.

Two more proteins have been recently implicated in mitochondrial fission in *Drosophila*: Pink1 (serine-threonine kinase) and Parkin (RING finger-containing E3 ubiquitin ligase). Genetic findings suggest that *pink1* and *parkin* are unlikely to be components of the canonical fission machinery controlled by *drp1*, rather they promote mitochondrial fission and/or inhibit fusion either directly or indirectly by means of a different pathway from *drp1*, as evidenced by flies mutant for *pink1* and *parkin* that show distinct mitochondrial phenotypes from *drp1* mutant flies (Deng et al., 2008).

Milton is a protein found associated with mitochondria and proposed to link directly or indirectly mitochondria to kinesin, since its property of binding kinesin, allowing for directed transport and

movement of mitochondria during spermatid elongation. By the connection of the outer mitochondrial membrane to the cytoplasmic microtubules, Milton would help the elongation of mitochondrial derivatives in developing spermatids. In addition to this role, Milton is also involved into anchoring the Nebenkern to the nucleus (Aldridge et al., 2007).

1.9 BASAL BODY FORMATION AND NUCLEUS ANCHORING TO THE AXONEME

Early after meiosis, the single centriole of each spermatid embeds into the spherical nuclear membrane and then converts into the basal body. Once the attachment of the basal body to the nuclear envelope has taken place, (process called basal body docking), the axoneme initiates to assemble from the basal body. More specifically, the axoneme assembly starts at the protein body stage, when an electron-dense, phase-dark structure appears in the nucleus. Two giant mitochondrial derivatives elongate along the growing axoneme, which becomes covered by a membranous axial sheath. As the axonemes elongate, the spermatid nuclei are moved toward the base of the testis. The process by which all nuclei within a cyst get grouped at one end of the bundle is termed cyst polarization. Some evidence from mutations accounting for the loss of the connection between the axoneme and the nucleus suggests that this linkage is required for proper nuclear position within the elongating cyst. However, axoneme assembly is independent of basal body docking, because flies mutant for γ-tubulin ring complex (γ-TuRC) proteins produce normal axonemes, yet their basal body fails to dock (Vogt et al., 2006), giving rise to spermatid cysts with nuclei scattered along the bundles.
Flagellar axoneme is composed of nine outer doublet microtubules (MTs) and a central pair of MTs (9+2).

Among the proteins recognized to be components of basal body there are Centrosomin, γ-tubulin which is, more correctly, a component of the centriolar adjunct, a torus-shaped structure around the middle of the basal body (Tokuyasu, 1975), Uncoordinated, Pericentrin-like protein, γTuRC cap proteins; the latter has been proposed having a function in microtubules anchoring at special

MTOCs, such as basal bodies, as evidenced by the detachment of γ-tub and, thereby, axoneme from the nuclei in *Grip128* and *Grip75* mutant spermatids (Vogt et al., 2006). As for the mechanism by which the connection between spermatid nucleus and flagellar basal body, hence, flagellar axoneme, is maintained, two structures have been implicated in this process: dynein-dynactin complex and dense complex. At the round spermatid nucleus stage, an hemispherical dynein-dynactin cap assembles over a nuclear side, juxtaposed to the associated flagellar basal body. This nuclear-associated dynein cap would have a role in the nuclear attachment of the basal body, supported by findings that spermatids mutant for the gene codifying 14-kDa dynein light chain, have nuclei scattered along the entire length of the bundles instead of being clustered at one end, as a consequence of the disrupted linkage between nucleus and basal body, proved by γ-tubulin mis-localization (Li et al., 2004).

In 1974, Tokuyasu in his description of the ultrastructural changes to the nuclei during elongation, introduced the term of "dense complex" referred to a specialized microtubule-rich structure and dense cytoplasm that runs the length of the nucleus. Early after meiosis, the single centriole of each spermatid gets embedded into the nuclear envelope at the center of the dense complex and becomes basal body. As the nuclei elongate, dense complex transform from a cap over one hemisphere of the round nuclei, to a stripe along the long axis of the nucleus and the basal body moves to the apical tip of the nucleus, immediately adjacent to the stripe of dense complex. Functions proposed for dense complex are the positioning of basal body and the strengthening of nuclei as they undergo extreme condensation. Yuri gagarin is a protein co-localizing with dense complex, required for actin accumulation in the dense complex and, if mutated, determines nuclear deformation and disorganization, the latter due to the mispositioning of the basal bodies on the nuclei (Texada et al., 2008). The dynein-dynactin complex is likely to interact with the cytoplasmic microtubules of the dense complex to facilitate the nuclear attachment of basal body, as already speculated by Li et al. (2004).

2. RATIONALE

Spermatogenesis in *Drosophila* is relatively simple, dispensable for adult viability, and amenable to genetic and biochemical investigation. The stages of spermatogenesis are well defined, cells are large and easily accessible, and there is evidence that many aspects of the genetic control of spermatogenesis are conserved. The presence or absence of a germ line, the number and quality of mitotic and meiotic divisions, and the production of motile sperm can all be easily scored in the light microscope. Sterile mutations can be easily generated at any step, identified and investigated, providing the starting point for molecular studies.

Strikingly, from transcriptome analysis of various *Drosophila* tissues, 1317 transcripts have been shown to be testis-specific. The genetic screens performed to date in *Drosophila* testes are far from exhaustive. Actually, complementation tests between mutants of similar phenotypes revealed only a few cases of potential allelism, suggesting that many male sterile loci remain still to be uncovered.

My research was focused on the analysis of a unique collection of 13 ethyl methanesulfonate (EMS)-induced male sterile recessive mutants (a generous gift of Barbara Wakimoto, Dept. of Biology, Washington University, Seattle), identified in a well known large screen for *Drosophila* male sterile mutations mapping to chromosomes 2 and 3 (Wakimoto et al., 2004). All these mutants have not been characterized until now. Preliminary *in vivo* cytological analysis had shown that the mutants mainly exhibit defects of entry into meiosis and cell cycle progression. However, these defects do not prevent the newly formed spermatids from undergoing further differentiation, producing sperm bundles that fail to individualize and to gain mobility, with consequent male sterility. Such a behavior indicates that the morphological maturation of sperms follows a pathway which is independent from the completion of meiosis, thus reminding the “Twine class” mutant phenotype. The “Twine class” includes genes as *boule*, *pelota*, *Dmcdc2*, besides *twine*, which is the founding member of this group. *twine* encodes the Cdc25 phosphatase, responsible for the activation of Cdc2-CyclinB complex, which, in turn, triggers G2/M transition. The loss-of-function mutation *twe* ^{HB5} is characterized by the presence of 16-cell cysts that undergo spermiogenesis without any evidence of meiotic divisions; whereas the hypomorphic allele *twe* ^{Z0758} shows a mutant phenotype characterized by spermatocytes that execute only one of the two meiotic divisions while undertaking the further spermatid differentiation.

Genetic analysis was performed of the phenotypically most interesting EMS-induced male sterile recessive mutations. More specifically, gene mapping was executed following two approaches, meiotic recombination and deficiency mapping. Recombination mapping was also exploited in order to recover the “clean” chromosome (clean means that the original mutant chromosome retains only the region where the mutation lies, whereas the rest of the chromosome is entirely derived

from the marker chromosome), in the event that was necessary. By this approach I could verify whether a given mutant retains sterility and the same cytological phenotype of the original mutant strain, as proof of the presence of a single mutation on the chromosome, responsible for a mutant phenotype. Genetic analysis of *twine*-complementing mutation *71-43*, was performed much more in detail until to narrow the region on chromosome 2, where it maps, to 40952 bp and, besides, the study of such a mutation was extended also to check possible effects on vitality and female fertility.

Genetic characterization was followed by molecular analysis of some *twine*-noncomplementing mutations and of *71-43*. In the first case, *twine* gene sequencing was executed in order to investigate whether the genes mapping in *twine* region were *twine* alleles and if the genes mapping far from *twine* but are *twine*-noncomplementing had a second mutation on *twine* sequence responsible for such a behavior. As for *71-43* mutation, a proteomic approach, consisting of comparative analysis of 2D-IEF-SDS-PAGE in mutant and wildtype, was accomplished, in order to overcome the difficulties of classical genetic methods to identify the gene responsible for mutant phenotype. A cytological analysis of the mutations, previously genetically and molecularly examined, was executed, pointed toward a sharp characterization of the impaired aspects of spermatogenesis leading to the mutant phenotype. This analysis was performed by standard microscopy investigation, and with the use of antibodies against a panoply of factors known to be involved in meiotic division execution and sperm maturation to precisely assess which aspect of spermatogenesis is impaired in the mutants.

The final aim of this research is the identification of new genes required for male fertility in *Drosophila melanogaster*, providing insights into the genetic pathway underlying *Drosophila* spermatogenesis and, in particular, the male meiosis process.

3. MATERIALS AND METHODS

3.1 *DROSOPHILA* STRAINS AND MAPPING EXPERIMENTS

The Z2-3162 (**12-228)**; Z2-5584 (**71-43**); Z2-4024 (**55-99**); Z2-4089 (**50-38**); Z2-1395 (**60-40**); Z2-0903 (**27-76**); Z2-1191 (**58-102**); Z2-0758 (**83-28**); Z2-2863 (**69-36**); Z2-1168 (**58-79**); Z2-2412 (**54-96**); Z3-2366 (**118-27**) and Z2-2345 (**54-23**) mutations were identified by a cytological screen of the Zuker's collection of male sterile mutants on chromosomes 2 and 3 (Wakimoto et al., 2004). The second chromosome lines of the Zuker's collection carry a mutagenized second chromosome marked with *cn* and *bw* balanced over *CyO, Cy* cn^2. Mutations on chromosome 2 were mapped by recombination using multiply marked chromosomes with *al dp b pr c px sp* and *al dp b pr Bl cn c px sp* and tested for failure to complement the deletions from the chromosome 2 deficiency kit provided by the Bloomington Stock Center (Department of Biology, Indiana University, Bloomington, IN). The genotype of deficiencies I used is described in the FlyBase server at Indiana (http://flystocks.bio.indiana.edu/Browse/df-dp/dfextract.php?num=all&symbol=bloomdef).

All genetic mutations and balancers are described and referenced by Lindsley and Zimm (1992).

"Chromosome cleaning" carried out on *12-228, 60-40, 54-23* and *50-38* strains was performed by meiotic recombination using the following multiply marked chromosome with *S Spt Tft nw-D px Pin*. "Clean" chromosomes were kept over *CyO* balancer.

All flies were raised on standard *Drosophila* medium. Complementation tests and mapping experiments were performed at 25°C. For each complementation test, two males heterozygous for the mutation under exam and the *Df* allele (originated by virgin females *mutation/CyO* mated to *Df/Balancer* males) were mated to two *yw* virgin females and then the offspring was counted through the 18th day after each mating. Reduced fertility meant a fewer progeny than 10 flies. In case of reduced fertility or sterility, such a cross was set up two more times. To analyze female fertility, mutant homozygous females were singularly mated to two *Oregon-R* males and scored for fertility after 18 days. For each mutation, two different crosses were set up.

To test for a possible delayed development or lethality of *Rec#57/Rec#57* flies, a cross between *Rec#57/St, Cy Tb* heterozygous males and females was set up and the progeny was scored within 18 days. The same experiment was repeated two more times, providing the following results:

	Rec#57/St, Cy Tb (adults n°)	*Rec#57/Rec#57* (adults n°)
First experiment	45	24
Second experiment	54	18
Third experiment	65	27

The observed frequencies were analyzed by Chi-Square Test, in order to assess whether the difference between observed and expected frequencies of such genotypes was statistically significant.

	Rec#57/St, Cy Tb (Obs. Freq.)	*Rec#57/St, Cy Tb* (Exp. Freq.)	*Rec#57/Rec#57* (Obs. Freq.)	*Rec#57/Rec#57* (Exp. Freq.)	Chi-Square Test (P value)
1st exp.	45	46	24	23	0.86
2nd exp.	54	48	18	24	0.27
3rd exp.	65	61.3	27	30.7	0.56

3.2 ANALYSIS OF LIVE AND FIXED TESTES CONTENTS

Live testes of young males (less than one day-old) were dissected, squashed in 2 μg/ml DAPI, added to testis buffer, TIB, (183 mM KCl, 47 mM NaCl, 10 mM Tris pH 6.8) and examined by phase contrast and fluorescence microscopy.

For statistical analysis, 100 cysts, both of one day-old mutant homozygous males and heterozygous males, were scored. To preserve cysts, testes were dissected in TIB on a slide. Once put on the slide a siliconized cover slip, the slides were frozen in liquid nitrogen and the cover slip was removed with a razor blade. Slides were dehydrated in cold ethanol and fixed in 2% paraphormaldehyde and 1X PBS for 7'. Then, slides were hydrated in 1X PBS for 5' and stained in DAPI (2 mg/ml) in 2X SSC for 10' and, finally, mounted in vectashield. Statistical analysis was executed by Chi-Square Test.

3.3 PREPARATION OF MITOTIC CHROMOSOME SQUASHES FROM LARVAL BRAINS

The clean *71-43* chromosome (*Rec#57*) was maintained over the *T(2;3)Cy Tb* balancer that carries the body shape marker *Tubby*. *Rec#57/Rec#57* homozygous larvae obtained from *Rec#57/T(2;3)Cy Tb* cross, were identified on the basis of their non-*Tubby* phenotype. Third instar larvae were selected and washed in a 35 x 10 mm petri dishes with 0.7% saline at room temperature, where brains were dissected. Then, brains were placed into a drop (50μl) of hypotonic solution on a siliconized slide and incubated at room temperature for 8'. Brains were moved to a 35 x 10 mm petri dishes containing a freshly prepared mixture of acetic acid/methanol/H20 (11:11:2) and left for approximately 30 seconds, before transferring a single brain into a small drop (2μl) of 45% acetic acid placed on a dust-free siliconized coverslip (20 x 20mm 22 x 22mm), where it left for 1-2

minutes. Afterward, a dust-free slide were put on the cover slip and, once flipped the slide over, it was squashed hard. Slides were, first, frozen in liquid nitrogen and then, once removed the cover slip using a razor blade, they were immediately plunged in cold (-20°C) absolute ethanol until they gradually reached room temperature. They, finally, were removed from ethanol, air dried, hydrated in 1X PBS and stained in DAPI.

Mitotic index was defined as the number of mitotic cells per optical field, with every optical field in the brain being scored. The optic field chosen for this analysis was the circular area defined by a phase-contrast 100x Zeiss objective, using 10x oculars. Statistical analysis was executed by Chi-square Test.

3.4 IMMUNOFLUORESCENCE STAINING OF MALE MEIOSIS

Very young adult males (up to one day-old), were dissected in cold TIB. Testes were transferred in a drop (10 μl) of TIB solution on a slide and, once put on a siliconized cover slip, the slide was frozen in liquid nitrogen and cover slip was removed with a razor blade. Tissues were fixed in cold MetOH for 7' and permealized in 1X PBS 0.1% Tween20 for 10'.

For double immunostaining of either spindle and centrosomes or lamin and centrosomes, testes were incubated in a wet chamber, for 1 hour at room temperature, with the monoclonal mouse anti-α-tubulin IgG (Sigma) diluted 1:50 in 1X PBS and rabbit anti-Spd2 (Giansanti et al., 2008) diluted 1:1000 in 1X PBS, and with monoclonal mouse anti-laminDm0 IgG (Developmental Studies Hybridoma Bank –DSHB- Department of Biological Sciences, University of Iowa) diluted 1:50 in 1X PBS and rabbit anti-Spd2 diluted 1:1000 in 1X PBS, respectively. These primary antibodies were detected by 1 hour incubation at room temperature in a wet chamber with Alexa^{488}-conjugated anti-mouse IgG (Molecular Probes) diluted 1:100 in 1X PBS and Alexa^{594}-conjugated anti-rabbit IgG (Molecular Probes) diluted 1:200 in 1X PBS.

For actin staining, testes were dissected in TIB and frozen in liquid nitrogen. Then, they were dehydrated in cold ethanol for 10' and fixed in 3.7% paraphormaldehyde and 1X PBS for 7'. After allowing the slides to hydrate in 1X PBS, they were soaked in the blocking solution (1X PBS + 0.1% Tween20 + 3% BSA) for 30' and incubated in a wet chamber for 2h at 37°C with rhodamine-phalloidin (Cytoskeleton).

All preparations were examined using a Zeiss Axiophot fluorescence microscope equipped with a 100-W mercury light source. Fluorescent images were captured with a CCD camera (series 200; Photometrics, Tucson, AZ) using IPLab software (Signal Analytics Corp., Vienna, VA) and processed using Adobe Photoshop software.

3.5 *TWINE* SEQUENCING

Standard phenol-chloroform extraction was performed to recover genomic DNA from young male and female *Oregon-R, 12-228/12-228, 50-38/50-38, 60-40/60-40* and *54-23/54-23* flies. More primer combinations (see below) were used in enzymatic amplification reactions to amplify the whole *twine* sequence plus 5'- regulatory region. The temperature cycle started at 95° C for 2 minutes, then 20 seconds at 95°C, 20 seconds at $T_{annealing}$ and 30 seconds at 72°C, and the cycle was repeated 30 times. Finally, 3 minutes at 72°C. The reaction product, after purification, was sequenced and compared with wildtype *twine* sequence by computational programs. In the event of a mutation in *twine* sequence of the mutant genotype under exam was found, one more enzymatic amplification reaction was set up and the reaction product sequenced.

***twine* sequence plus 5'- regulatory region (RELEASE 5.9) and primers used in enzymatic amplification reactions:**

```
3'-TGCATCTT TCATGACTGA AGGATTGTTT CCTTATGTAC TAAAACACCT ATTCTGGTCG
   >>>>>>>>>>>>>>>>>>>>>
TAATCTCTGA AGGCACACAC AGTAAAGCAT TTCAATATCT GAATTATGTT TCGAAATGTT
AGAAATTGTT TAAAAATGAA TAAAATGATA AGTATTTTAT AACTGTTCTC AAAAATAGTG
GTCCTTTTTA TTATCTCGAT CAGTAACAAA TTATTTGTTC TCTTCATATT TCTTCAATAG
CTTAAAGCAT TTAAAATTTT GTAATATATA TAAACTATAA TAGCATATAA ATTAAGGAAC
ATTTTTCTTC ATTTGATTTA AAATTTGTAT CACGAATTTT CTTGAAATAT TTTATGAGTA
TTCTTACATC TCCTGTTCTA ATTAAGCATT ATGCATCCTA AAACTTTTAA ATTGTGTATT
AAATGATTGT TTTTAGATAC TTTTAATAAA AGTTGACCGA TGTAGGTGGA ATCCACATAA
                                  >>>>>>>>>>>>>>>>>>>>>
ATAGTTTCAG CATAGTTTGT ATTCATACAT AGACAATTTT CGTAATTTCC TTTGAAGTTC
TTAAATCCAA TGGTTAGATT ATTATGCTTA AATACTAAAA TAAAATATGA AATACTTTCT
TAAGTTAACT TTTAAATTCC GAACACAAAA ATGAACTTTA ATTAATTTTG AAACTATTAC
ATACACTGAC TAGAGAACAT ATATCCATTT TCTGTTCTTC TTCCCATCTT TGGTGGTTCC
CATTTGGGTG CTCTGTGTCC ACACAACGTG GAACATAATA CAAAATCAAG AACTAAATAA
   <<<<<<<<<<<<<<<<<<<<
ATATAAAGTG CTTTCACAAC ATTTGAACAA CGCAACAAGA AATGAACCTT AAAATGTGCG
TCCTTAAATA TTACAAAATA ATTCTATGAG TAAAATTGGG CAGCCATCGT TTCTCATTGA
GATCTCTGTG AGCTTATGGC AGGTGGATCG ATTCGAGAAT TGTATCTATA GCCTGAAATG
GTCACTCGGC GTAGAGCAGT CGTGAACGTG ATTTCCGGAG GCCGCGAGAG CCTCCACCGC
CGATTCCACT GTCTCCGCCC TCGCCACATT GCCAGGACTT GGTCTTGGCC CGAAAATATC
GAAACTCATC ATTGTGCGCC GGTGCCAGCA TTGGTACATA TTGGCTGGGC TGGCATAGCT
GCGAGTATAG ACCGAAGAAC TCCTTGTACC CATTGTGCAG GATATAAAGT TCAGGATAGT
                                                              >>
CCAGTGCCGG ATAGTTGTGG GTATGCTGAC TTCTGTCGTT GCTCCGCAGG TAGCGCAATA
>>>>>>>>>>>>>>>>>>>
GCTTGGGACC CCGTTCCGAG GAGAACTCAC AGTGGAAGAC GTAGATGCGT CGATTTTCCT
GATTGGAGGT CAGCGTGGGA AACGCCTCCT GTATCTGCCC ACGTGTGTAC AAATTCTTCG
               <<<<<<<<<<<<<<<<<<<<
CTCCCCGTAT GTGTCCGCCA AGGAACTCGT ATGGGTAACG GCAGTCTATG ATCTCGTATC
                                 >>>>>>>>>>>>>>>>>>>>
CGCCCTGGCT TCCCAATTGT TCATCAAACT CGCCCTGAAT CAGTCTGGCC AATGTGTCAC
TGGAGATGGT CTTTAGATCA CGATGTCTAA TGCCTGTCGC CAAACAGGGC AGGGTACATG
GCTTGCTGAG ATCTCCGATT AACTCTGGTT CATCTCCCAG TGCTCTCATG ATCTCGGCGT
CGTTCATTGA TAGAGTTTTC CGTTGCATCT TCTTCATGGG CATGTTGGTC TCCTGATCTG
GTTCTTGAAC CGCTTCCTCT GGCTGTTCAC TGGGATACAT GCTAAGGCAG CGACGCAGGG
AGCCTTTTTT GTTGGACATC TCCTCTAAAT TGCTTTCCGA TTTCAGCTGT CCGCTGAGGA
                                  <<<<<<<<<<<<<<<<<<<<
GCACTTCCAA GTCATCGGGC AACTCAAGAT TGTGATTCTC GGCTGATTCC ATTTCGAACA
TGTCCATGTA CTCATCATCC AGCGAGTTGC CCGACTCGTA ACTCGAGCAG GAGCTACTGA
AACTGCCGAG TGTTCGCGAG GACAGGCTAT TAAAGTTATT CAGGGTCCTG TTGGCTGGGA
TTCTCTGGGT GGACTTGGGA GTGCCATCCA GGCGGGCTCC ATTCATATTC TGCGACAATT
                                                        >>>>>>>>
CGGTGATGGG CGACAGAACG GTGGTGCTGG CAGGAATATG CCGCTTCAGC ATCCATTGCA
>>>>>>>>>>
GCGGAGTCTC CTGCACGGCT GATTTTCGCC TTTTGGCCTG GTATTCCATA TCGGCATCAT
GGGGATCGAA ATTCTCCTGA CCACACGCTC CACTTTCATC ATCTTCTTCC TCCACATCGA
                                    <<<<<<<<<<<<<<<<<<<
GCATTAGCCG CTTGCTCGCC ATCTGCGCGT TAAAAAGAAA AAAAACAATG ATTTTTTTAT
<<
CAGCTGGAAG CTGCTAAAAT CAGCTGGATT TTCGCAATTG TTCTTACCCT GATCTATTTG
CGATATACGT AACTATTGGG AAGTTCAGAT TTTGGGTTCC AGCGTGCGCA GTGATTTCGA
TTGCCAAATC CTTGACGATT TTCTTGTTCT GTCGACTTGT TTGTTTCGCT TTTGGCGGTC
AACTTTATTG GCGCCTTTAT CAATTCCCCA TTCTACCGAT GCAAACCCAC CACCTGCTAA
CTCACCACTG CGCCGTATTT AAACAGGACG CTCTAGTTTG AATTTAAATT GCTTGTATAT
          <<<<<<<<<<<<<<<<<<<<
```

```
TTTTTTGTTG GTATTTGCAT GGCTGGTTCAACCAACtttatttgacaaagagcaatgaaattg
aatttaaaaagcgcagccatcttaatgataacgtgttctaccaccataatatgcgatgaaatcaa
tatattttcaatcaataaatttgtactttaaatagttataagaaaaagatacatagaataatcgt
taatgagcgtaataaaataaaaacattccacaattataattatgaatcatatcatttttccagtg
gaaaatttgacaaaaacatattaacATTTATTACATCTGGTCACACTGTCCGTTTGTT-5'
                                <<<<<<<<<<<<<<<<<<<<
```

XXXXX FORWARD PRIMER

XXXXX REVERSE PRIMER

3.6 PROTEIN EXTRACTION OF MUTANT AND WILDTYPE TESTES

About 990 testes of either *71-43/71-43* or *71-43/CyO* young males (one day-old) were dissected in TIB and stored at -80°C until protein extraction. Tissues were homogenized in 100 mL of a lysis solution (7M urea, 2M thiourea, 4% CHAPS) and sonicated. After centrifugation at 14000 rpm for 10' at 4°C, the supernatant was recovered and further subjected to a centrifugation at 14000 rpm for 3' at 4°C. Protein extraction was stored at -20°C until 2D-electrophoresis.

3.7 BI-DIMENSIONAL ISOELECTROFOCUSING SDS-PAGE (2D-IEF-SDS-PAGE) OF MUTANT AND WILDTYPE TESTES

To remove lipids, proteins were precipitated from a desired volume of each sample with a cold mix of tri-n-butyl phosphate:acetone:methanol (1:12:1). After incubation at 4°C for 90 min, the precipitate was pelleted by centrifugation at 14000 x g, for 20 min at 4°C. After washing with the same solution, the pellet was air-dried and then solubilized in the focusing solution containing 7 M urea, 2 M thiourea, 4%, w/v CHAPS, 1 % w/v pH 3-10 carrier ampholyte, Tris 40 mM, 5 mM TBP, 10 mM acrylamide, 0.1 mM EDTA (PH 8.5). Before focusing, the sample was incubated in this solution for 3h at room temperature, under strong agitation. IEF was carried out on a 17 cm long IPG 3–10 (Multiphor II, GE Healthcare) with a maximum current setting of 50 µA/strip at 20° C. The total product time voltage applied was 85 000 V for each strip. For the second dimension, the IPG strips were equilibrated for 30 min in a solution containing 6 M urea, 2% w/v SDS, 20% v/v glycerol, 375 mM Tris-HCl (pH 8.8), with gentle agitation. The IPG strips were then laid on a 10.5–14% T gradient SDS-PAGE gel with 0.5% w/v agarose in the cathode buffer (192 mM glycine, 0.1% w/v SDS and Tris to pH 8.3). The anode buffer was 375 mM Tris-HCl, pH 8.8. The electrophoretic run was performed at a constant current (10 mA for 60 min, followed by 40 mA until the run was completed). The proteins were visualized using Blue silver (Candiano et al.,

2004). Two (*71-43/71-43* and *71-43/CyO*) technical replicates were performed for each sample for a total of 4 2D maps. There was good reproducibility between the technical replicates of each sample.

3.8 STATISTICAL ANALYSIS

Four stained gels were digitalized using an ImageScanner and LabScan software 3.01 (Bio-Rad Hercules, CA). The 2DE image analysis was carried out and spots were detected and quantified using the Progenesis SameSpots software v.2.0.2733.19819 software package. Each gel was analyzed for spot detection and background subtraction. Within-group comparison of protein spot numbers was determined by repeated measures analysis. Spots which were significantly different between groups (wildtype vs mutant) and not significantly different in the two technical replicate samples were identified by ESI-MS/MS.

3.9 PROTEIN IDENTIFICATION BY MS/MS

Protein spots were carefully excised from Blue silver stained gels and subjected to in-gel trypsin digestion according to Shevchenko and colleagues with minor modifications. The gel pieces were swollen in a digestion buffer containing 50 mM NH_4HCO_3 and 12.5 ng/µL of trypsin (modified porcine trypsin, sequencing grade, Promega, Madison, WI) in an ice bath. After 30 min the supernatant was removed and discarded, 20 µL of 50 mM NH_4HCO_3 were added to the gel pieces and digestion allowed to proceed at 37° C overnight. The supernatant containing tryptic peptides was dried by vacuum centrifugation. Prior to mass spectrometric analysis, the peptide mixtures were redissolved in 10 µL of 5% FA (Formic Acid).

Peptide mixtures were separated using a nanoflow-HPLC system (Ultimate; Switchos; Famos; LC Packings, Amsterdam, The Netherlands). A sample volume of 10 µL was loaded by the autosampler onto a homemade 2 cm fused silica precolumn (75 µm I.D.; 375 µm O.D.; Reprosil C18-AQ, 3 µm (Ammerbuch-Entringen, DE)) at a flow rate of 2 µL/min. Sequential elution of peptides was accomplished using a flow rate of 200 nL/min and a linear gradient from Solution A (2% acetonitrile; 0.1% formic acid) to 50% of Solution B (98% acetonitrile; 0.1% formic acid) in 40 minutes over the precolumn in-line with a homemade 10-15 cm resolving column (75 µm I.D.; 375 µm O.D.; Reprosil C18-AQ, 3 µm (Ammerbuch-Entringen, Germany)).

Peptides were eluted directly into a High Capacity ion Trap (model HCTplus, Bruker-Daltonik, Germany). Capillary voltage was 1.5-2 kV and a dry gas flow rate of 10 L/min was used with a temperature of 230 °C. The scan range used was from 300 to 1800 m/z. Protein identification was

performed by searching the National Center for Biotechnology Information non-redundant database (NCBInr, version 20081128, www.ncbi.nlm.nih.gov) using the Mascot program (in-house version 2.2, Matrix Science, London, UK). The following parameters were adopted for database searches: complete carbamidomethylation of cysteines and partial oxidation of methionines, peptide Mass Tolerance ± 1.2 Da, Fragment Mass Tolerance ± 0.9 Da, missed cleavages 2. For positive identification, the score of the result of (- 10 x Log(P)) had to be over the significance threshold level ($P < 0.05$).

Even though high MASCOT scores are obtained with values greater than 60, when proteins were identified with only one peptide a combination of automated database search and manual interpretation of peptide fragmentation spectra was used to validate protein assignments. In this manual verification, the mass error, the presence of fragment ion series, and the expected prevalence of C-terminus containing ions (Y-type) in the high mass range, were all taken into account. Moreover, replicate measurements have confirmed the identity of these protein hits.

4. RESULTS

STARTING POINT

The current research is focused on the analysis of a unique collection of 13 ethyl methanesulfonate (EMS)-induced male sterile recessive mutants (a generous gift of Barbara Wakimoto, Dept. of Biology, Washington University, Seattle), identified in a well known large screen for *Drosophila* male sterile mutations mapping to chromosomes 2 and 3 (the Zuker collection, Wakimoto et al., 2004). All these mutants are still uncharacterized. For identification, they have been denoted with a Z (Zuker) followed by number 2 or 3, to indicate the chromosome in which the mutation resides, a four digit number and a further "label" number, in parenthesis, which I will refer to all over the thesis (bold numbers): Z2-3162 (**12-228)**; Z2-5584 (**71-43**); Z2-4024 (**55-99**); Z2-4089 (**50-38**); Z2-1395 (**60-40**); Z2-0903 (**27-76**); Z2-1191 (**58-102**); Z2-0758 (**83-28**); Z2-2863 (**69-36**); Z2-1168 (**58-79**); Z2-2412 (**54-96**); Z3-2366 (**118-27**); Z2-2345 (**54-23**). Following a preliminary *in vivo* cytological characterization, the 12 mutations on chromosome 2 basically appeared to affect the meiotic cell cycle in males, evidenced by their incapability to accomplish one or both meiotic divisions, yet allowing an, although incomplete, spermatid differentiation. Since these strains showed meiotic defects that remind those of *twine* class, a complementation analysis among the so far known genes of this class (*twine, pelo, cdc2*, mapping on chromosome 2) and each of these mutations in transheterozygous condition was executed to investigate whether they are alleles of genes already characterized. In this analysis was used the *twine* allele, *tweHB5*, a loss-of-function mutation which causes homozygous males to skip both meiotic divisions. The results of the complementation analysis showed that only *twine* seems to interact with some mutations on chromosome 2. More specifically, the strains: *50-38, 54-23, 60-40, 12-228, 83-28* failed to complement *twine*, while the other mutations on chromosome 2 did complement *twine* (Tab.1).

Since *Z*-mutants originate from heavily mutagenized lines and their phenotype strongly reminds that of *twine*, I followed two approaches in order to genetically characterize these *twine* non-complementing lines: i) gene mapping and "cleaning" of mutated chromosome to verify the potential presence of second-site mutations; and ii) sequencing of *twine* in each of these lines. Then, a cytological analysis has been conducted on some of the 12 mutations on chromosome 2 in order to pinpoint the function of the gene involved and, eventually, to identify the gene affected by the mutation under examination.

	twine	*60-40*	*50-38*	*54-23*	*12-228*	*55-99*	*71-43*	*83-28*	*27-76*	*69-36*	*54-96*	*58-79*	*58-102*
twine	-	-	-	-	-	+	+	-	+	+	+	+	+

Tab. 1 Complementation analysis among *Z*-mutations and *twine*.

4.1 *12-228; 50-38; 60-40; 54-23; 55-99; 27-76* CHARACTERIZATION

4.1.1 MAPPING RESULTS

The first approach to identify the genes affected by the mutations responsible for male sterile phenotype consisted in the recombination mapping. In order to get information about the localization of mutations on chromosome 2, I took advantage of strains with chromosome 2 bearing multiple recessive markers. The scheme of crosses used to get recombinants is shown below.

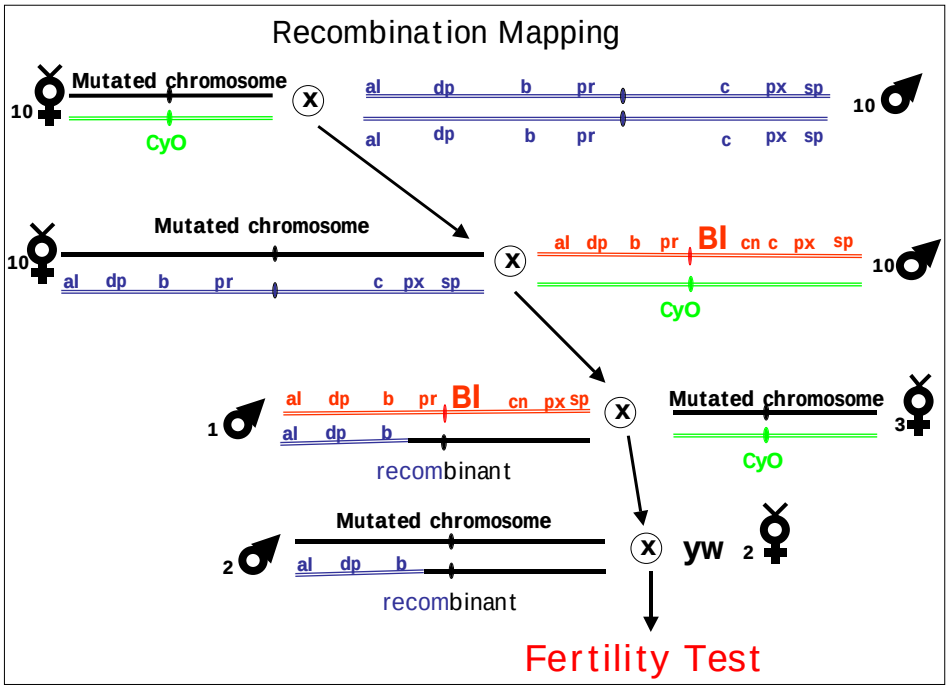

Scheme of crosses used for recombination mapping. (as example, only one among all the possible recombinants is indicated)

The resolution of a recombination-based mapping approach depends on the availability of markers, on the ease with which they can be scored, and on the number of recombinant chromosomes that can be scored. From the second cross, I recovered about 50 recombinants per each locus, which is considered enough to get a rather precise map. The map position of each mutation will be deduced

by the persistence of the male sterile phenotype on the recombinant chromosomes (to be scored in the 4th cross progeny), together with its genotype in terms of recessive markers, as deduced by the phenotype of the 2nd cross progeny. The map positions I got for the analyzed mutations are: 74.3 m.u. (*12-228*), 49-51 m.u. (*50-38*), 46-50 m.u. (*60-40*), 45-50 m.u. (*54-23*), 56.3 m.u. (*55-99*) and 82-89 m.u. (*27-76*). A diagram of the map positions of the just mentioned mutations is shown in Fig.1. The localization of *twine* gene on second chromosome is also displayed, in order to put in evidence which of the mutations under examination might be the potential *twine* alleles.

Two strategies were carried out to discern whether mutations mapping to the *twine* region were actual *twine* alleles: i) "chromosome cleaning" and ii) *twine* sequencing. The latter method will be further dealt with, in the paragraph 4.1.2. Both approaches were executed in *12-228* strain as well, because, even if it maps far away from *twine* gene, yet, it failed to complement *twine*. Cleaning of the chromosome ("clean" means that the original mutant chromosome retained only the region where the mutation lies, whereas the rest of the chromosome was entirely derived from the marker chromosome) was carried out by recombination with a chromosome bearing visible phenotypic markers useful to verify the effective formation of recombinants.

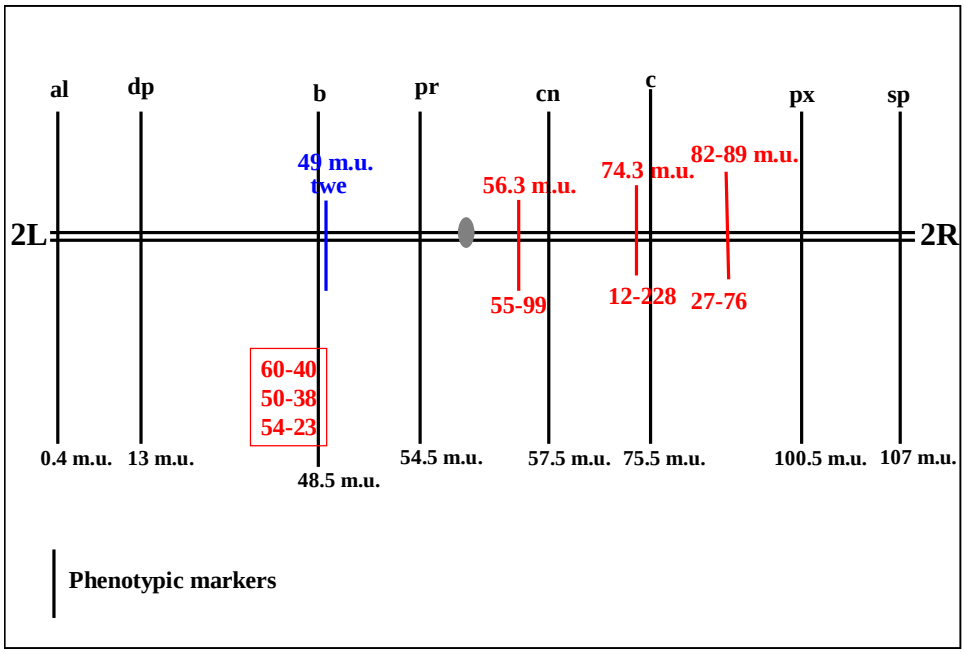

Fig.1 Diagram of map positions of mutations *60-40, 50-38, 54-23, 55-99, 12-228* and *27-76* (red bars) on chromosome 2. Map position of *twine* gene (blue bar) is also shown. Phenotypic markers are indicated in black.

To this aim, I availed of strains bearing the 2nd chromosome with different markers from those used to get the recombination map. Once I got the recombinants, I checked whether they were in fact "clean" mutant chromosomes by looking if the recombinant chromosome in heterozygosity with the original mutant chromosome retained both sterile and meiotic phenotypes. This was accomplished by testing recombinant males for fertility and looking at the *in vivo* cytology of their testes. The outcomes were the following: the clean strains *60-40*, *54-23* and *12-228* retained sterile phenotype but they lost meiotic phenotype, suggesting the presence in the original mutant chromosome of a second mutation, contributing to the meiotic phenotype, which is lost in the clean chromosome. On the other hand, the clean strain *50-38* retained both sterile and meiotic phenotype. As I mentioned before, these data was integrated by *twine* sequencing outcomes (see below).
Fertility in females was also investigated to get information on the sex-specificity of the tested mutation. An easy scheme of crosses was set up, eventually obtaining the virgin female homozygotes for *55-99* locus, while, in the case of clean chromosomes *12-228*, *60-40*, *50-38* and *54-23*, these were tested in heterozygous combination with their original mutated homologs. Females bearing *55-99* mutation, and females bearing clean chromosomes *12-228* and *60-40* resulted fertile; females with clean chromosome *50-38* resulted sterile whereas females with clean chromosome *54-23* showed reduced fertility (progeny < 10 flies).

4.1.2 SEQUENCING OF *twine* IN NON-COMPLEMENTING MUTANTS: *12-228; 60-40; 50-38; 54-23*

As I said above, I exploited two strategies to characterize *50-38, 54-23, 60-40* and *12-228* mutations which failed to complement *twine*, in order to see whether the first three mutations, which map close to *twine*, were *twine* alleles and whether *12-228*, which instead maps to the right arm of chromosome 2, had a second mutation in *twine* gene that accounts for the non-complementation with *twine*. The first approach was the already described cleaning of the mutated chromosome from *twine* region, while the second was based on the sequencing of *twine* gene in the genome of these mutants. According to Maines and Wasserman (1999), a 3.7-kilobase genomic region that fully rescues the loss-of-function twe^{HB5} mutant defines the *twine* gene and its regulatory regions. They also found in the mutant twe^{Z0758} a point mutation, 418 base pairs upstream of the open reading frame, thus locating a potential transcriptional regulatory element, responsible for the hypomorphic phenotype, consisting of the ability of undergoing only one meiotic division. Hence, I focused the sequencing work on 2460 bp, spanning from the first bases of the CG4935, which is the gene next

to *twine* at 5' to the 3'-UTR (Fig. 2). This interval encompasses the regulatory region at 5' identified by Maines and Wasserman (1999).

Sequencing of PCR products that overall cover the entire sequence interval of 2460 bp, pointed out the presence of mutations in the *twine* coding region in *54-23, 60-40* and *12-228* mutants whereas *50-38* strain did not exhibit any variation in *twine* sequence. More specifically, in *60-40* strain there was a non-conservative missense mutation (C-T) in the *twine* ORF, giving rise to an aminoacidic transition from Glycine (Gly) to Arginine (Arg). In *54-23* strain, the point mutation in *twine* open reading frame (G-A) determined a transition from Proline (Pro) to Serine (Ser), whereas in *12-228* mutants two mutations in *twine* ORF were found: (A-T) causing the change from Histidine (His) to Glutamine (Gln) and (G-A) responsible for the transition from Arginine (Arg) to a stop codon (Fig. 3).

Fig. 2 Sequenced *twine* region.

Legend:

XXX…XXX: *twine* gene (2460 bp) XXXXXXX: *twine* ORF XXXXXXX: 3’- UTR

XXXXXXX: 5’- UTR xxxxxxxxxx: intron xxxxxxxxxx: 5’ regulatory region

c: point mutation in *twe*^{Z0758} mutant XXXXXXX: CG4935

3′-TGCATCTTTC
ATGACTGAAGGATTGTTTCCTTATGTACTAAAACACCTATTCTGGTCGTAATCTCTGAAG
GCACACACAGTAAAGCATTTCAATATCTGAATTATGTTTCGAAATGTTAGAAATTGTTTA
AAAATGAATAAAATGATAAGTATTTTATAACTGTTCTCAAAAATAGTGGTCCTTTTTATT
ATCTCGATCAGTAACAAATTATTTGTTCTCTTCATATTTCTTCAATAGCTTAAAGCATTT
AAAATTTTGTAATATATATAAACTATAATAGCATATAAATTAAGGAACATTTTTCTTCAT
TTGATTTAAAATTTGTATCACGAATTTTCTTGAAATATTTTATGAGTATTCTTACATCTC
CTGTTCTAATTAAGCATTATGCATCCTAAAACTTTTAAATTGTGTATTAAATGATTGTTT
TTAGATACTTTTAATAAAAGTTGACCGATGTAGGTGGAATCCACATAAATAGTTTCAGCA
TAGTTTGTATTCATACATAGACAATTTTCGTAATTTCCTTTGAAGTTCTTAAATCCAATG
GTTAGATTATTATGCTTAAATACTAAAATAAAATATGAAATACTTTCTTAAGTTAACTTT
TAAATTCCGAACACAAAAATGAACTTTAATTAATTTTGAAACTATTACATACACTGACTA
GAGAACATATATCCATTTTCTGTTCTTCTTCCCATCTTTGGTGGTTCCCATTTGGGTGCT
CTGTGTCCACACAACGTGGAACATAATACAAAATCAAGAACTAAATAAATATAAAGTGCT
TTCACAACATTTGAACAACGCAACAAGAAATGAACCTTAAAATGTGCGTCCTTAAATATT
ACAAAATAATTCTATGAGTAAAATTGGGCAGCCATCGTTTCTCATTGAGATCTCTGTGAG
CTTATGGCAGGTGGATCGATTCGAGAATTGTATCTATAGCCTGAAATGGTCACTCGGCGT
AGAGCAGTCGTGAACGTGATTTCCGGAGGCCGCGAGAGCCTCCACCGCCGATTCCACTGT
CTCCGCCCTCGCCACATTGCCAGGACTTGGTCTTGGCCCGAAAATATCGAAACTCATCAT
TGTGCGCCGGTGCCAGCATTGGTACATATTGGCTGGGCTGGCATAGCTGCGAGTATAGAC
CGAAGAACTCCTTGTACCCATTGTGCAGGATATAAAGTTCAGGATAGTCCAGTGCCGGAT
AGTTGTGGGTATGCTGACTTCTGTCGTTGCTCCGCAGGTAGCGCAATAGCTTGGGACCCC
GTTCCGAGGAGAACTCACAGTGGAAGACGTAGATGCGTCGATTTTCCTGATTGGAGGTCA
GCGTGGGAAACGCCTCCTGTATCTGCCCACGTGTGTACAAATTCTTCGCTCCCCGTATGT
GTCCGCCAAGGAACTCGTATGGGTAACGGCAGTCTATGATCTCGTATCCGCCCTGGCTTC
CCAATTGTTCATCAAACTCGCCCTGAATCAGTCTGGCCAATGTGTCACTGGAGATGGTCT
TTAGATCACGATGTCTAATGCCTGTCGCCAAACAGGGCAGGGTACATGGCTTGCTGAGAT
CTCCGATTAACTCTGGTTCATCTCCCAGTGCTCTCATGATCTCGGCGTCGTTCATTGATA
GAGTTTTCCGTTGCATCTTCTTCATGGGCATGTTGGTCTCCTGATCTGGTTCTTGAACCG
CTTCCTCTGGCTGTTCACTGGGATACATGCTAAGGCAGCGACGCAGGGAGCCTTTTTTGT
TGGACATCTCCTCTAAATTGCTTTCCGATTTCAGCTGTCCGCTGAGGAGCACTTCCAAGT
CATCGGGCAACTCAAGATTGTGATTCTCGGCTGATTCCATTTCGAACATGTCCATGTACT
CATCATCCAGCGAGTTGCCCGACTCGTAACTCGAGCAGGAGCTACTGAAACTGCCGAGTG
TTCGCGAGGACAGGCTATTAAAGTTATTCAGGGTCCTGTTGGCTGGGATTCTCTGGGTGG
ACTTGGGAGTGCCATCCAGGCGGGCTCCATTCATATTCTGCGACAATTCGGTGATGGGCG
ACAGAACGGTGGTGCTGGCAGGAATATGCCGCTTCAGCATCCATTGCAGCGGAGTCTCCT
GCACGGCTGATTTTCGCCTTTTGGCCTGGTATTCCATATCGGCATCATGGGGATCGAAAT
TCTCCTGACCACACGCTCCACTTTCATCATCTTCTTCCTCCACATCGAGCATTAGCCGCT
TGCTCGCCATctgcgcgttaaaaagaaaaaaaacaatgatttttttatcagctggaagct
gctaaaatcagctggattttcgcaattgttcttacCCTGATCTATTTGCGATATACGTAA
CTATTGGGAAGTTCAGATTTTGGGTTCCAGCGTGCGCAGTGATTTCGATTGCCAAATCCT
TGACGATTTTCTTGTTCTGTCGACTTGTTTGTTTCGCTTTTGGCGGTCAACTTTATTGGC
GCCTTTATCAATTCCCCATTCTACCGATGCAAACCCACCACCTGCTAACTCACCACTG**CG**
CCGTATTTAAACAGGACGCTCTAGTTTGAATTTAAATTGCTTGTATATTTTTTTGTTGGT
ATTTGCATGGCTGGTTCAACtttatttgacaaagagcaatgaaattgaatttaaaaagcg
cagccatcttaatgataacgtgttctaccaccataatatgcgatgaaatcaatatatttt
caatcaataaatttgtactttaaatagttataagaaaaagatacatagaataatcgttaa
tgagcgtaataaaataaaacattccacaattataattatgaatcatatcatttttccag
tggaaaatttgacaaaaacatattaacATTTATTACATCTGGTCACACTGTCCGTTTGT-5′

Fig. 3 Sequenced *twine* region and mutations in *twe* ORF found in *12-228*, *60-40* and *54-23* strains.

Legend:

XXXXXXX: *twine* ORF

G A: mutated bases in *12-228* strain

C: mutated base in *60-40* strain

G: mutated base in *54-23* strain

4.2 *71-43* CHARACTERIZATION

4.2.1 RECOMBINATION MAPPING AND CHROMOSOME CLEANING

71-43 is the mutant strain I characterized more in depth in the present study. Meiotic recombination mapping was performed taking advantages of the same previously mentioned strains, bearing visible phenotypic recessive markers. By these means I mapped *71-43* mutation around 96.2 m.u, to the left of *plexus* (*px*, 100.5 m.u.) (Fig. 4). The accuracy resides on the number of recombinants scored, more than 100.

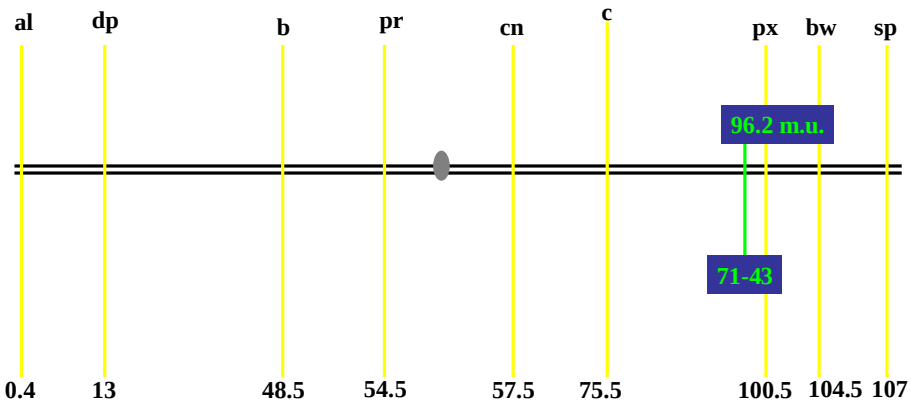

Fig. 4 Graphic illustration of chromosome 2, showing all phenotypic recessive markers used to map *71-43* mutation and the map position of such a mutation, which is around 96.2 m.u. Numbers under markers indicate map units.

Meiotic recombination mapping was also useful to clean chromosome 2, in order to get a recombinant bearing only the region where *71-43* lies deriving from the original mutant chromosome, while the rest of chromosome belongs to marker chromosome (Fig. 5). Once I recovered such a recombinant, it was tested in homozygous combination for male fertility and cytological meiotic phenotype (images are shown in the section of cytological results), showing preservation of both male sterility and the same mutant cytological phenotype as the original *71-43* strain. On the other hand, male homozygotes for the reciprocal recombinant (Fig. 5) were fertile and underwent a normal spermatogenesis.

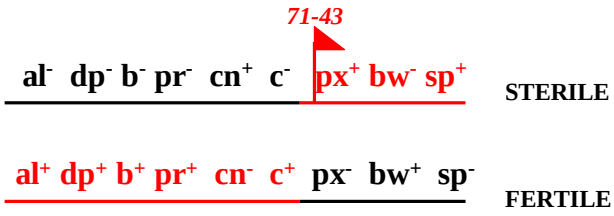

Fig. 5 Clean *71-43* chromosome and its reciprocal, obtained by meiotic recombination.

Clean *71-43* sterile recombinant is displayed above. The part of chromosome 2 derived from marker chromosome is shown in black, whereas the region coming from the original *71-43* chromosome is in red. Flag points out the position of *71-43* mutation on the recombinant. Below is shown the reciprocal recombinant which is fertile in homozygosity.

Hence, cleaning of chromosome 2 provided evidence that only one mutation, mapped to the left of *px*, is responsible for male sterile phenotype in *71-43* flies.

4.2.2 DEFICIENCY MAPPING

The reliability of recombination mapping data was further proved by deficiency mapping findings. First, I screened, by complementation, throughout the chromosome 2 by means of 133 chromosomal deficiencies, belonging to Chromosome 2 Deficiencies Kit and covering 95% of the euchromatin on chromosome 2. These deletions were tested in hemizygous combination with *71-43* mutation in order to check fertility in males having this genetic background. I found that 4 Dfs failed to complement the *71-43* male sterile phenotype: **6507** (23F3-4; 24A1-2), **3813** (25A5; 25E5), **1547** (55A; 55F) and **5246** (57D2-8; 58D1). Through the conversion from map units to cytological bands and viceversa available on Flybase website, I found that the Df 5246 uncovered interval corresponding to that established by recombination analysis. Next step consisted of narrowing down, as much as possible, this region on chromosome 2, testing by complementation sub-deficiencies covering almost entirely the Df 5246, available at Bloomington Stock Center. Tested sub-deficiencies are shown in the Fig. 6.

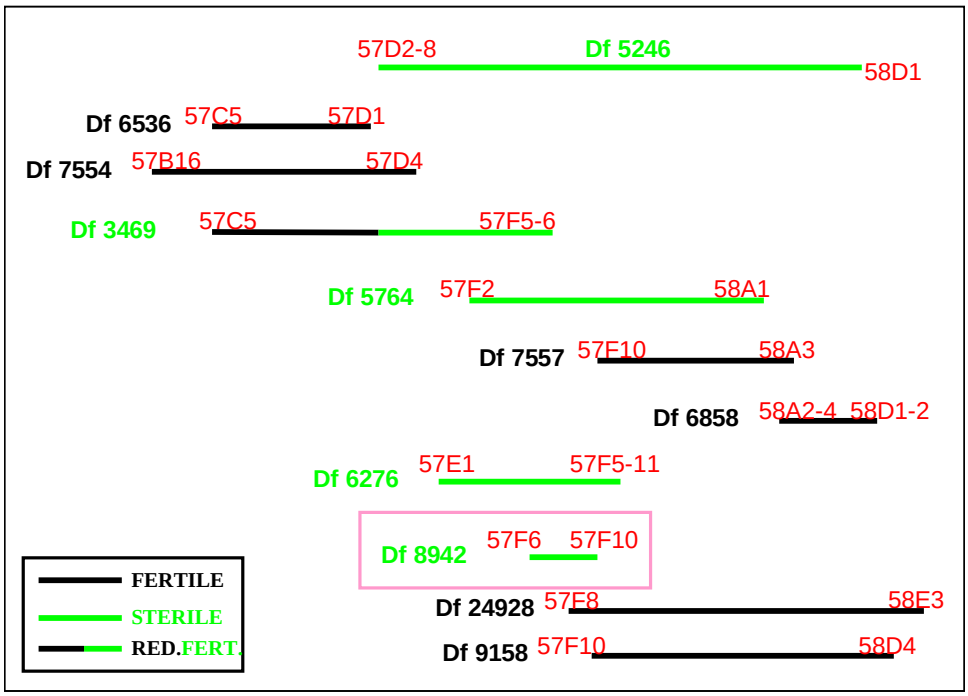

Fig. 6 Schematic representation of the sub-deficiencies tested for complementation against the *71-43* chromosome. Dfs giving fertility are depicted by black bars, whereas those giving sterility by green bars. Df 3469, that gave reduced fertility, is shown as a middle black and middle green bar. Cytological boundaries of each Df are indicated in red. The smallest deletion, commercially available, uncovering *71-43* mutation, is in the pink box.

The smallest deletion uncovering *71-43* mutation was Df 8942 (57F6; 57F10), whose cytological interval corresponds to 96 m.u., thus confirming map position obtained by meiotic recombination. Besides, testing Df 24928 (57F8; 58E3) I could further narrow down the right limit of the region identified by Df 8942. Thus, the *71-43* locus must reside in a chromosome 2 region of 40952 bp, whose sequence coordinates, according to Release R5, run from 17534119 bp to 17575071 bp. In this area are embedded several genes. Their localization in the region is shown in the Fig. 7.

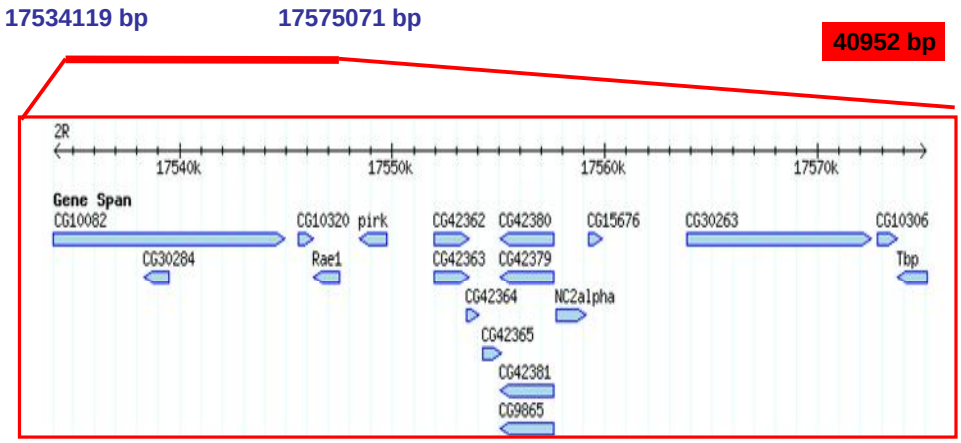

Fig. 7 Region of chromosome 2, spanning from 17534119 bp to 17575071 bp, and genes mapped to the sequence embedded in. Sequence R5. (Image from FlyBase)

4.2.3 CYTOLOGICAL CHARACTERIZATION

Looking at the *in vivo* whole testis of *71-43* mutants, in comparison with *wildtype* testis (Fig. 8), the most evident difference was the strongly reduced number of sperm bundles, which in *wildtype* testis fill up the structure throughout its length. A more detailed *in vivo* cytological characterization, then, pointed out to early defects, in young primary spermatocytes of *71-43* homozygotes. Interestingly, this mutant phenotype was also confirmed in the hemizygotes *71-43* over Df (*71-43/Df 8942*), which is the smallest *71-43* non-complementing deficiency I found. More specifically, such defects consisted in the presence of nuclear membrane evaginations, resembling hernias (Fig. 9, upper panel, arrows). As regards the male germ cells development, *71-43* homozygotes and hemizygotes *71-43/Df 8942*, showed an impaired meiotic cell cycle, as evidenced by the presence at onion stage of variable sized nuclei and Nebenkernes (Nebs), that also exhibited an irregular shape, in addition to the presence of cells exhibiting only Neb but lacking in nucleus (Fig. 9, middle panel). In *71-43* homozygotes as well as hemizygotes, spermiogenesis too exhibited striking defects, particularly apparent in early elongating sperm bundles. At this stage, from a comparison with *wildtype* bundles, it emerged the presence of cyst polarization defects and of large round nuclei, an evidence of

nuclear shaping impairment (Fig.9 lower panel). Moreover, nuclei were dispersed all over the bundle (Fig. 9, lower panel, arrows).

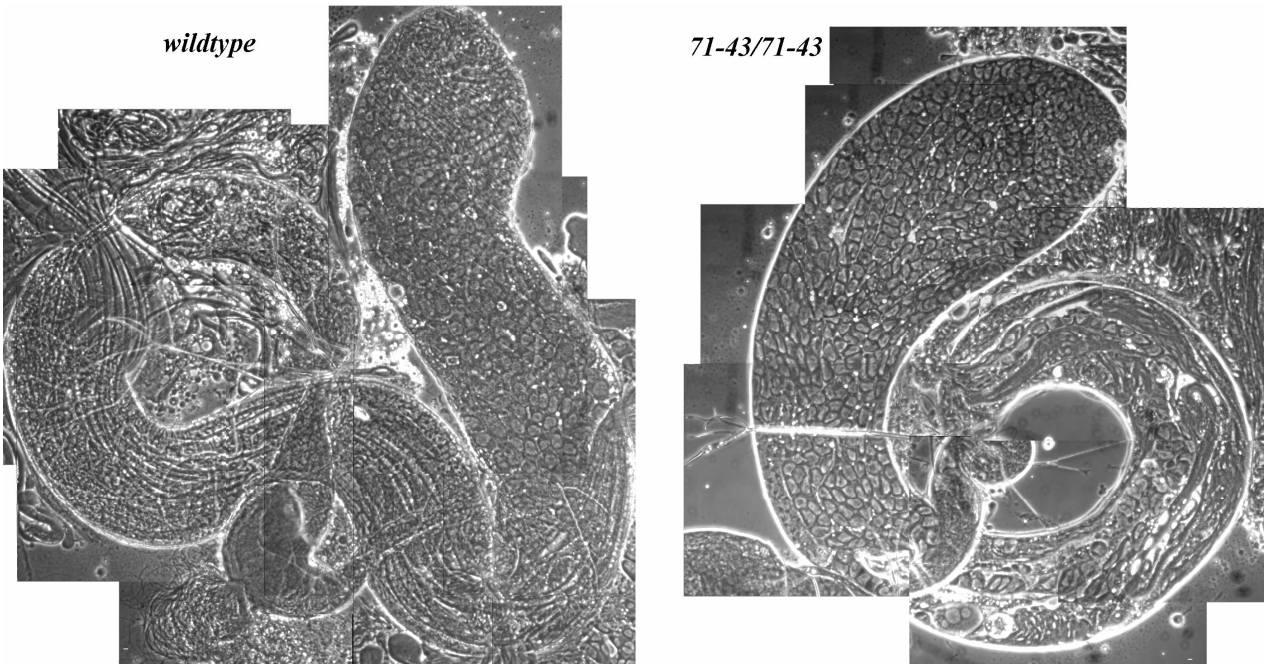

Fig. 8 *In vivo* whole testis. Phase contrast images. From left to right: *wildtype* and *71-43/71-43* testes. Note the highly reduced number of long sperm bundles in *71-43* mutant testis in comparison with *wildtype* testis, where long tails of sperm bundles fill up testis all over its length. Scale bar: 10 μm.

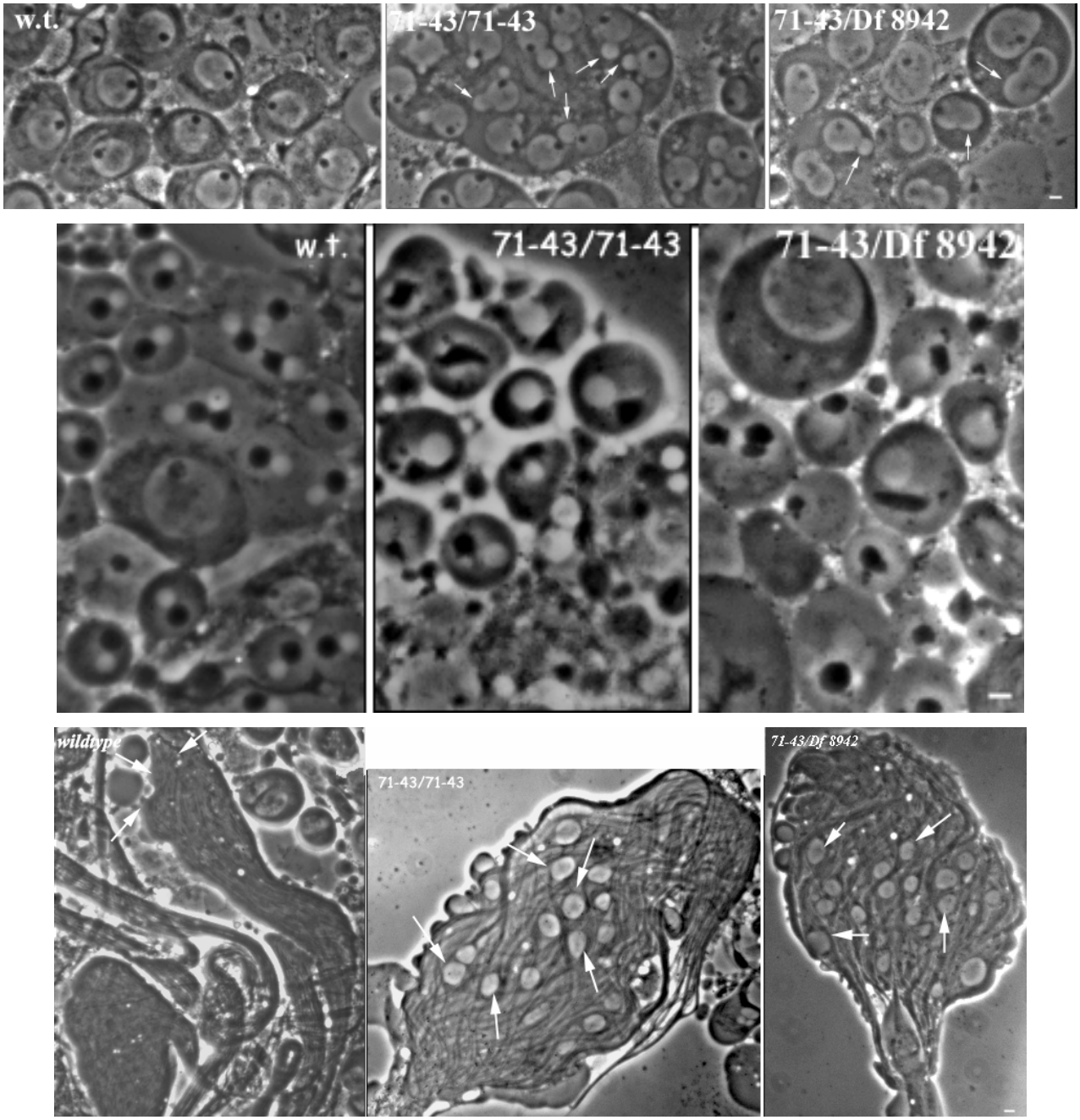

Fig. 9 *In vivo* cytological analysis by phase contrast microscopy.

Upper panel: young primary spermatocytes, showing herniations leaving from nuclear membrane of *71-43/71-43* and *71-43/Df 8942* spermatocytes. Arrows point out the hernias.

Middle panel: onion stage spermatids. Note variable sized nuclei (white spheres) and Nebs (black spheres) in *71-43/71-43* and *71-43/Df 8942* spermatids.

Lower panel: early elongating sperm bundles. Look at the large round nuclei (arrows), spread out throughout the bundle in *71-43/71-43* and *71-43/Df 8942* mutants. Arrows in *wildtype* image indicate the end of the bundle where all the nuclei are grouped. In all panels, from left to right: *wildype, 71-43/71-43, 71-43/Df 8942.*

Scale bars represent 10 μm.

As already mentioned in 4.2.1, I recovered the recombinant *71-43* chromosome (*Rec#57*), that retained only the region where the mutation maps while replacing all the remaining of the original

71-43 mutated 2nd chromosome. This "cleaned" *71-43* chromosome was analyzed by *in vivo* cytology in homozygous condition (*Rec#57/Rec#57*) and over *71-43* original chromosome (*Rec#57/71-43*), in order to verify the presence of the same defects as *71-43* homozygotes displayed. A comparison among onion stage spermatids of *71-43* homozygotes, *71-43* over *Rec#57*, *Rec#57* homozygotes and *71-43* over the non complementing *Df 8942* hemizygotes, showed a marked phenotypic similarity among all these genotypes (Fig. 10). The correspondence of the mutant phenotype was also valid seen in young primary spermatocytes as well as early elongating sperm bundles (not shown).

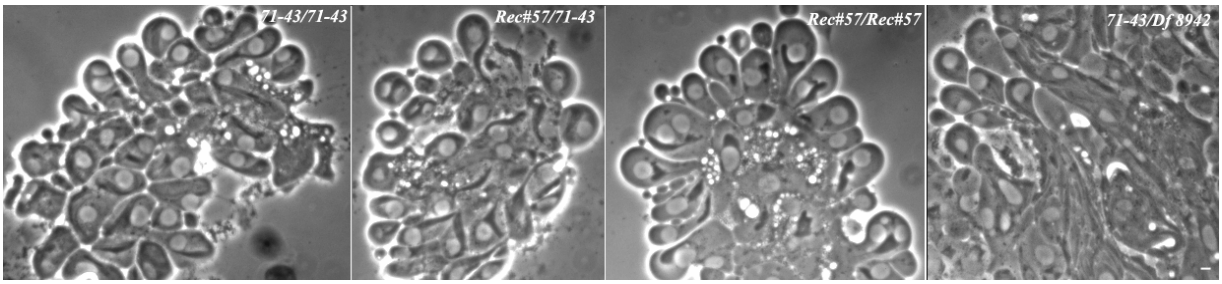

Fig. 10 *In vivo* cytological analysis by phase contrast microscopy. Onion stage spermatids.
From left to right*: 71-43/71-43*, *Rec#57/71-43*, *Rec#57/Rec#57* and *71-43/Df 8942* mutants. Note the similarity of phenotype of all different genotypes. Scale bar represents 10 μm.

A statistical analysis, aimed to detect the presence of 16 primary spermatocytes-, 32 secondary spermatocytes- and 64 spermatids- cysts in *71-43* homozygotes, was performed in parallel with *wildtype* and *twine* mutants (Fig. 11). Besides the absence of either 32 cell- or 64 cell- cysts in *71-43* mutants, as proof of failure of accomplishing both first and second meiotic division (same behaviour as *twine* mutants), the most relevant finding obtained by this kind of investigation, was the unexpected presence of cysts with a number of nuclei ranging from 16 to 32.
In order to reveal the stage at which meiotic cell cycle arrests in these mutants a statistical analysis was performed, focused to assess the relative abundance of specific meiotic stages. I counted more than 100 cysts per genotype (*wildtype*, *71-43* and *twine* homozygotes), and I found that, despite a fully and/or partial meiotic failure, both *twine* and *71-43* mutants, presented onion stage cysts, in a statistical significant higher number than that of wildtype (Fig. 12).

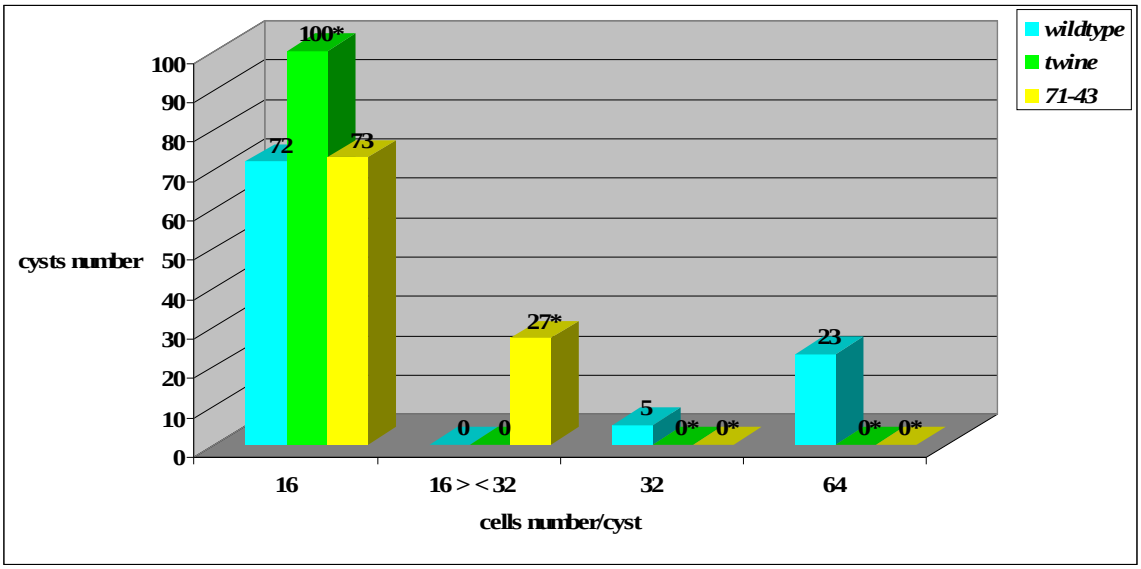

Fig. 11 Bar chart showing cysts comparison among *wildtype*, *71-43* and *twine* homozygotes.
On the x axis, the cells number per cyst is displayed whereas, on the z axis, the cysts number is indicated. *Wildtype* is in blue, *twine* in green and *71-43* in yellow. The asterisks point out statistically significant data. Note the unexpected presence of cysts between 16 and 32 cells in *71-43* mutants.

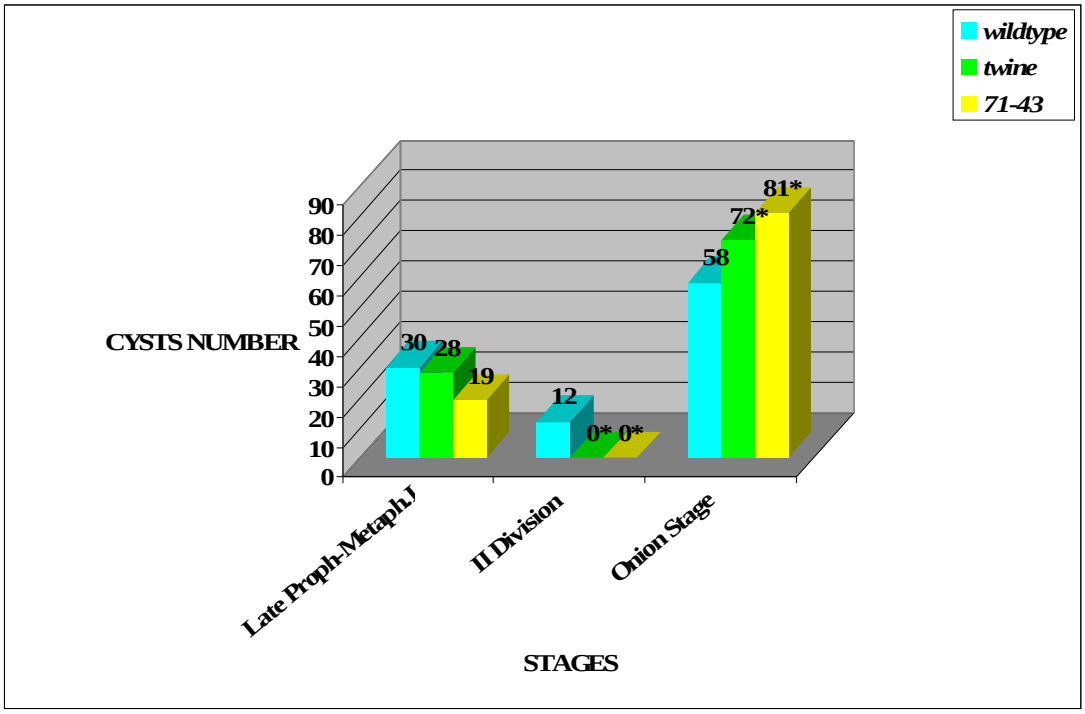

Fig. 12 Bar chart showing stages comparison among *wildtype*, *71-43* and *twine* homozygotes.
On the x axis, different stages are displayed –late prophase-metaphase, II division, onion stage- whereas, on the z axis, the cysts number is shown. *Wildtype* is in blue, *twine* in green and *71-43* in yellow. The asterisks point out statistical significant data.

Once proved that homozygotes for clean *71-43* chromosome retained the same mutant phenotype as *71-43* homozygotes, the immunofluorescence experiments were executed on fixed preparations of

71-43/71-43 mutant males, aimed to assess which specific aspects of meiosis and spermatogenesis are impaired, and, eventually, to gain insight on the molecular function of the mutated gene.
As before mentioned, the earliest spermatogenesis defect I observed in *71-43* homozygotes, was the presence of nuclear herniations in primary spermatocytes, well visible by phase contrast optics (arrows in Figs. 9, upper panel, and 13, leftmost image). In order to investigate the nature of such nuclear evaginations and whether they housed DNA, I immunostained fixed preparations of *71-43* mutant testes by Ab anti-lamin, to look at nuclear envelope, and then the slides were coloured by DAPI to visualize DNA. Nuclear lamin was always detectable around the hernias, which, in most cases, contained DNA (Fig. 13).

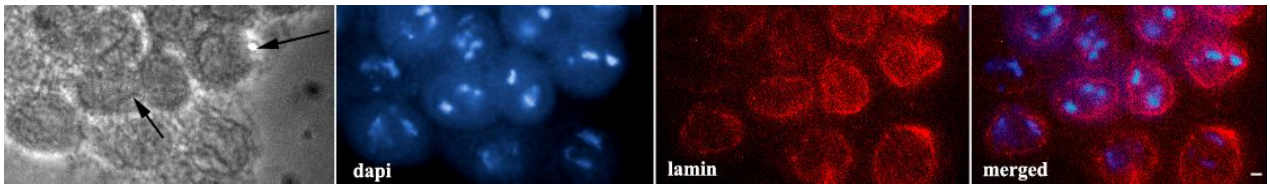

Fig. 13 *71-43/71-43* primary spermatocytes stained with DAPI and antibody directed to lamin, in order to visualize nuclear hernias. From left to right: phase contrast image, DAPI staining (blue), immunofluorescence by anti-lamin Dm0 Ab (red) and merged image. Arrows point out primary spermatocytes displaying hernia. Note the presence of nuclear lamin around such hernias and DNA in them. Scale bar: 10 μm.

DAPI staining, also, allowed to notice chromatin condensation defects starting from primary spermatocytes throughout prometaphase stage, where they become strongly evident. At this stage, three pairs of homologs and the pair of dot-like fourth chromosomes are recognizable as condensed chromatin clumps in *wildtype* cells (Fig. 14, left). In *71-43* primary spermatocytes, instead, distinct chromatin clumps were difficultly visible, owing to an impaired chromatin condensation, resulting into decondensed state (Fig. 14, right).

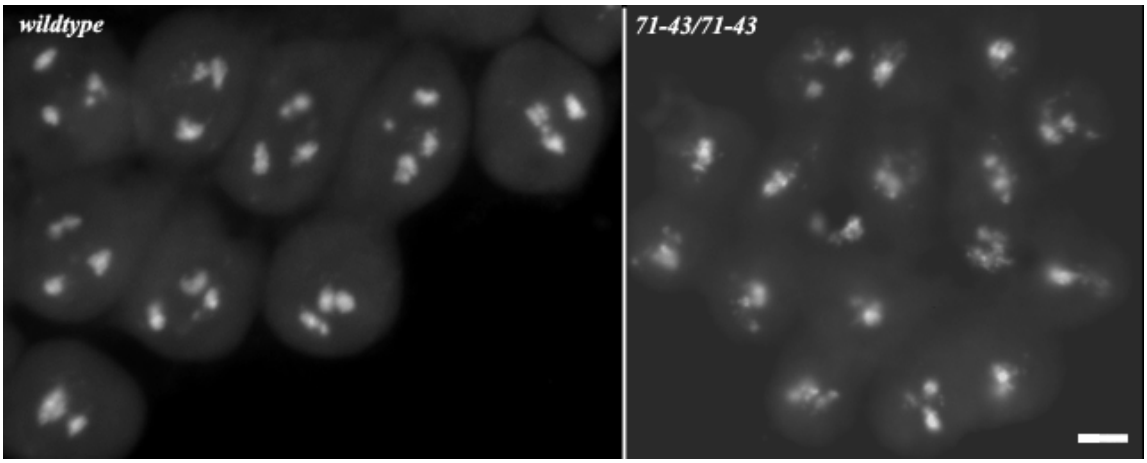

Fig. 14 Primary spermatocytes at prometaphase stage. DAPI staining to look at chromatin conformation and spatial distribution. Note the chromatin organization in three clumps and a dot, representing the pair of fourth chromosomes not always visible, in *wildtype* spermatocytes, differently from what is observable in *71-43* mutant spermatocytes, where diffuse chromatin makes impossible discern the three chromatin masses. Scale bar represents 10 μm.

Going on spermatogenesis process, meiotic division defects became apparent, which are likely responsible for the meiotic arrest occurring in these mutants. Abnormal metaphase plates showing chromosomes misalignment were frequent as well as irregular chromosomes migration to the opposite poles of cell (Fig. 15, **c**, **d**. Compare with *wildtype* image, **b**).

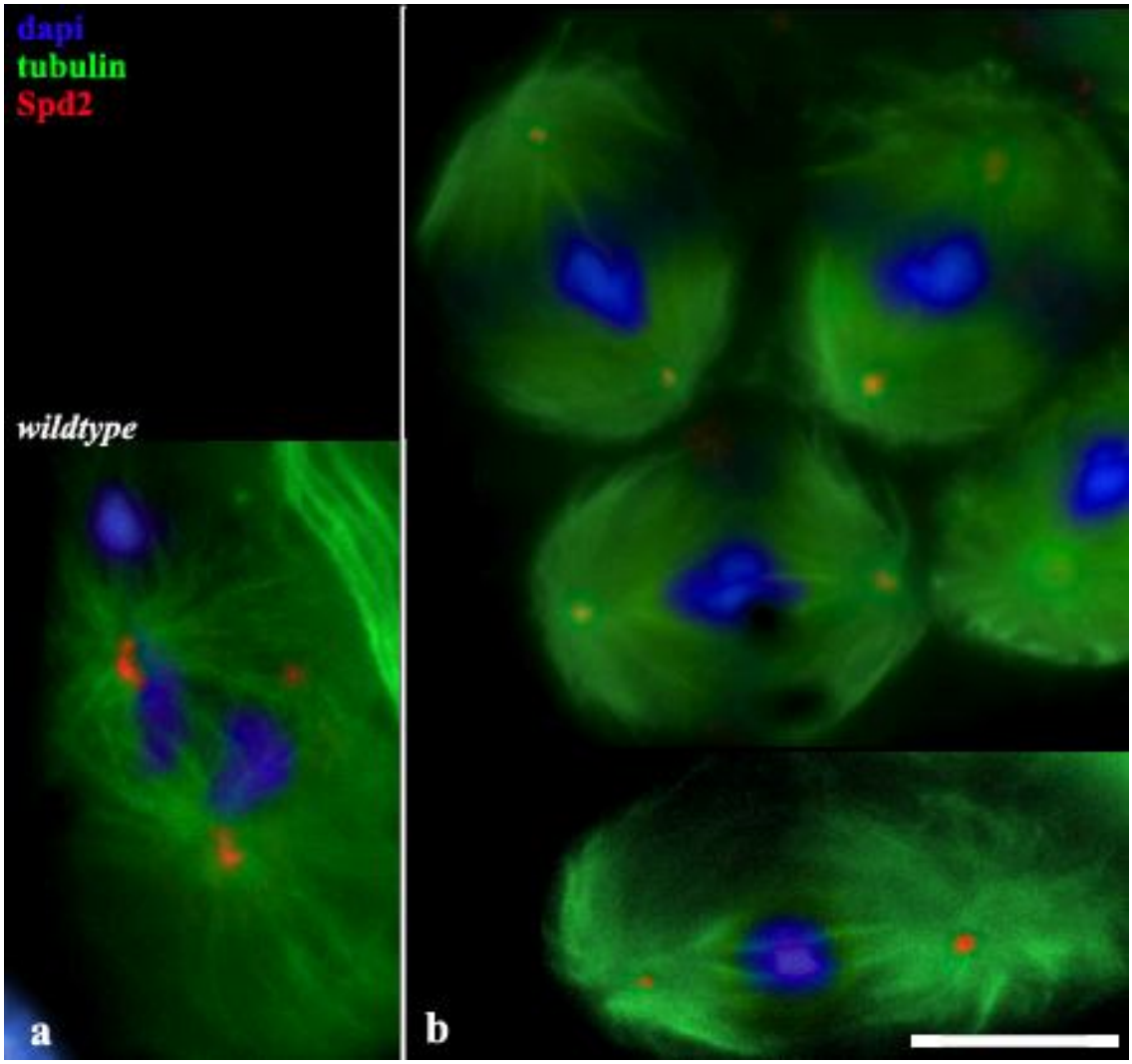
dapi
tubulin
Spd2
wildtype
a
b

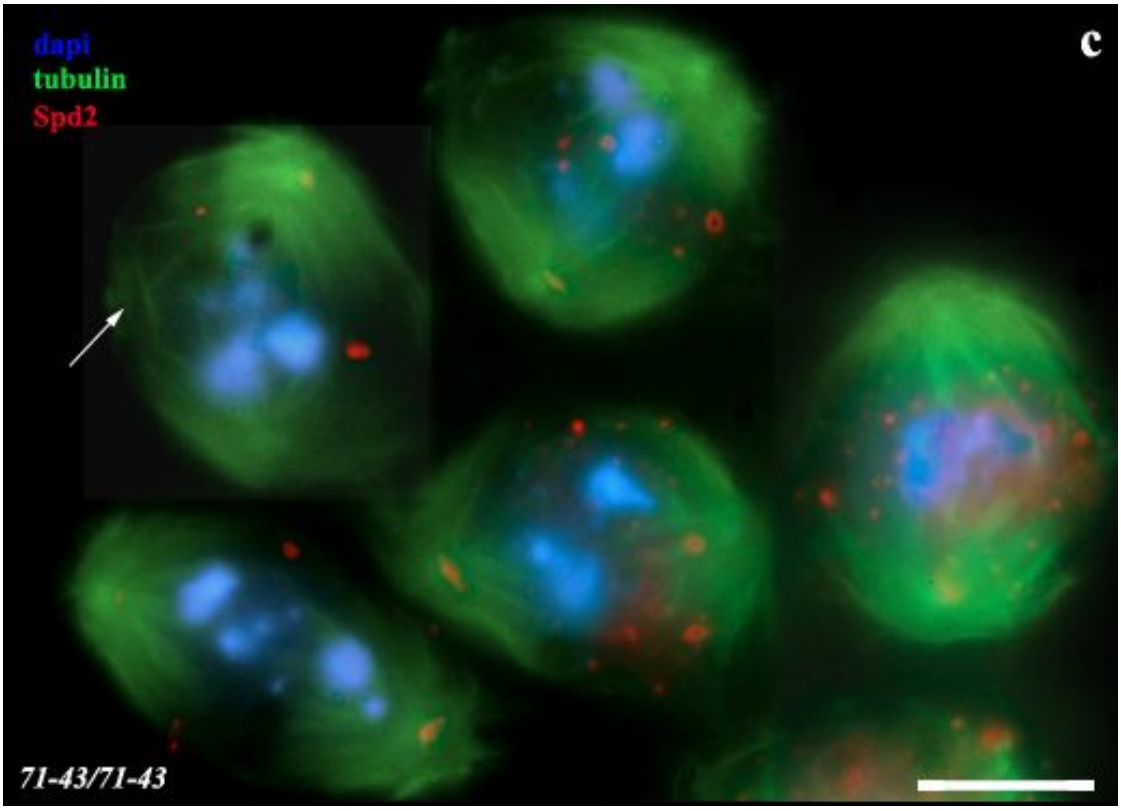
dapi
tubulin
Spd2
c
71-43/71-43

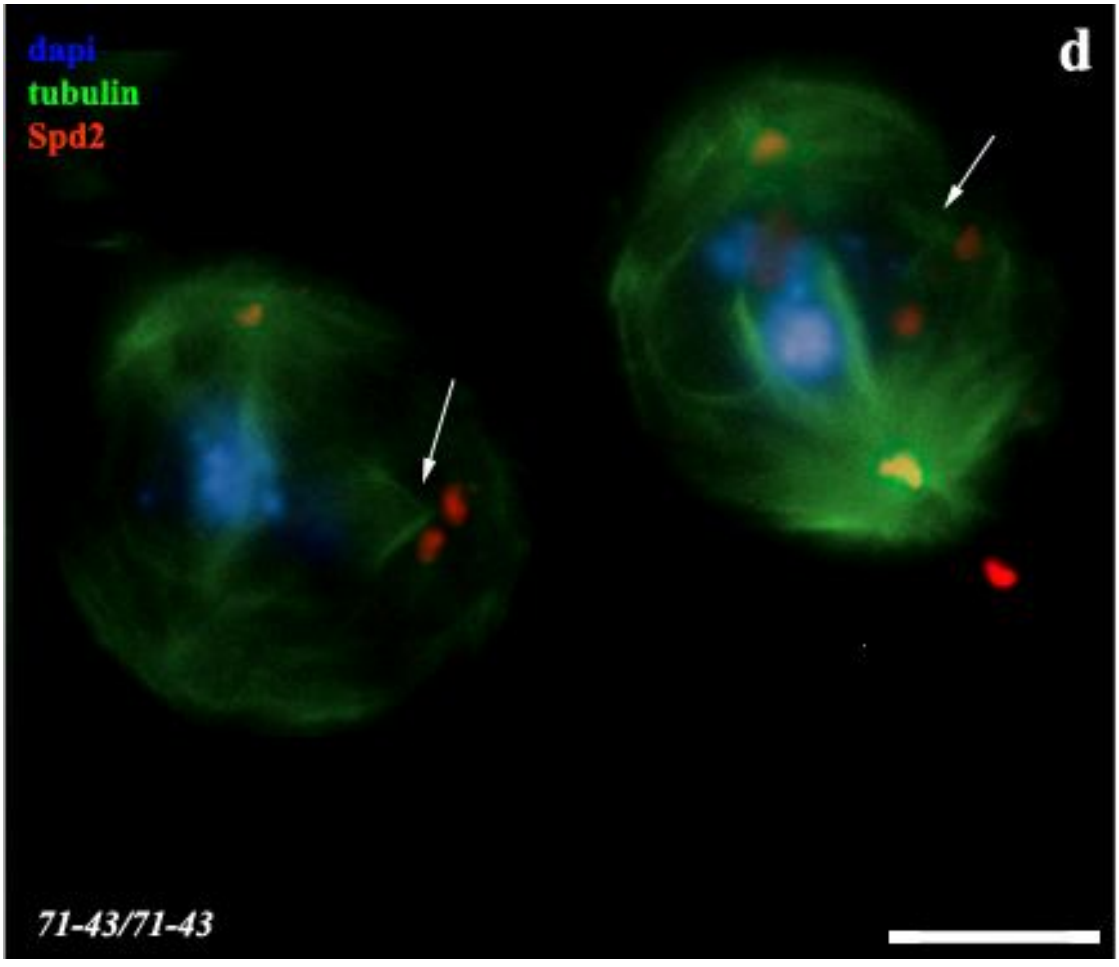
dapi
tubulin
Spd2
d
71-43/71-43

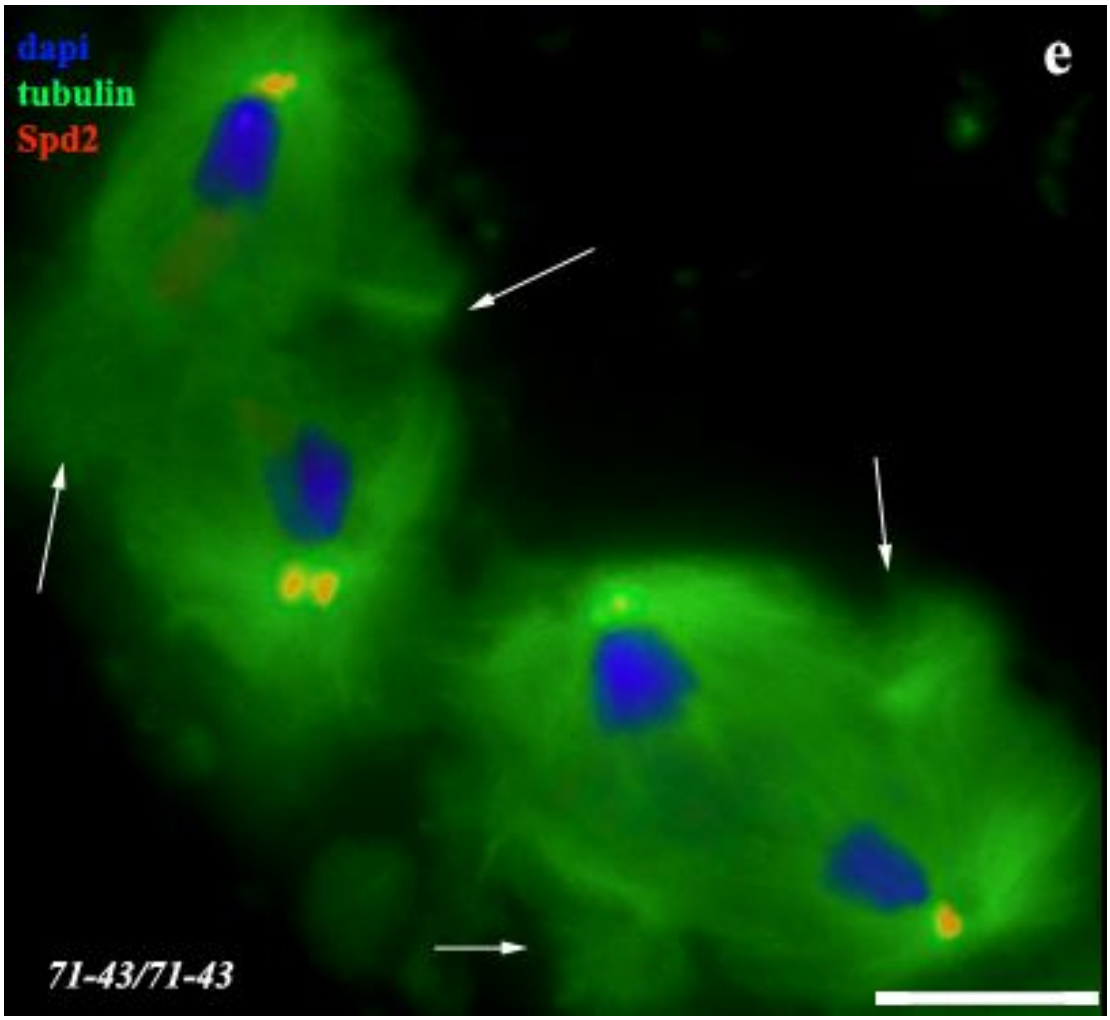

Fig. 15 Indirect immunofluorescence of meiotic cells stained for DNA with DAPI and tubulin with anti-αtubulin Ab and centrosomes with anti-Spd2 Ab, in order to look at defects of spindle structure, chromatin condensation and segregation, and centrosomes number and localization. Panels **a** and **b**: *wildtype* meiotic cells. **a** prophase. **b** metaphase I cells. Panels **c**, **d** and **e**: *71-43* mutant meiotic cells. **c** metaphase I and early anaphase I cells. **d** metaphase I cells. **e** late anaphase I cells. All images show merged figures simultaneously stained for DNA (DAPI, in blue), for tubulin and centrosomes (anti-αtubulin, green and anti-Spd2, in red, respectively). Arrow in **c** points out misoriented microtubules, self-organizing in absence of centrioles, while arrows in **d** show microtubules originating from extra-centrosomes and in **e** misoriented microtubules out of the spindle axis. Scale bars: 10 μm.

The analysis of meiotic divisions defects was performed using antibodies directed against α-tubulin and Spd2, a centriolar component, to gain information about meiotic spindle organization and centrosome behaviour. Cells displaying either monoastral (Fig. 16 **a**, **b**) or tripolar spindles (Fig. 16, **c**) were observed, together with centrosome defects like the presence of multiple or mislocalized centrosomes (Fig. 15, **c**, **d**, and Fig. 16, **b**, **c**, Spd2 immunostaining in red). The α-tubulin antibody, also, showed metaphase spindles with abnormal microtubules either self organizing in absence of the Spd2 Ab signal (Fig. 15, **c**, arrow) or originating from extra-centrosomes localized out of the so-

called spindle envelope (Fig. 15, **d**, arrows). Misoriented microtubules were evident at late anaphase too (Fig. 15, **e**, arrows).

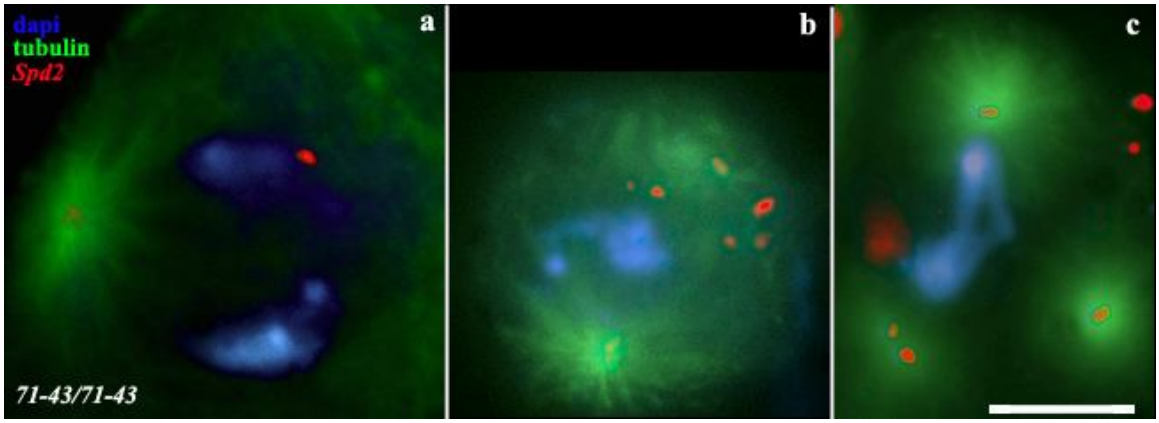

Fig. 16 Immunohystochemistry on fixed cells to look at DNA, spindle microtubules and centrosomes. Merged images simultaneously stained for DNA by DAPI (in blue), for tubulin and centrosomes by immunofluorescence by anti-αtubulin (in green) and anti-Spd2 (in red) Abs, respectively. Monoastral spindles are shown in **a** and **b**, whereas tripolar spindle is displayed in **c**. Multiple centrosomes are visible in **b** and **c**. Note the abnormal chromatin condensation in **b** and the irregular DNA spatial conformation in **c**. Scale bar represents 10 μm.

The immunostaining with antibodies pointed to highlight meiotic spindle and centrosomes allowed to emphasize the presence of chromosome segregation defects, showing, for example, asters and centrosomes devoid of chromatin (Fig. 17, lower panel, white arrows), which, instead, totally migrated to the same spindle pole (Fig. 17, lower panel, pink arrows). Such defects in chromosome segregation were further proved by means of DAPI staining of nuclear and mitochondrial DNA in onion stage mutant spermatids. Cells without nuclei, only showing nebenkernes were scored (Fig. 18, arrows). Moreover, chromatin bridges (Fig. 17, lower panel, pink arrowhead) and pairs of aster-less centrioles (Fig. 17, lower panel, white arrowheads) were observed in meiotic cells of *71-43* mutants.

To have an overall picture of meiotic division anomalies due to *71-43* mutation, I also analyzed two key events of cytokinesis process, i.e. central spindle formation and actomyosin ring assembly. In *wildtype* cells, a dense network of microtubules between the two cell poles starts to become visible by late anaphase (Fig. 19, upper panel, leftmost image, arrow). At telophase, central spindle is progressively squeezed (Fig. 19, upper panel, image in the middle, arrows) up to, eventually, attain an hourglass shape at late telophase (Fig. 19, upper panel, rightmost, arrow). In *71-43* homozygotes, spermatocytes displayed central spindles formed by a very reduced set of microtubules (Fig. 19, lower panel, leftmost image, arrows), sometimes even misoriented or positioned out of the spindle axis (Fig. 19, lower panel, rightmost image, arrows).

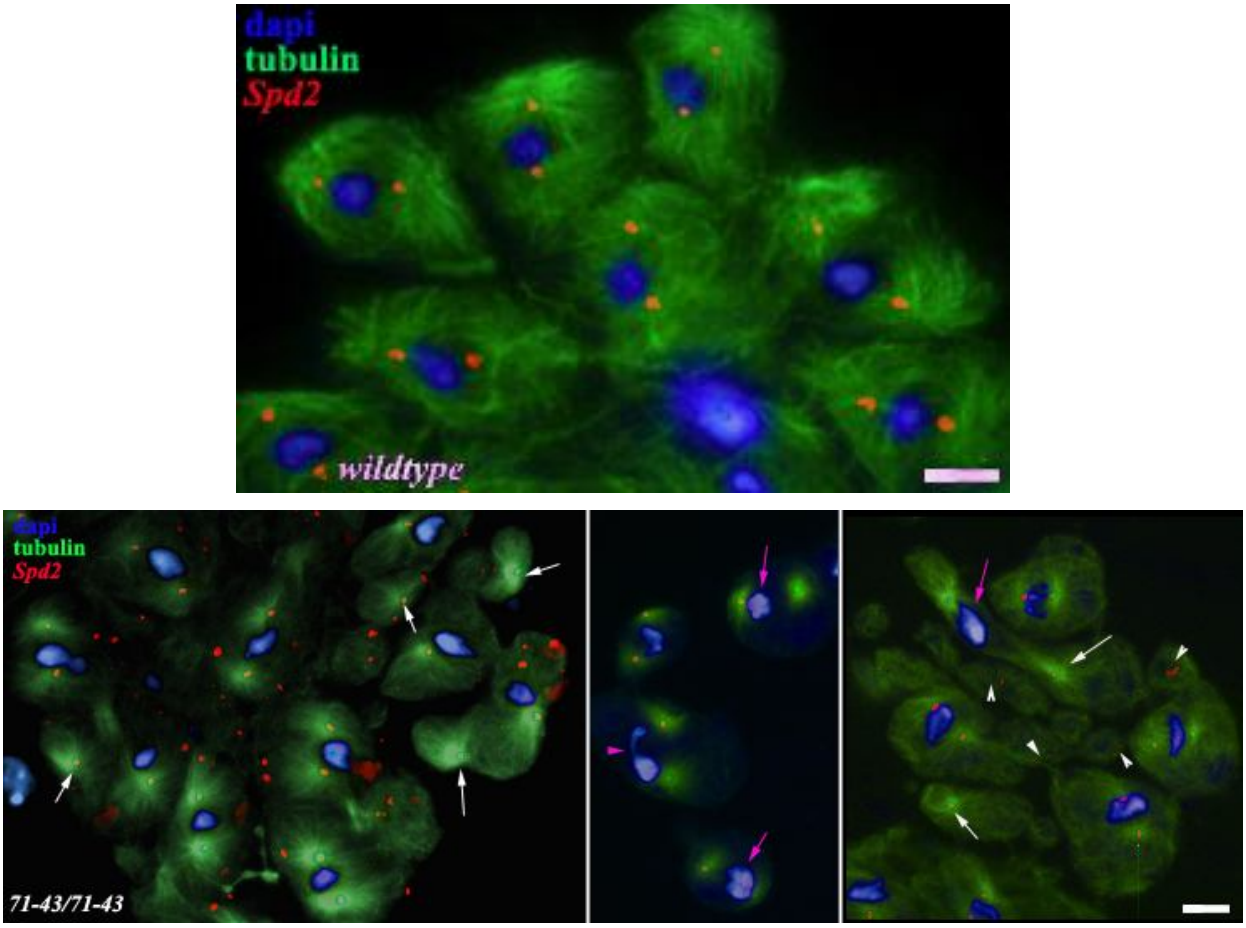

Fig. 17 Indirect immunofluorescence of meiotic cells stained for DNA with DAPI, tubulin with anti-αtubulin Ab and centrosomes with anti-Spd2 Ab, in order to look at defects of chromatin segregation, spindle organization and centrosomes localization. Upper panel: *wildtype* meiotic cells at metaphase I. Lower panel: *71-43* mutant meiotic cells. All panels show merged figures simultaneously stained for DNA by DAPI (in blue), for tubulin and centrosomes by immunofluorescence by anti-αtubulin (in green) and anti-Spd2 (in red) Abs, respectively. White arrows point out asters and centrosomes devoid of chromatin; white arrowheads indicate pairs of centrioles without either aster or chromatin. Pink arrows show uneven chromatin segregation, with all chromosomes migrated to the same spindle pole, while pink arrowhead displays a chromatin bridge. Scale bars are 10 μm.

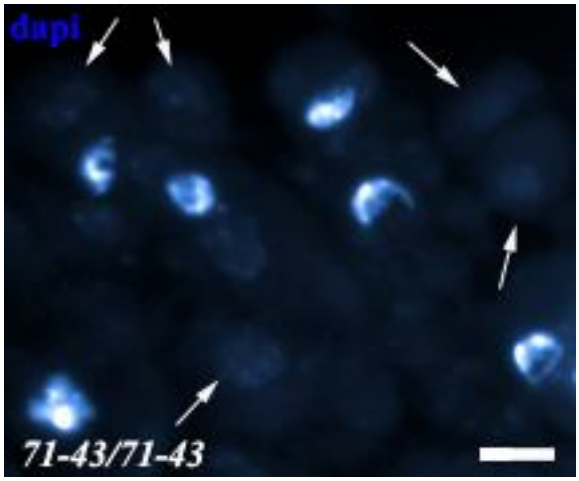

Fig. 18 DAPI staining of fixed *71-43* mutant cells at onion stage. Arrows point out cells with nebenkernes not associated with nuclei. Note that DAPI staining allows to visualize not only nuclear DNA but also mitochondrial one (nebenkern). Scale bar: 10 μm.

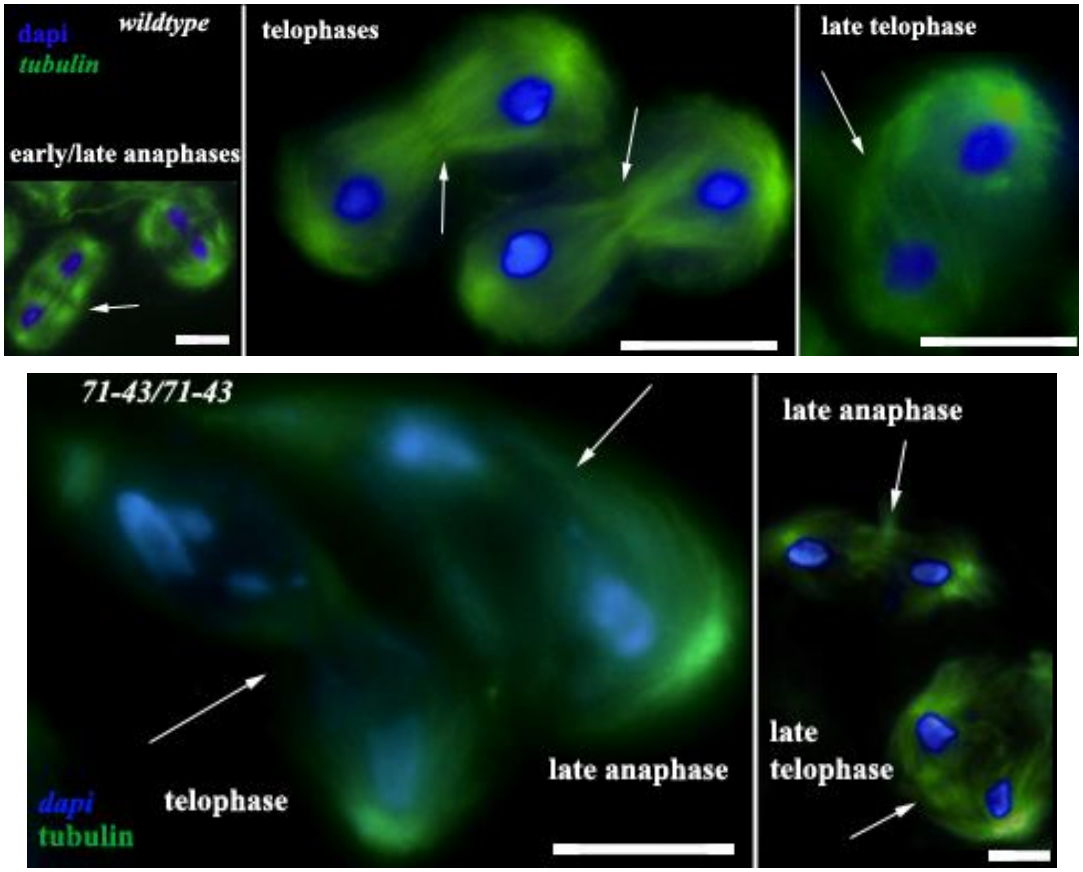

Fig. 19 Analysis of central spindle by immunofluorescence with anti α-tubulin Ab to visualize microtubules.
Upper panel: *wildtype* cells at anaphase I and telophase I. Lower panel: *71-43* mutant meiotic cells at anaphase I and telophase I. Merged figures simultaneously stained for DNA by DAPI (in blue) and for tubulin by immunofluorescence by anti-αtubulin Ab (in green). Arrows in upper panel, point out central spindle, forming in late anaphase and constricting more and more up to late telophase, where it displays a hourglass shape. Arrows in lower panel, point out the paucity of microtubules forming the central spindle and their misorientation relative to spindle axis. Note lagging chromatin in *71-43* mutant cells, lower panel, figure on the left. Scale bars: 10 μm.

The study of actomyosin ring assembly was allowed by means of staining with rhodamine phalloidin, a fluorescent marker specific for actin. The actomyosin ring is visible as a band at the midzone, between the telophase nuclei, that progressively constricts until becoming ring-shaped (Fig. 20, upper panel, arrows). In *71-43* mutant cells actomyosin ring failed to assembly at the midzone (Fig. 20, lower panel, arrow).

Then, immunocytological analysis was focused on some crucial aspects of spermiogenesis, starting from the post-meiotic positioning of the centriole, that will give rise to the future basal body. *Wildtype* spermatids, coming out from the meiotic divisions, have only one centriole per nucleus, owing to the lack of centriole duplication by the end of first meiotic division. The single centriole is juxtaposed to each spermatid nucleus, between nucleus and nebenkern, where it will become the basal body. I took advantage of the availability of the antibody against Spd2, to look at basal body formation and location, since Spd2 is a basal body constituent too (Fig. 21, upper panel. See the arrows). In *71-43* mutant spermatids, multiple Spd2-positive signals were evident per each nucleus. Moreover, they were mispositioned, since they were neither anchored to nucleus nor situated between nucleus and nebenkern (Fig. 21, lower panel).

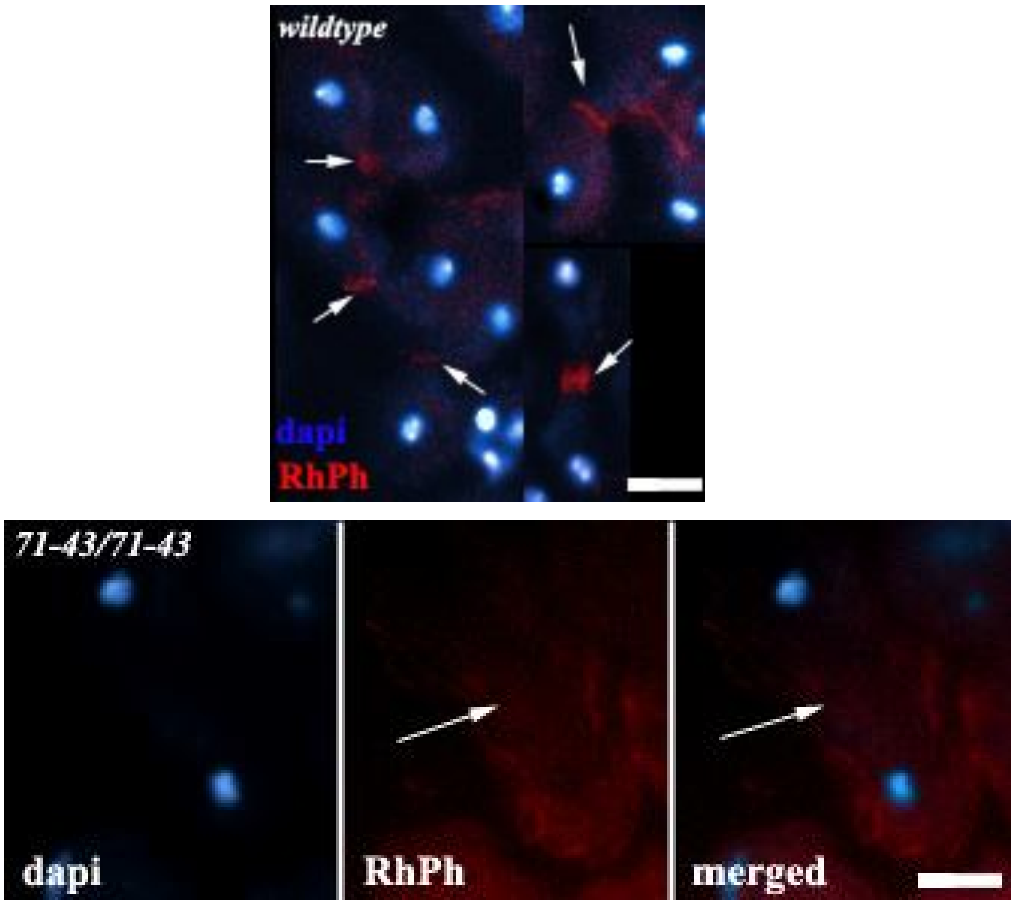

Fig. 20 Analysis of actomyosin ring by rhodamine phalloidin fluorescence.
Upper panel: merged figures of *wildtype* late anaphase to telophase cells, simultaneously stained for DNA by DAPI and actomyosin ring by fluorescence with rhodamine phalloidin. Arrows point out the actomyosin ring visible at the midzone of dividing cells. Lower panel: *71-43* homozygous telophase cell. From left to right: DAPI staining, rhodamine phalloidin fluorescence and merged image. Arrows point out the absence of rhodamine phalloidin signal at the midzone. Scale bars: 10 μm.

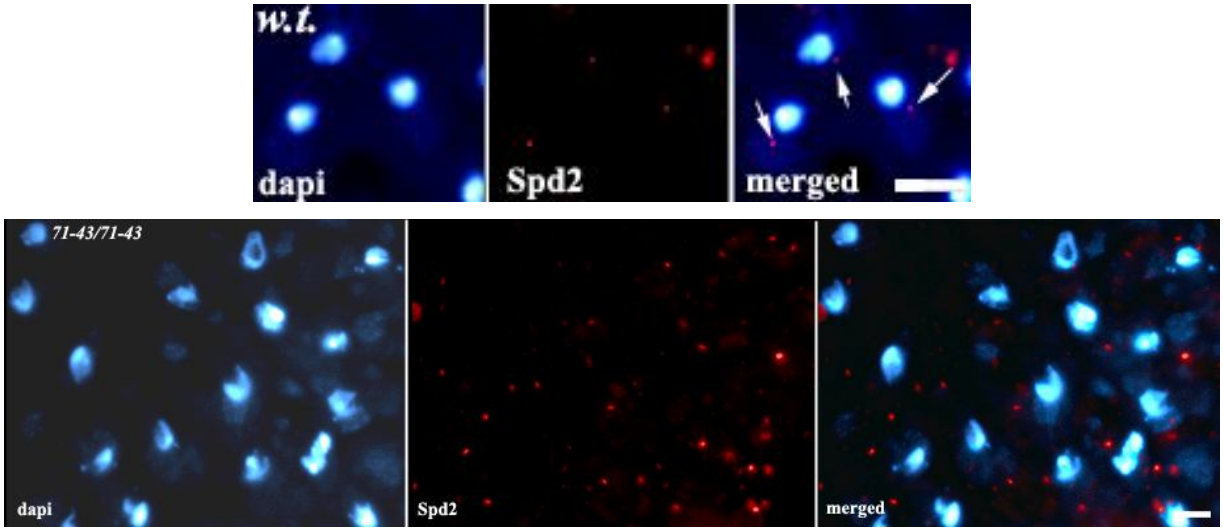

Fig. 21 Onion stage spermatids stained with DAPI and the antibody against Spd2, to visualize DNA and the centriole or basal body.

Upper panel: *wildtype* onion stage spermatids. Arrows point out the single centriole positioned at the base of each nucleus, between nucleus and nebenkern. Lower panel: *71-43* homozygous onion stage spermatids. In all panels, from left to right: DAPI staining (blue), anti-Spd2 immunostaining (red) and merged image.

71-43/71-43 mutant spermatids exhibit multiple, mispositioned centrioles per nucleus. Note that DAPI staining also allows to see nebenkern. Scale bars represent 10 μm.

Immediately after onion stage, *wildtype* early elongation spermatids displayed a regular set of growing microtubules and a dense chromatin mass, flattened against the side of the nucleus underlying the elongating axoneme (Fig. 22, upper panel), whereas *71-43* spermatids showed a disorganized network of microtubules and diffuse chromatin (Fig. 22, lower panel).

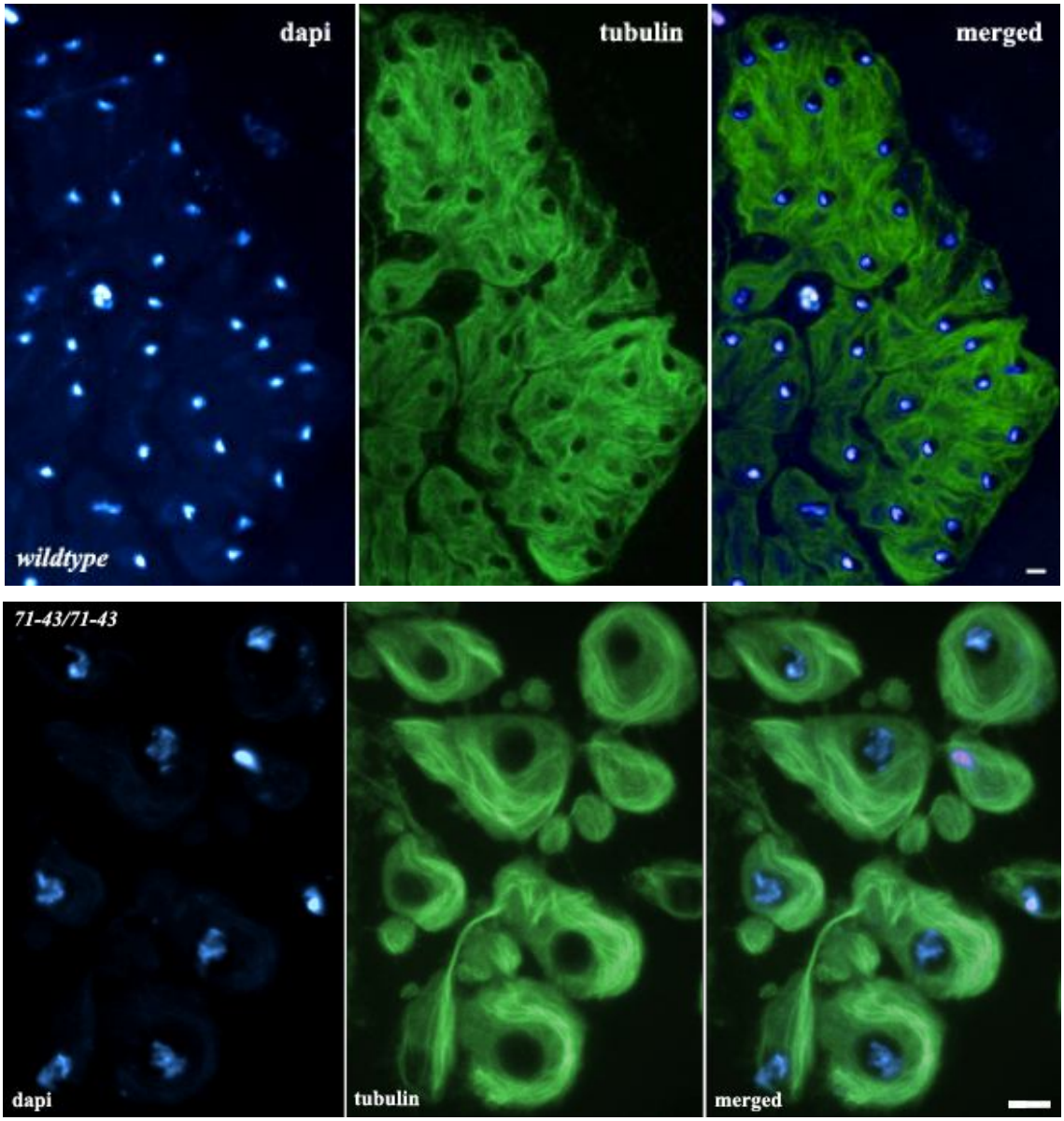

Fig. 22 Early elongating spermatids, stained with DAPI and antibody directed to α-tubulin, to see chromatin condensation and microtubules arrangement.

Upper panel: *wildtype* young spermatids. Lower panel: *71-43* homozygous young spermatids. In all panels, from left to right: DAPI staining (blue), α-tubulin immunostaining (green) and merged image.

Note the diffuse chromatin state and the disorganized network of microtubules in the mutant in comparison with compact chromatin, flattened against a side of the nucleus, and the regular pattern of microtubules in the *wildtype*.

Scale bar: 10 μm.

In vivo cytological analysis showed the presence of empty seminal vesicles (data not shown), as proof of sperm individualization defects. As early mentioned, in *Drosophila*, cytokinesis process during mitotic and meiotic spermatogenetic divisions is incomplete, so that all spermatid nuclei descended from a primary spermatocyte remain connected via an extensive network of cytoplasmic bridges. A late step in sperm maturation requires the physical resolution of the cyst, into individual cells, a process referred to as sperm individualization. I, therefore, investigated such a process

taking place by means of the individualization complex (IC), which assemblies in each individual spermatid nucleus and translocates along the tail towards the end in a synchronous way, with each IC assembled on each of the 64 spermatid nuclei forming a bundle. The ICs consist of actin-based cones (also referred as investment cones), thus, I observed their assembly and movement over the sperm bundles by means of rhodamine phalloidin staining. While investment cones were well visible in proximity of spermatid nuclei in a *wildtype* background (Fig. 23, upper panel), ICs were absent in *71-43* mutant bundles, evidencing the failure of assembly of investment cones (Fig. 23, lower panel). Such an analysis was performed with DAPI staining as well, to look at nuclear shaping and cyst polarization. Interestingly, *71-43* spermatid nuclei were round instead of being needle-shaped (Fig. 23; compare *wildtype* and *71-43* nuclei in the inserts); moreover, they were scattered all over the bundle instead of being polarized at one end of the bundle as in *wildtype* (Fig. 23; compare DAPI staining in wildtype and mutant), proving the impairment of both processes.

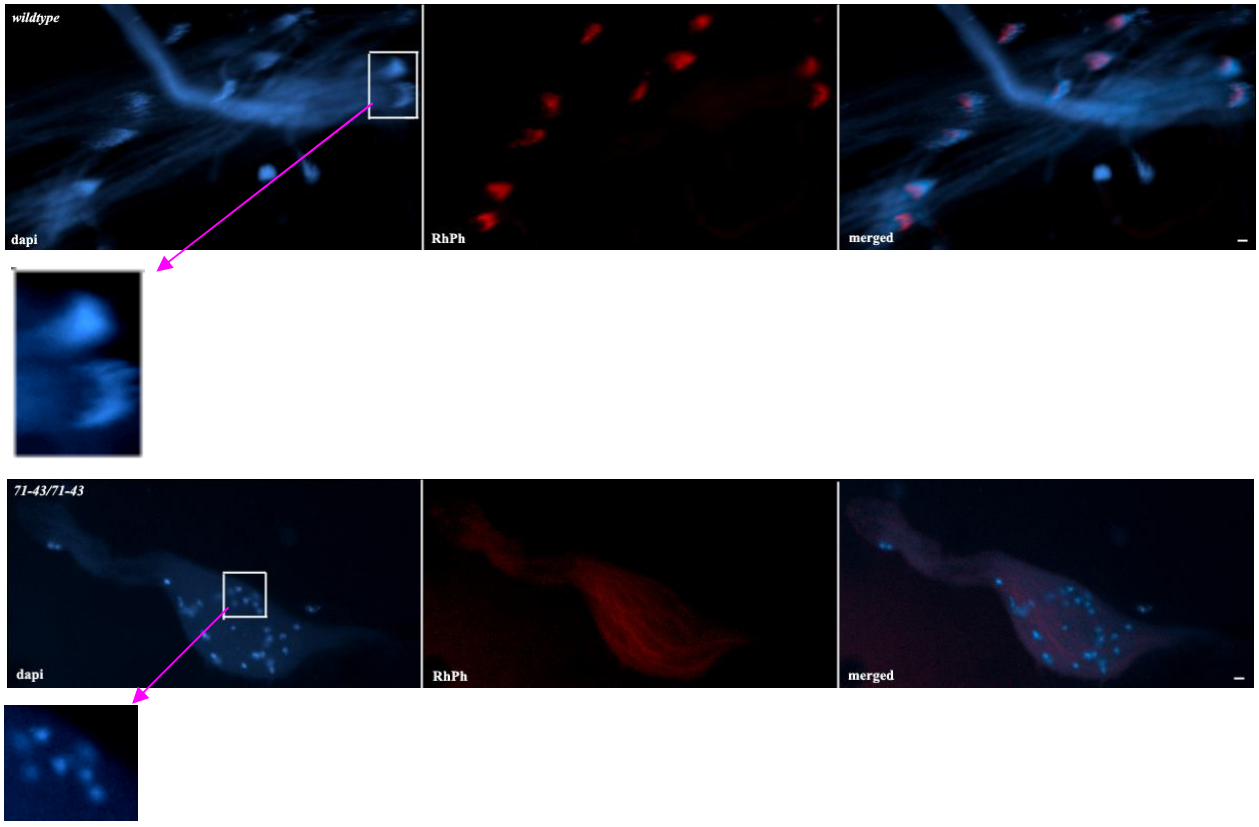

Fig. 23 Spermatid bundles stained with DAPI and rhodamine phalloidin (RhPh) to look at spermatid heads and individualization complex (IC).

Upper panel: *wildtype* spermatid bundles. The insert, indicated by the pink arrow, points out the needle-shape heads at one end of two spermatid bundles. Lower panel: *71-43/71-43* spermatid bundle. The insert, indicated by the pink arrow, points out the abnormally round shape heads spread out all over a spermatid bundle. In all panels, from left to right: DAPI staining (blue), rhodamine phalloidin (red) and merged image.

Note the absence of actin-based cones and the presence of round nuclei scattered all over the bundle in *71-43* mutant. Scale bars: 10 μm.

4.2.4 IS *71-43* ALSO A MITOTIC MUTANT?

I investigated the effect of *71-43* mutation in mitotic cell cycle by calculating the mitotic index (the fraction of cells undergoing mitosis), as the number of mitotic cells per optical field (Gatti and Baker, 1989; Gatti and Goldberg, 1991) in larval mutant brains as compared to the wild-type. The analysis was accomplished by means of a particular balancer which bears both *Cy* as dominant marker of 2nd chromosome and *Tb* as dominant larval marker of 3rd chromosome, this latter allows to discriminate between tubby (wildtype genotype) and not tubby (mutant genotype) larvae. Thus, I scored mitotic cells in larval brains of males bearing clean *71-43* chromosome in homozygous condition (named *Rec#57/Rec#57*) versus heterozygotes, (*Rec#57/St,CyTb*) as control. I recorded a statistically significant lower mitotic index of the mutant males in comparison with the control (Tab.2), as a proof that *71-43* mutation affects mitosis as well as meiosis.

	Optical fields	Mitotic cells	MITOTIC INDEX
Rec#57/ St,Cy Tb	568	808	1.42
Rec#57/ Rec#57	637	638	1.00

χ^2 test: P= 0.000

P≤0.05 STATISTICALLY SIGNIFICANT

Tab.2 Mitotic index estimated in larval brains of clean *71-43* homozygotes versus heterozygotes. *Rec#57/Rec#57* represents clean *71-43* homozygotes, whereas *Rec#57/St, Cy Tb* are the heterozygotes used as control. On the right, the outcome of χ^2 test provides statistical significance to mitotic index data, since if the probability (P) is fewer than or equal to 0.05, data are not due by chance.

To test whether a lower mitotic index had negative effects on the development of the mutant flies in terms of delayed development or lethality, I scored the progeny coming out from a cross between *Rec#57/St, Cy Tb* heterozygous males and females, within 18 days, and I observed frequencies of homozygotes and heterozygotes nearly identical to the expected ones (45 observed heterozygous adults vs 46 expected and 24 observed homozygotes vs 23 expected). This analysis was repeated setting up many independent crosses, always confirming the same outcome (See Materials and Methods, paragraph 3.1).

4.2.5 DOES *71-43* ALSO AFFECT FEMALE FERTILITY?

To investigate the effects of *71-43* mutation in female fertility, 8 virgin females, homozygote for the clean chromosome 2, were singularly tested for fertility. This analysis provided as result reduced fertility in six cases and sterility in two, thus, indicating that *71-43* mutation has not only a specificity of action in male spermatogenesis but affects female fertility as well.

4.2.6 TOWARDS THE IDENTIFICATION OF THE *71-43* GENE

4.2.6i GENETIC APPROACH

I exploited two strategies to identify the gene mutated in *71-43* strain: complementation analysis and proteomics. The former consisted in a test of complementation of available null or ipomorphic alleles of the genes, mapped to such a region, to see whether the combination of *71-43* mutation over each mutated candidate gene failed to complement male fertility. The outcomes of tests carried out on the alleles of *CG10082, CG10320, CG42362* and *CG42363* allowed to rule out these genes as possible candidates for *71-43* mutation, since their heterozygous combination with *71-43* mutation resulted into male fertility. (Before the smallest region uncovering *71-43* mutation was discovered, some other genes spanning to the right of it were also tested giving full complementation with the *71-43* mutation). The parameters for the genes to be chosen and tested by complementation were, first of all, the availability of their mutant alleles, the expression in testis, evidenced by the presence of ESTs in testis and the predicted molecular function. One limit of this approach is, definitely, represented by the potential inability to test all the candidate genes for *71-43* mutation due to the unavailability of the required mutant alleles. To overcome this difficulty, in parallel, I followed an alternative route, embarking on a proteomic analysis that will be introduced and explained further on, in the following paragraph.

4.2.6ii PROTEOMIC APPROACH

As I said in the previous paragraph, some genes, that lie in the interval of chromosome 2 uncovering the mutation, cannot be tested by complementation, owing to the unavailability of their alleles. Hence, I started a proteomic analysis, taking advantage of a collaboration with the Mass

Spectrometry Facility of the University of Tuscia. Proteomic study consisted in the analysis of testis protein extracts from *71-43* homozygous males as compared to heterozygous males by bi-dimensional gel electrophoresis (2D-IEF-SDS-PAGE). My main interest was on those genes that could not be tested by complementation (see Tab.3), thus, the analysis was focused on those protein spots that should correspond, because of molecular weights and isoelectric points, to the putative products of each *71-43* aspirant gene. Such an investigation was feasible by the availability on FlyBase of predicted molecular weights and isoelectric points of proteins codified by given gene sequences.

Genes	predicted MW (kDa)	theoretical pI
CG30284-PA	39.6	11.01
CG30284-PB	36.6	10.70
Rae1	38.6	7.64
CG15678	21.2	9.59
CG9865-PA	54.1	9.49
CG9865-PB	54.1	9.49
NC2alpha-PA	36.3	7.50
NC2alpha-PB	33.9	4.87
CG15676	20.9	5.09
CG10306	25.7	6.40
Tbp	38.5	9.79

Tab.3 Genes to test by proteomics. MW: molecular weight. pI: isoelectric point.

At the same time, the comparison between protein patterns of mutant versus wildtype testes was informative about the differences in terms of presence/absence of specific spots. By this way, two replicates of 2D-IEF-SDS-PAGE for both mutant and wildtype were performed and elaborated by computational programs, giving rise to a final 2D-gel per each genotype (Fig.24). Those spots present in one genotype but absent in the other (highlighted by numbers over both gels) were selected and subjected to mass spectrometry analysis.

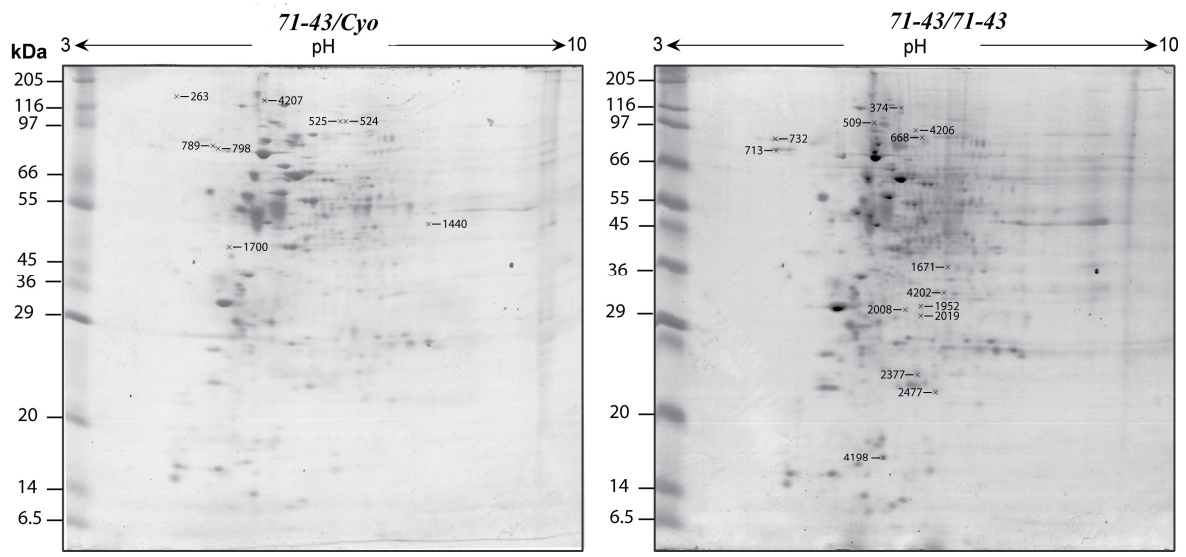

Fig. 24 Final 2D-gel, coming from the computational elaboration of two replicates per each genotype (*71-43/CyO* and *71-43/71-43*). On the Y axis, molecular weights (kDa) are displayed while, on the X axis, pH range (3-10) is shown. Numbers in both gels point out the spots present in a genotype but absent in the other, selected for the analysis by mass spectrometry.

Proteins, identified by such spots, that resulted misregulated could be categorized into the following functional groups: Protein/DNA metabolism, Redox and ion homeostasis, Hsp and protein folding, Cytoskeleton and microtubules, Energy production, Ecdysone puffs and growth factors, Comet genes, unknown function (see Tab.4).

Spots # 524 and 525 likely identify two isoelectric variants of the protein with unknown function, codified by CG1979, which are both present in *71-43/CyO* gel but absent in *71-43/71-43* one. In the same way, spots # 789 and 798 are likely to identify two different isoforms of the protein codified by the comet gene spaw. Both isoforms are visible in *71-43/CyO* gel but not in the mutant one, where, instead, two probable isoforms of the polypeptide with predicted ATPase activity, codified by CG34434, are present differently from *71-43/CyO* gel. All the testis proteins with an altered expression profile detected by such a 2D-IEF-SDS-PAGE technique were codified by loci mapping outside of the region of chromosome 2 to which I mapped *71-43*, allowing to rule out all of them as putative products of the mutated gene in *71-43* homozygote males.

Proteins with altered expression profiles in *71-43* heterozygous *vs* homozygous as identified by mass spectrometry:

	71-43/CyO	*71-43/71-43*
Protein/DNA metabolism		
CG17331 (2L) endopeptidase	-	+
CG4904 (2L) pros35	-	+
CG4494 (2L) smt3 (sumo)	-	+
CG8023 (3L) eIF4E-3	-	+
Redox and ion homeostasis		
CG1633 (X) thioredoxin peroxidase 1, isoform A	-	+
CG5495 (3L) thioredoxin-like protein	-	+
Hsp and protein folding		
CG31449 (3R) Hsp70Ba	-	+
CG1242 (3L) Hsp83 (or Hsp90)	-	+
Cytoskeleton and microtubules		
CG5939 (3L) paramyosin	-	+
CG10540 (2R) capping protein alpha	-	+
Energy production		
CG34434 (X) ATPase activity	-	+
CG31169 (3R) glycerol-3-phosphate dehydrogenase	+	-
Ecdysone puffs and growth factors		
CG32031 (3L) arginine-kinase	-	+
CG6143 (3L) protein on ecdysone puffs	-	+
CG4559 (2L) imaginal disc growth factor 3	+	-
Not known function		
CG1979 (3R)	+	-
CG1324 (X)	+	-
Comet genes		
CG30365 (2R) spaw	+	-

Tab.4 Proteins with altered expression profiles identified by Mass Spectrometry.
"-" and "+" point out the absence and presence, respectively, of a protein in either *71-43/CyO* or *71-43/71-43* testes protein extracts.

4.3 *50-38* CYTOLOGICAL CHARACTERIZATION

50-38 was worth to be investigated more in depth than the other non-complementing mutants since it failed to complement *twine,* yet did not show any mutation in *twine* sequence.

The *in vivo* cytological characterization of *50-38* mutants basically showed defective initiation of male meiosis, as evidenced by the abnormally large size of both nuclei and Nebenkern (Neb) at the onion stage (Fig. 25), which is the stage immediately following the two meiotic divisions, usually used as an indicator of meiotic alterations during the processes of nuclear and cytoplasmic division. Since such a phenotype is reminiscent of that of twe^{HB5}, cytological characterization of *50-38* mutants was performed in parallel with twe^{HB5}, in order to compare them.

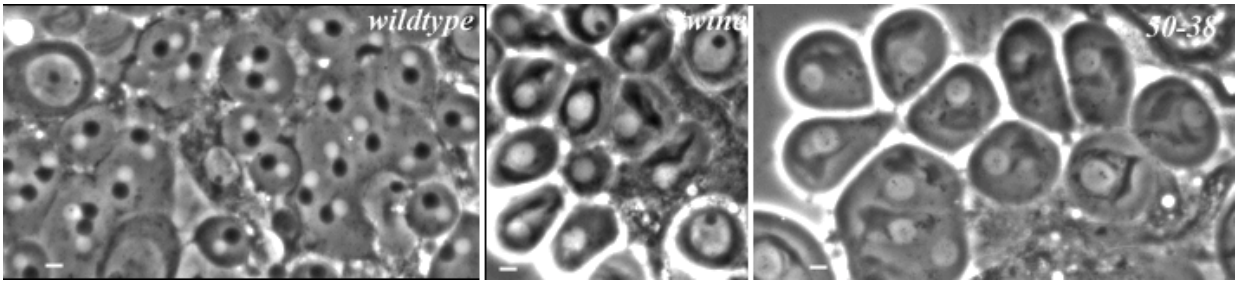

Fig. 25 *In vivo* cytology. Onion stage spermatids observed by phase contrast microscope.
From left to right: *wildtype*, *twine* and *50-38* spermatids. Spermatid nuclei are pale while the Nebenkernes are darker. Note the abnormally larger size of both nuclei and Nebs in *twine* and *50-38* mutants in comparison with those of wildtype.
Scale bars:10 μm.

The failure of meiotic entry suggested by looking at the size of both nucleus and Neb of onion stage spermatids was confirmed by a statistical approach. I scored the relative number of 16 cell-, 32 cell- and 64 cell-cysts in testes from *50-38* homozygous individuals and I compared the final score with that of *wildtype* and *twine*. The outcomes, showed in the bar chart (Fig. 26), displayed a total absence of either 32-cell or 64-cell cysts in *50-38* and *twine* mutants in comparison with *wildtype* males.

In order to get much more insights on the stage at which meiotic cell cycle halts in these mutants a statistical analysis was performed focused to assess the relative abundance of specific spermatogenesis stages (Fig. 27). This kind of investigation, based on the score of 100 cysts per genotype, revealed that both *50-38* and *twine* homozygous have a statistically significant fewer number of cysts than *wildtype* at the growth phase. No cysts underwent first meiotic division, as evidenced by the absence of meiotic cysts ready to execute second division. Nevertheless, 16-cell

onion stage cysts are present in these mutants, with a statistical significant higher number than that found in *wildtype*.

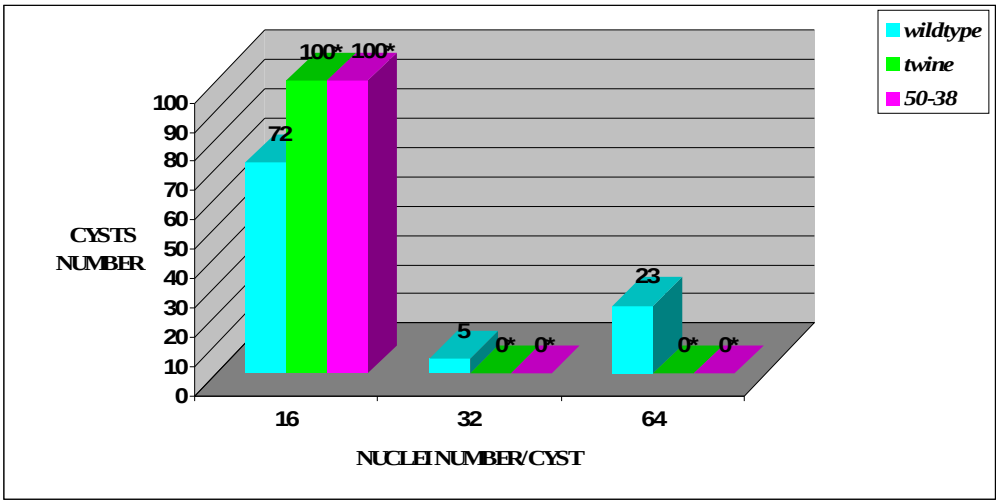

Fig. 26 Bar chart showing cysts comparison among *twine* and *50-38* mutants and *wildtype*.
On the x axis, the nuclei number per cyst is displayed whereas, on the z axis, the cysts number is indicated.
Wildtype is in blue, *twine* in green and *50-38* in pink. The asterisks point out statistical significant data.

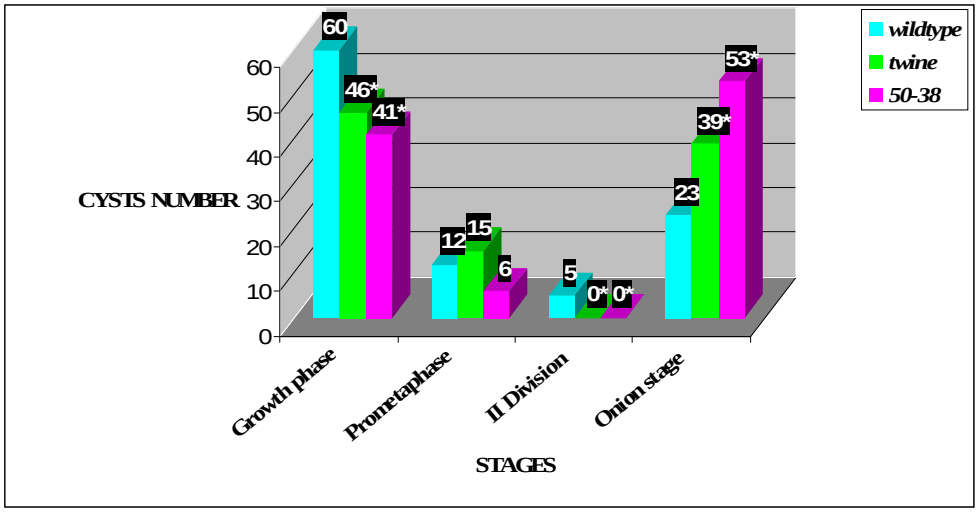

Fig. 27 Bar chart showing stages comparison among *twine* and *50-38* mutants and *wildtype*.
On the x axis, different stages are displayed whereas, on the z axis, the cysts number is indicated.
Wildtype is in blue, *twine* in green and *50-38* in pink. The asterisks point out statistical significant data.

The *in vivo* cytological analysis of testis preparations stained with DAPI staining, to visualize DNA, spotlighted in *twine* and *50-38* mutants the arrest of primary spermatocytes at the late prophase stage where chromatin clumps are apposed to the inner nuclear envelope (Fig. 28, middle and lower panels, see DAPI staining on the right).

During normal spermatogenesis, chromatin clumps, representing pairs of homologous chromosomes, migrate from the internal sheet of the nuclear envelope to the middle of nucleus,

where they start to line up (Fig. 28, upper panel, see DAPI staining on the right), in order to align in metaphase plate. In *twine* and *50-38* mutants, chromatin clumps remained at periphery of the nucleus, in proximity of nuclear membrane, and never congregated in metaphase plate, showing that primary spermatocytes never reached late prometaphase/metaphase stage (Fig. 28, middle and lower panels).

Despite the failure of *twine* and *50-38* primary spermatocytes to undergo meiotic divisions, yet giant onion stage spermatids were visible in their testes, characterized by peculiar larger nuclei and Nebs as respect to wildtype (Fig. 29, left panels; compare phase contrast images of *twine* and *50-38* onion stages with that of *wildtype*). Dapi staining (Fig. 29, right panels) evidenced that in *twine* spermatid nuclei chromatin was still organized in separate clumps, instead of being condensed in a single mass as in *wildtype* onion stage spermatids. On the other hand, in *50-38* spermatids chromatin masses clumped together, although in a less condensed state than that seen in *wildtype*.

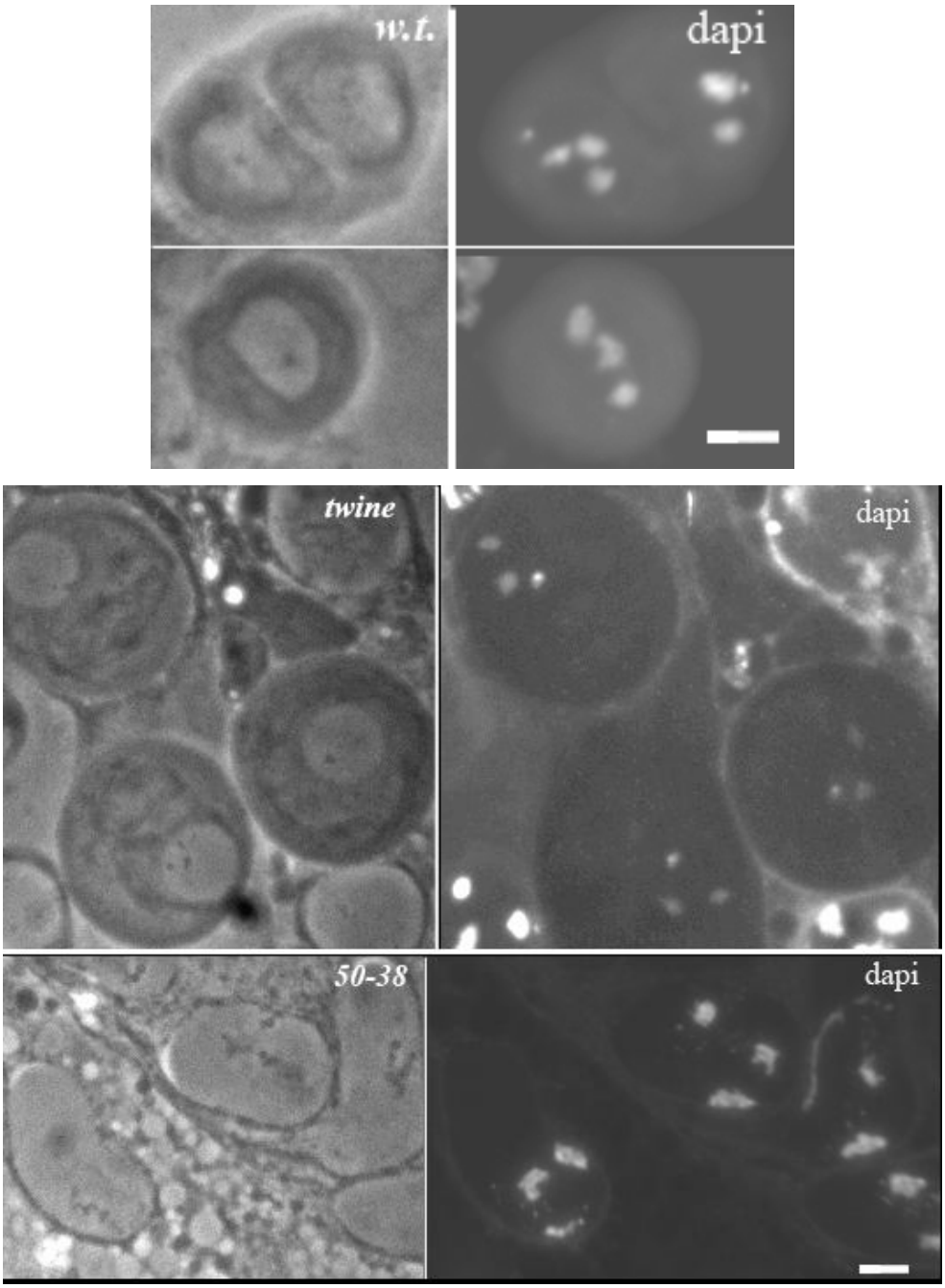

Fig. 28 *In vivo* cytology and DAPI staining. Primary spermatocytes at late prophase and prometaphase.
Upper panel: *wildtype* primary spermatocytes at prometaphase. In the cell displayed below, lined up chromatin clumps are shown. See dapi staining. Middle panel: *twine* primary spermatocytes at late prophase. Lower panel: *50-38* primary spermatocytes at late prophase. In all panels, phase contrast images are shown on the left whereas dapi staining is on the right. Scale bars represent 10 μm.

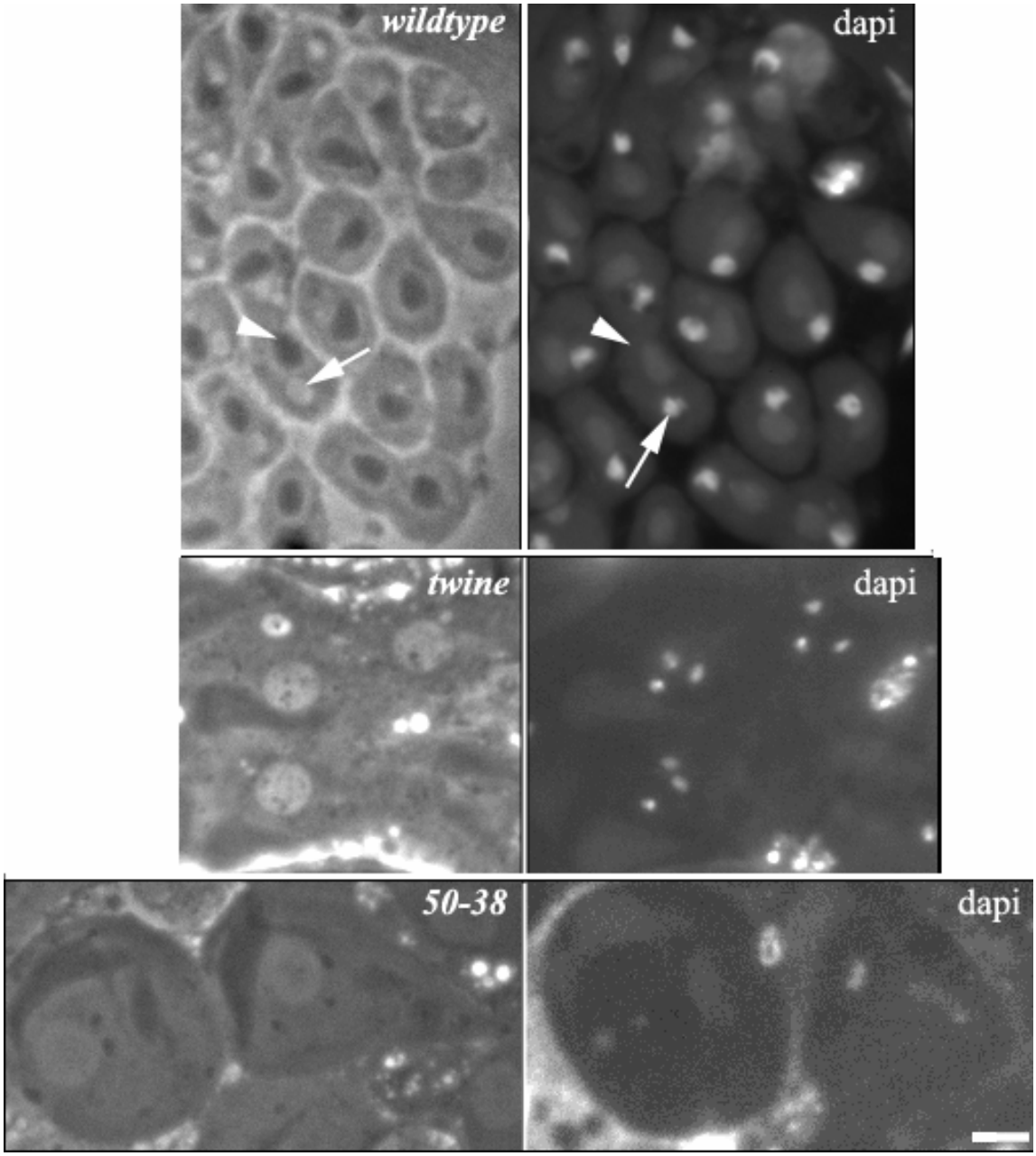

Fig. 29 *In vivo* cytology and DAPI staining. Onion-stage spermatids.
Upper panel: *wildtype* onion stage spermatids. Middle panel: *twine* onion stage spermatids. Lower panel: *50-38* onion stage spermatids. In all panels, phase contrast images are shown on the left whereas dapi staining is on the right.
In the upper panel, arrows point out nuclei, while arrowheads indicate Nebenkernes. Note that dapi staining allows to evidence Neb as well. Scale bar: 10 μm.

Since the *in vivo* cytological characterization of the *50-38* mutants, basically, showed the arrest of male meiotic cell cycle at some point of prophase before metaphase onset, I investigated, by means of specific antibodies, the presence and the behaviour of some known actors of cell division machinery, as centrosomes, meiotic spindle and nuclear envelope. This analysis was performed in parallel with *twine* mutants.

The analysis of nuclear envelope was executed by means of an antibody against lamin proteins, which are known components of nuclear membrane, simultaneously to centrosomes staining through an antibody specific for Spd2 protein, a centriolar constituent, whose pattern is useful to recognize cellular stage. In wildtype spermatogenesis, primary spermatocytes at early prometaphase still show an intact nuclear envelope, under which chromatin clumps are closely apposed; at this stage, centrosomes migrate from the cell membrane to the nuclear one (Fig. 30, panel **a**). Upon late prometaphase, pairs of homologous chromosomes start to congregate toward the metaphase plate, while centrosomes migrate to opposite poles of nucleus and lamin envelope disappears (Fig. 30, panel **b**). In *twine* and *50-38* late prometaphase spermatocytes, centrosomes migrated to opposite poles of nucleus, however neither bivalents congregation to metaphase plate took place nor lamin broke down (Fig. 30, **c** and **d**). The peculiarity of *50-38* primary spermatocytes was the presence of dot-like extra-centrosomes, besides the two conventional V-shaped pairs of centrioles (Fig. 30, **d**, and Fig. 31, **d**).

This characterization was further deepened by looking at meiotic spindle through an antibody directed against α-tubulin. Differently from *wildtype* primary spermatocytes, that show microtubules originating from centrosomes and organize asters (Fig. 31, panel **a**), which migrate to opposite poles of nucleus where they arrange a meiotic spindle (Fig. 31, panel **b**), *twine* and *50-38* mutants failed to assemble a meiotic spindle. In *twine* mutants, microtubules originating from centrosomes organized themselves into aster-like structures, less dense than those of *wildtype* (Fig. 31, **c**). *50-38* mutant primary spermatocytes, also, failed to accomplish the assembly of a canonical meiotic spindle, showing in particular aster-like structures rather poor of microtubules and dot-like extra centrosomes, well visible in Fig. 31, **d**.

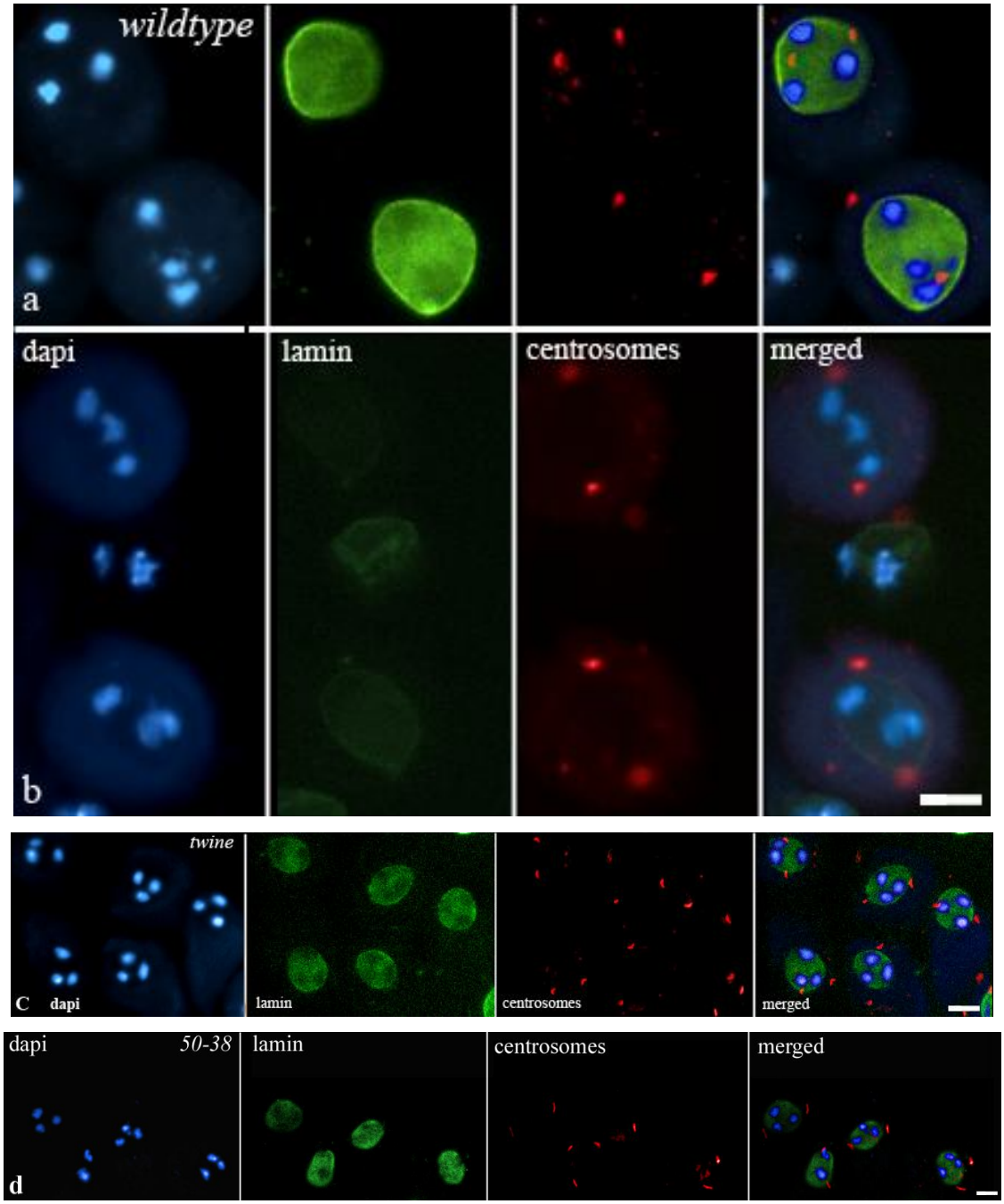

Fig. 30 Immunohystochemistry on fixed cells. DNA, lamin and centrosomes stainings.

Panels **a** and **b**: *wildtype* early (**a**) and late prometaphase (**b**) primary spermatocytes. Panel **c**: *twine* late prometaphase primary spermatocytes. Panel **d**: *50-38* late prometaphase primary spermatocytes. Look at centrosomes staining. In all panels, from left to right: dapi staining (blue), lamin immunostaining (green), centrosomes immunostaining (red) and merged image. DNA is showed by DAPI staining. The Ab used to recognize nuclear envelope is anti-laminDm0, while the Ab used to visualize centrosomes is anti-Spd2, a centriolar constituent. Scale bars represent 10 μm.

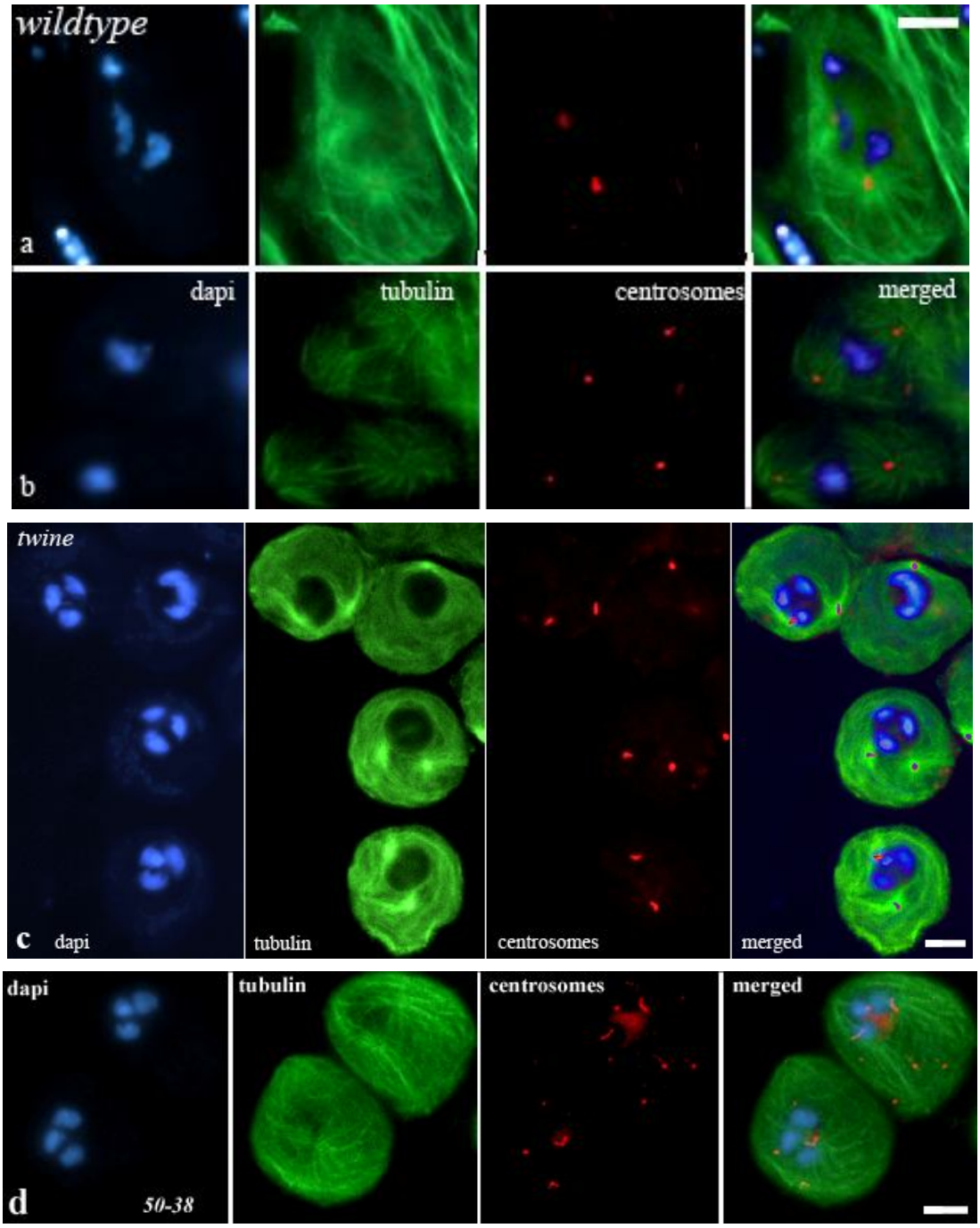

Fig. 31 Immunohystochemistry on fixed cells. DNA, tubulin and centrosomes stainings.
Panels **a** and **b**: *wildtype* early prometaphase (**a**) and metaphase (**b**) primary spermatocytes. Panel **c**: *twine* late prometaphase primary spermatocytes. Panel **d**: *50-38* late prometaphase primary spermatocytes. In all panels, from left to right: dapi staining (blue), tubulin immunostaining (green), centrosomes immunostaining (red) and merged image. DNA is showed by DAPI staining. The Ab used to visualize meiotic spindle is anti α-tubulin, while the Ab specific for centrosomes is anti-Spd2, a centriolar constituent. Scale bars represent 10 μm.

The failure of *twine* and *50-38* mutants to accomplishing both meiotic divisions was also provided by the number of centrioles that can be observed in the onion stage spermatids. As I already mentioned in the paragraph 4.2.3, *wildtype* spermatids exiting from meiotic divisions each have a

single centriole per nucleus, that will become the basal body, docked to nuclear envelope (Fig. 32, upper panel). In *twine* and *50-38* onion stage spermatids, both V-shaped pairs of centrioles were still visible and, moreover, they were detached from the nucleus, where chromatin clumps were still recognizable (Fig. 32, middle and lower panel), differently from *wildtype* nucleus, which shows a single dense chromatin mass (Fig. 32, upper panel). *50-38* spermatids showed another peculiarity in number of centrosomes, because, besides the two pairs of centrioles, dot-like, anti-Spd2 positive signals were visible (Fig. 32, lower panel), reminiscent of extra-centrosomes seen in primary spermatocytes (Fig. 31, d).

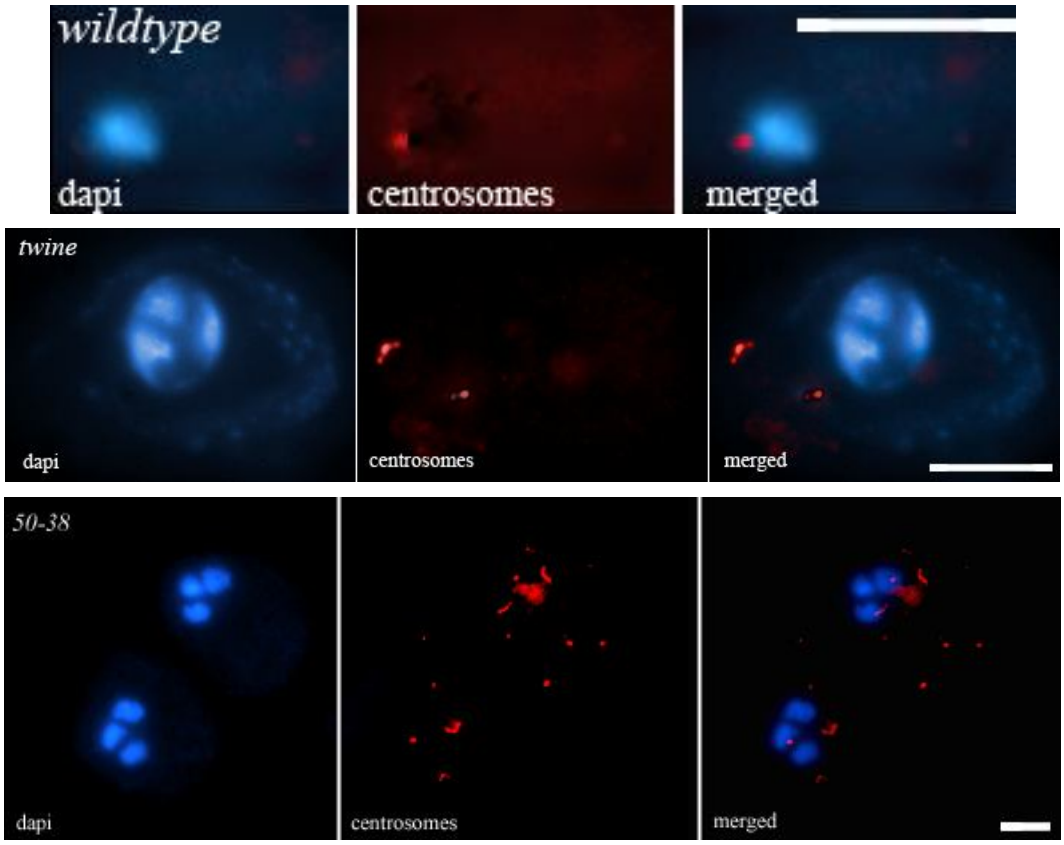

Fig. 32 Immunohystochemistry on fixed cells. DNA and centrosomes stainings. Onion stage spermatids.
Upper panel: *wildtype* onion stage spermatid. Middle panel: *twine* onion stage spermatid. Scale bars 10 μm. Lower panel: *50-38* onion stage spermatids. Scale bar: 10 μm. In all panels, from left to right: dapi staining (blue), centrosomes immunostaining (red) and merged image. DNA is visualized by DAPI staining. The Ab used to recognize centrosomes is anti-Spd2, a centriolar constituent.

5. DISCUSSION

In the previous chapter I showed the results obtained by the study carried out on a set of male sterile mutants belonging to Zuker Collection. An approximate *in vivo* cytological characterization of these 13 mutations, performed in the Wakimoto's laboratory, in Seattle, classified them as *twine*-like phenotype, owing to their difficulty to properly execute male meiotic divisions, yet exhibiting some spermatid differentiation. Complementation analysis carried out in transheterozygous condition with twe^{HB5} allele, showed that *12-228, 50-38, 60-40, 54-23* and *83-28* mutations fail to complement *twe* mutation for male sterility (Tab.1). *83-28* was not taken in consideration in this research project because data from Wakimoto's laboratory indicated it as *twine* allele. As for the other four mutations, their failure to complement *twine* together with their cytological phenotype strongly resembling that of twe^{HB5}, are both strong clues they are *twine* alleles. Gene mapping of *12-228* to 2R allowed to rule out it is allelic to *twine*, whereas *50-38, 60-40* and *54-23* mutations map close to *twine* locus on 2L, further strengthening that they are new alleles of *twine*. Alternatively, they could identify new genes, mapping very close to *twine* and sharing the same cytological phenotype, or these stocks could possess a second-site mutation, right in *twine* gene, responsible for their *twine*-like phenotype. The hypothesis of a second-site mutation is also proper for *12-228* stock, which could have, in addition to the mutation on 2R, a second mutation in *twine* underlying the mutant meiotic phenotype. Moreover, *Z*-lines Collection is well known to have been heavily mutagenized by EMS-treatment, further supporting the presence of multiple mutations on chromosome 2, selected for male sterility.

Chromosome cleaning, i.e. the recombination-mediated elimination of the *twine* region from the original mutated chromosome 2 shed light on the true nature of the male sterile mutations. Chromosome cleaning of *60-40, 54-23* and *12-228* stocks led to the loss of mutant meiotic phenotype, although the male sterile phenotype was retained. These findings suggest the presence in the original mutant chromosome of at least two mutations, one responsible of the male sterility and another one, likely located in the *twine* gene, contributing to the mutant meiotic phenotype, which was lost in the clean chromosome. On the other hand, the clean strain *50-38* retained both sterile and meiotic phenotype, thus, ruling it out as potential *twine* allele. As a whole, these conclusions were strengthened by the outcomes of *twine* sequencing. The alignment of *twine* aminoacidic sequence with the mitotic paralog *string* from *Drosophila*, the three *cdc25* homologs isolated from humans (CDC25A, CDC25B, CDC25C) (Sadhu et al., 1990; Galaktionov and Beach, 1991) and the cdc25 protein from *S.pombe* (Russell and Nurse, 1986) revealed extensive similarities in the C-terminal domain, allowing to identify the HC motif, a sequence containing residues essential for catalysis that are conserved in all the tyrosyl phosphatases (Courtot et al., 1992). The mutation

found in *twine* sequence of *60-40* strain is a missense non-conservative substitution (Gly to Arg) in the ORF, which affects an aminoacid which is identical in all the cdc25 homologs. The mutation in *twine* sequence of *54-23* stock is downstream of the active site, and as in *60-40*, it changes a conserved non-polar aminoacidic residue (Pro) into a polar (Ser) aminoacid. *12-228* strain showed two mutations in *twine* ORF; the former was in the N-terminal region which, by aminoacidic sequence comparison of cdc25 homologs does not display similarities except for two motifs (Courtot et al., 1992). Such a mutation caused the switch from a basic (polar and positively charged) aminoacid (His) to a polar and neutral one (Gln). The latter was a non-sense mutation that generated the transition from an Arginine to a stop codon, downstream of the catalytic motif. The mutations found in *twine* ORF of *60-40, 54-23* and *12-228* strains altered positions which are identical in all the studied cdc25 homologs, except for *12-228* strain where, however, two mutations are present and one of these gives rise to a truncated protein, devoid of 55 aminoacids. The identity of *twine* sequence with cdc25 of *S.pombe* and the three human homologs is not high (22-28%), differently from *twine* and *string* that share 43% identity (Courtot et al., 1992). This low sequence similarity strongly suggest that the conserved regions are likely essential for the proper functionality of the protein. A missense non-conservative mutation in these regions could be deleterious for the catalytic activity of the enzyme.

All the point mutations identified in the *Z*-lines I analyzed but one, were G/C to A/T transitions, consistent with the preponderance of G/C to A/T transitions seen in previous studies of EMS-induced mutations in *Drosophila* (Bentley et al., 2000; Winkler et al., 2005). Such a result is probably the result of the guanine alkylating activity of EMS (Cooper et al., 2008).

The only data about *twine* regulatory region came from the paper by Maines and Wasserman in 1999, describing a hypomorphic allele of *twine*, generated by a mutation 418 base pairs upstream of the *twine* ORF. I designed the *twine* sequencing experiments in *60-40, 54-23, 50-38* and *12-228* strains in order to obtain the entire *twine* genomic sequence, spanning the whole ORF and the 5' region up to the first bases of the *CG4935*, the closest gene 5' of *twine*. To date, the promoter elements conferring testis-specificity are poorly characterized. Early studies have been carried out on the testis-specific beta tubulin isoform, β*2tubulin*, which is, astonishingly, regulated by a relatively short promoter (53bp plus the first 71bp of the 5'UTR). Later, other testis-specific genes have been found that require small control elements (Michiels et al., 1989; White-Cooper, 2009). Little is known about signature sequences for testis-specific expression and the system conferring testis specificity to gene expression remains still unresolved.

Twine sequencing in *50-38* strain revealed the absence of mutations in the *twine* sequence as well as in its regulatory region, consistent with chromosome cleaning results. Accordingly, *50-38* stock has

only a mutation, accounting for meiotic and sterile phenotype, localized on chromosome 2, close to *twine* locus. On the other hand, a significant clustering of testis-specific genes has been found in the *Drosophila* genome, probably related to higher order chromatin structure in primary spermatocytes (White-Cooper, 2009). A more refined recombination mapping will allow to finely assess the position of such a mutation in the 2^{nd} chromosome.

The behaviour of *50-38* mutants was fully comparable with that of twe^{HB5} mutants, since both of them displayed only 16-cell cysts (Fig.26), diagnostic of a failure to accomplish both meiotic divisions. The exact stage of cell cycle arrest is at early prometaphase, when homologs are visible as three condensed clumps attached to the inner membrane of nuclear envelope, which, therefore, is still present, as evidenced by the staining with anti-lamin antibody (Fig.30). Figures of canonical meiotic spindles and chromosomes congregated in metaphase plate were never visible in both mutants (Fig.31). This cytological characterization of twe^{HB5} phenotype is partially in contrast with that of White-Cooper et al. (1993) who reported that in twe^{HB5} mutants nuclear envelope breakdown still occurred. On the other hand, Eberhart and Wasserman in 1995 showed that in *twine* homozygotes some chromosome condensation occurred, no spindle formed and the nuclear lamin did not disperse or degrade until spermatid differentiation had occurred; however, in full agreement with what I found. Centrosomes partially migrated in both mutants, and they were not able to arrange microtubule-dense asters. Additional dot-like centrosomes, seen in *50-38* primary spermatocytes and further visible in spermatids as well (Fig.31 and 32), may be diagnostic of either abnormal cycles of centrosome duplication or defective centrosome migration during the previous mitotic divisions.

The growth phase of primary spermatocyte usually lasts 3.5 days during which cell increases its nuclear volume, due to a high transcriptional activity, necessary to transcribe most of the genes underlying meiosis and spermiogenesis processes. These transcripts are then regulated post-transcriptionally to ensure the proper timing of the processes they handle. However, in a recent paper it has been shown that transcription does not fully shut off at the end of growth phase but rather it stops during meiotic divisions and re-starts in the elongating spermatids, immediately before the histone-protamine transition at late canoe stage (Rathke et al., 2007; Barreau et al., 2008). Except for these few genes, the growth phase seems to be extremely important to allow that the transcriptional program is fully accomplished, in order to get the cell ready to properly carry out meiotic divisions and spermatid differentiation. Primary spermatocytes have to reach the correct cell size, in order to coordinate the initiation of meiotic division and differentiation (Franklin-Dumont et al., 2007). Consistent with this, *twine* and *50-38* primary spermatocytes seem to spend less time than *wildtype* in growth phase (Fig.27), thus indicating that the defect appears before the

beginning of meiotic cell cycle. The relative higher number of onion stage cysts than *wildtype* (Fig.27) is justified by a brief growth phase span and the skip of the two meiotic divisions. The absence, on the one hand, of a strong monitoring system, able to arrest the development of abnormal male germ line cells, when necessary, and the presence, on the other hand, of several morphological processes that, as revealed by genetic analysis, are independently regulated, allow to explain the observation of partially differentiated spermatid cysts in *50-38* and *twine* mutants, despite the failure of the previous meiotic events.

Recombination mapping carried out to localize the *twine*-complementing mutation *71-43* on chromosome 2, allowed to accurately assess the map position of such a mutation (Fig.4). Then, taking advantage of available molecularly mapped deficiencies, I was able to narrow down the region where *71-43* maps down to 40952bp. Many genes are embedded in this interval (Fig.7). Some of them are mapped to the sequence whereas some others are mapped to the interval but not to the sequence. I investigated, by complementation analysis, also the possibility that *71-43* was an allele of one of this second class of genes, focusing my attention on the most interesting ones, like *humpy*, since it showed a male sterile phenotype, and *CG15675* because it was fully uncharacterized. However, the outcomes allowed to discard them as potential candidates for *71-43* gene. Among the genes mapped to the sequence, there are some extremely attractive because of their molecular function or abundance of expression in testis. For example, *CG10082* has been described to have an inositol or phosphatidylinositol kinase activity. Plasma membrane at the cell equator has been shown to be enriched in phosphatidylinositol (PtdIns) molecules, required, because of their biophysical properties, for a successful cytokinesis (Szafer-Glusman et al., 2008). This gene, together with others considered as good candidates for *71-43* gene, was tested by complementation in transheterozygous condition with *71-43* mutation, taking advantage of the availability of their alleles, but none of them furnished evidences of allelism with *71-43*. However, such a kind of analysis is not resolving, because the outcome of the complementation test might depend on the penetrance or expressivity of the tested allele. Alternatively the mutation could affect an isoform not acting in the spermatogenesis process. In addition to this genetic approach, a second approach, based on proteomics, was exploited for the molecular identification of *71-43* locus. Among the genes mapped to the minimal *71-43* interval and not genetically tested, there are *CG30284*, which seems to have a testis-specific expression; *Rae* and *CG9865*, that show some ESTs in the testis; *NC2alpha*, which has a transcriptional repressor activity; *CG15676*, involved in the biological process of protein folding; *CG10306*, that has a translational initiation factor activity and is expressed in several tissues, including testis; and *Tbp* (TATA-binding protein), a well known transcriptional initiation factor. However, the putative protein spots corresponding to these genes

did not show differences in homozygote mutants with respect to heterozygotes. On the other hand, from the Mass Spectrometry comparative study of the whole proteomic profiles of *71-43/CyO vs 71-43/71-43* testes, some interesting polypeptides were identified as being differentially expressed in wildtype *vs* mutant condition, whose coding genes do not map to the *71-43* interval. In such an analysis, only spots that differed for presence/absence of the protein were taken under exam (qualitative analysis), whereas differences in terms of quantity of protein expression (quantitative analysis) were not considered at the moment, because they would have need more experiments to validate the outcomes. Misregulated proteins in *71-43* mutants were categorized into functional groups (Tab. 4). Apart from the genes whose function is unknown (*CG1979* and *CG1324*), the most informative spots evident in wildtype gel and absent in mutant gel identified a "comet" gene, called *spaw*, which codifies for a protein homologous to proteins with the DM6, a cystein-rich domain (Barreau et al., 2008) and the CG31169, whose predicted function is glycerol-3-phosphate dehydrogenase. According to Flybase website, the protein codified by CG31169 is involved into the metabolism of glycerol-3-phosphate that, eventually, generates energy. Such a result would be consistent with the absence of motility of the mutant sperms, which is, definitely, due to the impairment of energy production into the mitochondria along the mutant sperm tails. Interestingly, most of the spots visible in the mutant gel and absent in the wildtype one, identified polypeptides involved in protein/DNA metabolism and redox and ion homeostasis, both processes diagnostic of stress conditions. *Smt3* or *sumo*, indeed, codifies for a ubiquitin-like protein whereas *CG17331* and *pros35* codify for proteasome components, which, in turns, has been shown to be related not only to a general house-keeping role but also to the turnover or processing of abnormal polypeptides arising as a result of a mutation or damage and that can potentially interfere with normal cell function (Yuan et al., 1996). *CG17331* was particularly noteworthy since it, normally, does not show ESTs in the testis, thus, its presence into the mutant testes and absence in the wildtype one, suggested a real alteration of normal protein degradation pathway. Also the heat-shock proteins identified into the mutant gel are symptomatic of a stressed environment. Among these, Hsp83 (or Hsp90) shows a male-sterile allele, whose phenotype is characterized by defects in microtubule dynamics (Yue et al., 1999). A gene extremely interesting both for map position (close to the region where *71-43* maps) and molecular function, *CG10540*, normally not expressed in the testis, as evidenced by the absence of testis ESTs, turned out to be present into the protein profile of *71-43* mutant testes. This gene codifies for the capping protein alpha, a cellular component of dynactin complex, also involved into actin cytoskeleton organization (data from Flybase). The dynein-dynactin complex has been shown to play essential functions underlying a correct spermatogenesis process and the alteration of the pathways where such a complex acts, gives rise to several defects (Li et al., 2004),

most of them are comparable to those evident in *71-43* mutant homozygotes (see below). The deficiency which destroys the function of this gene was, actually, already tested in heterozygous condition with *71-43* mutation, resulting into fertility of the hemizygote males, nonetheless, a complementation test of the transheterozygotes for *71-43* mutation over *CG10540* mutated allele is in progress.

2D-IEF-SDS PAGE is an innovative proteomics approach that, however, is unable to reveal all the proteins expressed in a cell or a tissue (Takemori et al., 2009). It, indeed, shows some limits as, for example, the pH range that, necessarily, restricts the search of the protein I'm interested in, to only those polypeptides included into the established range (in this case between 3 and 10). Nonetheless, only one gene (*CG302-84*) embedded into the region where *71-43* would map, codifies for a protein with a theoretical isoelectric point upper than 10 (Tab. 3).

Another drawback of such a technique is given by the fact that, in the most of the cases, proteins which have a high pH do not manage to be separated by the second dimension and tend to remain on the strip of the first dimension, not allowing to visualize them on the gel. In spite of these limits, 2D-IEF remains, definitely, a powerful method of analysis of the protein components of male reproductive system in *Drosophila* (Takemori et al., 2009).

Taken together, the results come out via forward and reverse genetic approaches, did not allow to identify the putative protein encoded by the mutated gene in *71-43* homozygotes; however, they provided intriguing clues about the putative pathways where the gene I'm looking for could act and, therefore, new roads to pursue.

The analysis of *in vivo* cytology of *71-43* onion stage spermatids showed large nuclei and variable sized Nebenkernes (mostly, huge Nebs), in comparison with wildtype spermatids (Fig.9). Moreover, the comparison of testes between *71-43* homozygous mutants and hemizygotes did not reveal substantial differences of phenotype (Fig.9). This may induce to hypothesize that the allele I've been handling can be a null mutation, since its action was comparable with that originating by the absence of the gene, caused by a chromosomal deletion. Once verified that the male sterile phenotype visible in *71-43* flies depended solely on a mutation on chromosome 2 right arm, all the further cytological experiments, carried out to characterize the mutant phenotype, were conducted on the homozygotes for the original *71-43* chromosome. *71-43* male mutants showed no 32-cell or 64-cell cysts, diagnostic of a failure of accomplishing both meiotic divisions, but they, surprisingly, exhibited peculiar cysts with a variable number of nuclei ranging from 16 to 32 (Fig.11). A likely explanation of this finding is that in such cysts a subset of primary spermatocytes undertook one meiotic division. Cells which undertook one meiotic division, in some cases, did not carry it out properly, producing cells with variable sized nuclei, diagnostic of defects of chromosome

segregation. Furthermore, immunofluorescence experiments provided proof of an extreme segregation distortion with all chromosomes segregating to only one pole (Fig.17). The final outcome was the presence of meiotic cysts constituted by spermatids with a large diploid nucleus associated with a variable sized nebenkern and spermatids with only a variable sized nebenkern and no nucleus. My findings are indicative, on a side, of a failure of nuclear division and, on the other side, of a failure of cytokinesis that gives rise to larger nebenkernes than wildtype even if, sometimes, a correct cellular division takes place that allows mitochondria to be evenly partitioned between the two daughter cells. At the basis of these defects there is an impairment of meiotic cell cycle machinery, more precisely, of meiotic spindle and centrosomes, as immunostaining with antibodies against α-tubulin and Spd2, a centriolar constituent (Fig.15 and 16), disclosed (see below). Strikingly enough, the few *71-43* primary spermatocytes that accomplished a defective first meiotic division, (first meiotic division was recognizable by the centrosome composition, constituted of a pair of centrioles), yet they failed to execute the second meiotic division. Such a behaviour is different from what is reported in the literature. Bucciarelli et al. (2003), for example, showed that *fusolo* and *solofuso* mutants, where the achromosomal spermatocytes II entered meiosis II, assembled an apparently normal spindle, initiated anaphase, organized a central spindle, and underwent cytokinesis, despite the absence of chromosomes. The lacking of an efficacious spindle checkpoint in *Drosophila* spermatocytes, as the experiments by Rebollo and Gonzalez had shown in 2000, and the existence of several independent mechanisms underlying spermatogenesis program with little cross talk between pathways, should allow the execution of the second meiotic division in *71-43* mutants, despite the impairment of the previous events. As I said in the Introduction, the regulation of second meiotic division is poorly understood. No genes have been identified for which loss-of-function mutations specifically block MII. The only evidence is about *Dmcdc2*, *twine* and *roughex*, that have been shown to play a critical role in control of MII (See Paragraph 1.5).

The frequency of spermatid cysts at onion stage is relatively higher in *71-43* mutants than *wildtype* (Fig. 12) right because of the absence of cysts at second meiosis.

On the basis of an approximate cytological analysis, *71-43* mutant was first classified as meiotic mutant, for its resemblance with the phenotype of *twine*. My detailed investigation, revealed defects, that precede the beginning of meiotic cell cycle. Nuclear herniations were visible in young primary spermatocytes, before they entered growth phase (Fig.9 and 13). Accordingly, the *71-43* main defect could affect primary spermatocytes well before they arrange the machinery of meiotic divisions. Hence, two hypothesis could be guessed: the former is that the gene influenced by the mutation is involved in such a function that allows to explain all the defects seen in *71-43* mutant spermatogenesis. This model is reasonable, especially in the light of the recent findings about

asunder mutants. The protein product of *asunder* is required for a correct perinuclear localization of dynein-dynactin complex in spermatocytes and spermatids. The loss of function of such a gene causes spermatocytes exhibit severe defects in meiotic spindle assembly, chromosome segregation and cytokinesis, while postmeiotic spermatids show loss of nucleus-basal body attachment, round nuclei, spread out all over the bundle and individualization defects (Anderson et a., 2009). Hence, *Asunder* mutants display multiple anomalies, very similar to those of *71-43*. Based on this, a model could be exploited to explain all the defects visible in *71-43* mutant males as originating from the alteration of only one gene, controlling many pathways. Nuclear pore complexes have been proposed as likely candidates for sites of dynein-dynactin attachment to the nuclear envelope (Salina et al., 2002). Nuclear evaginations visible in *71-43* primary spermatocytes are reminiscent of the herniations near the nuclear pore complexes described in the *Nup154* mutant spermatocytes (Gigliotti et al., 1998) as well as in some nucleoporin yeast mutants (Wente and Blobel, 1993; Bastos et al., 1995). Consistent with these data, *71-43* gene could codify a protein involved in the formation or the functioning of nuclear pores, which, in turn, are essential for a correct localization of dynein-dynactin complex to nuclear envelope. In support of this model, another analogy to *Nup154* mutants should be taken into consideration: no evident defects in lamin localization were observed in *71-43* mutants (Fig.13), indicating that such a mutation did not affect the overall integrity of the nuclear envelope. Hence, any impairment of this pathway underlying the proper localization of dynein-dynactin complex would provoke the series of defects displayed in *asunder* and *71-43* mutants.

The latter hypothesis is that the mutation *71-43* is responsible for a rather early defect during spermatogenesis, that indirectly might compromise the correct accomplishment of further events, originating a cascade of defects. Consequently, a cumulative effect of impairments, starting from the primary defect due to the mutation, is responsible for the multiple defects evident in *71-43* mutant phenotype. This is consistent with the abnormalities caused by hypomorphic mutations. When the intensity of a mutation is not very strong, the ensuing mutant phenotype is not very severe. In this case, instead of blocking the execution of both meiotic divisions, mutant cells undertake meiosis, yet not resulting in normal diploid spermatids. However, the similarity of phenotype of mutant *71-43* homozygotes with hemizygotes suggests that we have been handling a presumably null mutation, thus, favouring the former hypothesis rather than the latter.

Only the molecular identification of the *71-43* gene, and, hence, the discovery of its function, will allow to discern between these hypotheses.

Given the correlation between aster, central spindle microtubules and mitochondria inheritance suggested by Ichihara et al. in 2007, variabled sized nebenkernes seen in *71-43* mutants could be

diagnostic of impairments of such structures. Indeed, immunofluorescence experiments showed asters exhibiting misoriented microtubules and central spindles formed by a paucity of microtubules, often not aligned along spindle axis (Fig.15 and 19), thus providing a proof in support of an uneven mitochondria partition. However, the presence of onion stage cells with Nebs of different sizes is in contrast with a cytokinetic phenotype, suggested by the failure of acto-myosin ring assembly in *71-43* mutants, since the failure of cytoplasm division should give rise to a large nebenkern associated with a number of nuclei, depending on the accomplishment of nuclear divisions.

The later defects observable during spermiogenesis of *71-43* mutants, affecting cyst polarization (Fig.23), are likely due to the loss of basal body-nucleus anchoring. It has been proposed a model where dynein-dynactin complex would interact with the microtubules of dense complex in order to mediate the nuclear attachment of basal body (Li et al., 2004). Hence, the impairment of such a system would cause the basal body to be mislocalized, preventing polarization of spermatid heads of a bundle, and causing the nuclei to spread out all over the bundle as observed in *71-43* mutants.

The large round nuclei visible in *71-43* elongating spermatids also displayed uncondensed chromatin, in contrast with the extremely dense and compact chromatin of *wildtype* spermatids (Fig.22). Such an uncondensed state of chromatin could be responsible for the abnormal nuclear shape of these spermatids preventing nuclei from shifting to a needle shape. Chromatin defects were already apparent in the primary spermatocytes, at prometaphase, where chromatin seemed to be strongly disorganized and decondensed instead of being condensed and arranged into three masses, corresponding to bivalents (Fig.14). A likely hypothesis might be that such chromatin condensation defects would contribute to chromosome misalignment and missegregation in *71-43* mutants. A marker of condensed chromatin state, immediately before entering meiosis is the phosphorylation of Serine 10 of histone 3. An investigation about the presence of this post-translational histone modification in prometaphase mutant spermatocytes would be worth to be performed. The impairment of epigenetic modifications underlying higher order chromatin structure could be responsible for the abnormal chromatin state of later stages of spermatogenesis, as well.

The analysis of centrosome behaviour during spermatogenesis was carried out by means of an antibody directed against Spd2, a centriolar constituent, allowing to reveal the presence of multiple and mislocalized centrosome foci in *71-43* mutant spermatocytes. Giansanti et al., in 2008, showed that Spd2 acted downstream of Asl but upstream of Cnn, γ-tubulin, Dgrip91 and D-TACC. According to this, it could be hypothesized an impairment of the centrosome assembly pathway; thus, an analysis of the localization of these proteins acting downstream of Spd2 could provide

whether a proper centrosome formation and ensuing localization and function are compromised in *71-43* mutants.

The *71-43* mutation also affects female fertility. This finding let hypothesize that the mutation acts in a process which is conserved in both males and females. Hence, the *71-43* gene must act at an early stage of germ cell development in males and females, since the later stages of oogenesis and spermatogenesis are strikingly different, and probably under a sex-specific genetic control. Consistent with this idea, the homologous pairing and recombination, which occurs only in female and not in male meiosis, may definitely be ruled out as potential process affected by the mutation *71-43*. However, it's worth to be noticed that such a mutation induced 100% of sterility in male homozygotes whereas most of the *71-43* homozygote females exhibited reduced fertility, suggesting a redundant function for this gene in oogenesis.

Another feature of the *71-43* mutant phenotype has come from the estimate of mitotic index in the larval brains. *Drosophila* brains contain mostly neuroblasts (NBs) and ganglion mother cells (GMCs). NBs are stem cells that divide asymmetrically, giving rise to another NB and a smaller GMC which, instead, divides symmetrically just once to generate equally sized daughter cells that differentiate into neurons or glia. The finding of a statistically significant lower mitotic index in mutant *vs* wildtype brains allowed to classify *71-43* flies as mitotic mutants as well. The influence of this mutation on mitosis could bear as a consequence the delayed development of mutant flies and/or lethality. However, from the score of the progeny of many independent crosses between *Rec#57/St, Cy Tb* heterozygous males and females, I observed frequencies of homozygotes and heterozygotes nearly identical to the expected ones, thus, ruling out the possibility of a negative effect of the mutation either on development or vitality of the flies. In order to understand the reason why fewer mitotic cells were scored in mutant brains in comparison with wildtype ones, it will be informative to check structure and functionality of the mitotic apparatus, i.e. spindle and centrosomes.

Collectively, these data provide the evidence of conserved mechanisms underlying meiosis and mitosis. Actually, many works on yeast, frogs and other species, had already demonstrated that mitosis regulators, also act during male meiosis in *Drosophila* (reviewed by Nurse, 1990). An important regulator of entry into mitosis is the phosphatase encoded by *cdc25* gene. The *cdc25* gene was initially identified in *Schizosaccharomyces pombe* (Russel and Nurse, 1986) and later its *Drosophila* homolog was found at the *string* locus (Edgar and O'Farrell, 1989). Mutations in the *cdc25* and in *string* block the mitotic cell cycle at G2-phase. In *Drosophila*, a second *cdc25* phosphatase homolog (*twine*) was identified in 1992 (Courtot et al., 1992). As I've already said in the Introduction, *twine* does not operate during mitosis, but it is required only in meiosis, and

mutations in *twine* do not affect the embryonic development or viability of the fly (Alphey et al., 1993; Courtot et al., 1992; White-Cooper et al., 1993). Thus, *twine* is an example of a germ line-specific gene, whereas *71-43*, even though mainly expressed in testis, given the full penetrance of male sterile phenotype, should also present somatic expression since the mitotic index is also affected. Once molecularly identified the gene affected by the mutation in *71-43* strain, experiments, to finely assess the tissue expression pattern of *71-43* gene, will be, definitely, need.

6. REFERENCES

Adams R.R., Tavares A.A., Salzberg A., Bellen H.J. and Glover D.M.
Pavarotti encodes a kinesin-like protein required to organize the central spindle and contractile ring for cytokinesis. (1998)
Genes Dev. 12, 1483-1494.

Adams R.R., Maiato H., Earnshaw W.C. and Carmena M.
Essential roles of *Drosophila* inner centromere protein (INCENP) and aurora B in histone H3 phosphorylation, metaphase chromosome alignment, kinetochore disjunction, and chromosome segregation. (2001)
J. Cell Biol. 153, 865-880.

Aldridge A.C., Benson L.P., Siegenthaler M.M., Whigham B.T., Stowers R.S. and Hales K.G.
Roles for Drp1, a Dynamin-Related Protein, and Milton, a Kinesin-Associated Protein, in mitochondrial segregation, unfurling and elongation during *Drosophila* spermatogenesis. (2007)
Fly 1(1), 38-46.

Alphey L., Jimenez J., White-Cooper H., Dawson I., Nurse P. and Glover D.M.
twine, a cdc25 homolog that functions in the male and female germline of Drosophila. (1992)
Cell 69(6): 977-88.

Anderson M.A., Jodoin J.N., Lee E., Hales K.G., Hays T.S. and Lee L.A.
asunder is a critical regulator of dynein-dynactin localization during *Drosophila* spermatogenesis.
Mol. Biol. Cell 20, 2709-2721.

Baker C.C. and Fuller M.T.
Translational control of meiotic cell cycle progression and spermatid differentiation in male germ cells by a novel eIF4G homolog. (2007)
Development 134, 2863-2869.

Baker B. and Hall J.
Meiotic mutants: genetic control of meiotic recombination and chromosome segregation. (1976)
The Genetics and Biology of Drosophila 351-434.

Barreau C., Benson E., Gudmannsdottir E., Newton F. and White-Cooper H.
Post-meiotic transcription in *Drosophila* testes. (2008)
Development 135, 1897-1902.

Bastos R., Pantè N. and Burke B.
Nuclear pore complex proteins. (1995)
Int. Rev. Cytol. 162, 257-302.

Basu J. and Li Z.
The Des-1 protein, required for central spindle assembly and cytokinesis, is associated with mitochondria along the meiotic spindle apparatus and with the contractile ring during male meiosis in *Drosophila melanogaster*. (1998)
Mol. Gen. Genet. 259, 664-673.

Beall E.L., Lewis P.W., Bell M., Rocha M., Jones D.L. and Botchan M.R.
Discovery of tMAC: a *Drosophila* testis-specific meiotic arrest complex paralogous to Myb-Muv B. (2007)
Genes & Development 21, 904-919.

Bentley A., MacLennan B., Calvo J. and Dearolf C.R.
Targeted recovery of mutations in *Drosophila*. (2000)
Genetics 156, 1169-1173.

Bonaccorsi S., Pisano C., Puoti F. and Gatti M.
Y chromosome loops in *Drosophila melanogaster*. (1988)
Genetics 120, 1015-1034.

Bonaccorsi S., Giansanti M.G. and Gatti M.
Spindle self-organization and cytokinesis during male meiosis in *asterless* mutants of *Drosophila melanogaster*. (1998)
J. Cell Biol. 142(3), 751-761.

Bridges C.B.
Non-disjunction as a proof of the chromosome theory of heredity. (1916)
Genetics 1: 1-52 and 107-163.

Brill J.A., Hime G.R., Scharer-Schuksz M. and Fuller M.T.
A phospholipid kinase regulates actin organization and intercellular bridge formation during germline cytokinesis. (2000)
Development 127, 3855-3864.

Bucciarelli E., Giansanti M.G., Bonaccorsi S. and Gatti M.
Spindle assembly and cytokinesis in the absence of chromosomes during *Drosophila* male meiosis. (2003)
J. Cell Biol. 160(7), 993-999.

Candiano, G., Bruschi, M., Musante, L., Santucci, L., Ghiggeri, G. M., Carnemolla, B., Orecchia, P., Zardi, L., Righetti, P. G.
Blue silver: a very sensitive colloidal Coomassie G-250 staining for proteome analysis. (2004) Electrophoresis 25, 1327-33.

Carmena M., Riparbelli M.G., Minestrini G., Tavares A.M., Adams R., Callaini G. and Glover D.M.
Drosophila polo kinase is required for cytokinesis. (1998)
J. Cell Biol. 143, 659-671.

Cenci G., Bonaccorsi S., Pisano C., Verni F and Gatti M.
Chromatin and microtubule organization during premeiotic, meiotic and early postmeiotic stages of *Drosophila melanogaster* spermatogenesis. (1994)
Journal of Cell Science 107, 3521-3534.

Ceprani F., Raffa G.D., Petrucci R. and Piergentili R.
Autosomal mutations affecting Y chromosome loops in Drosophila melanogaster. (2008)
Genetics 9:32.

Chen X., Hiller M., Sancak Y. and Fuller M.T.
Tissue-specific TAFs counteract Polycomb to turn on terminal differentiation. (2005)
Science 310, 869-872.

Church K., Nicklas R.B. and Lin H.P.
Micromanipulated bivalents can trigger mini-spindle formation in *Drosophila melanogaster* spermatocyte cytoplasm. (1986)
J. Cell Biol. 103, 2765-2773.

Courtot C., Fankhauser C., Simanis V. and Lehner C.F.
The Drosophila cdc25 homolog twine is required for meiosis. (1992)
Development 116(2): 405-16.

Cooper J.L., Greene E.A., Till B.J., Codomo C.A., Wakimoto B.T. and Henikoff S.
Retention of induced mutations in a *Drosophila* reverse-genetic resource. (2008)
Genetics 180, 661-667.

Day J.W. and Grell R.F.
Synaptonemal complexes during premeiotic DNA synthesis in oocytes of Drosophila melanogaster. (1976)
Genetics 83(1), 67-79.

Deng H., Dodson M.W., Huang H. and Guo M.
The Parkinson's disease genes *pink1* and *parkin* promote mitochondrial fission and/or inhibit fusion in *Drosophila*. (2008)
PNAS 105(38), 14503-14508.

Dunphy W.G. and Newport J.W.
Fission yeast p13 blocks mitotic activation and tyrosine dephosphorylation of the Xenopus cdc2 protein kinase. (1989)
Cell 58(1): 181-91.

Eberhart C.G. and Wasserman S.A.
The *pelota* locus encodes a protein required for meiotic cell division: an analysis of G2/M arrest in *Drosophila* spermatogenesis. (1995)
Development 121, 3477-3486.

Edgar B.A. and O'Farrell P.H.
Genetic control of cell division patterns in the Drosophila embryo. (1989)
Cell 57(1): 177-87.

Edgar B.A. and O'Farrell P.H.
The three postblastoderm cell cycles of Drosophila embryogenesis are regulated in G2 by string. (1990)
Cell 62(3): 469-80.

Fabrizio J.J., Hime G., Lemmon S.K. and Bazinet C.
Genetic dissection of sperm individualization in Drosophila melanogaster. (1998)
Development 125, 1833-1843.

Farkas R.M., Giansanti M.G., Gatti M. and Fuller M.T.
The *Drosophila* Cog5 homologue is required for cytokinesis, cell elongation, and assembly of specialized Golgi architecture during spermatogenesis. (2003)
Mol. Biol. Cell 14, 190-200.

Franklin-Dumont T.M., Chatterjee C., Wasserman S.A. and DiNardo S.
A novel eIF4G homolog, Off-schedule, couples translational control to meiosis and differentiation in *Drosophila* spermatocytes. (2007)
Development 134, 2851-2861.

Fuller M.T.
Spermatogenesis. (1993)
In *The development of Drosophila melanogaster*. Vol 1, 71-147.

Fuller M.T.
Genetic control of cell proliferation and differentiation in *Drosophila* spermatogenesis. (1998)
Cell & Dev. Biol. 9, 433-444.

Galaktionov K. and Beach D.
Specific activation of cdc25 tyrosine phosphatases by B-type cyclins: evidence for multiple roles of mitotic cyclins. (1991)
Cell 67, 1181-1194.

Gao S., Giansanti M.G., Buttrick G.J., Ramasubramanyan S., Auton A., Gatti M. and Wakefield J.G.
Australin: a chromosomal passenger protein required specifically for *Drosophila melanogaster* male meiosis. (2008)
J. Cell Biol. 180(3), 521-535.

Gatt M.K. and Glover D.M.
The *Drosophila* phosphatidylinositol transfer protein encoded by *vibrator* is essential to maintain cleavage-furrow ingression in cytokinesis. (2006)
J. Cell Sci. 119, 2225-2235.

Gatti M. and Baker B.S.
Genes controlling essential cell-cycle functions in *Drosophila melanogaster*. (1989)
Genes Dev. 3, 438-453.

Gatti M. and Goldberg M.L.
Mutations affecting cell division in *Drosophila*. (1991)
Methods Cell Biol. 35, 543-585.

Gatti M., Giansanti M.G. and Bonaccorsi S.
Relationships between the central spindle and the contractile ring during cytokinesis in animal cells. (2000)
Microscopy Research and Technique 49, 202-208.

Gautier J., Matsukawa T., Nurse P. and Maller J.
Dephosphorylation and activation of Xenopus p34cdc2 protein kinase during the cell cycle. (1989)
Nature 339(6226): 626-9.

Giansanti M.G., Bonaccorsi S., Williams B., Williams E.V., Santolamazza C., Goldberg M.L. and Gatti M.
Cooperative interactions between the central spindle and the contractile ring during *Drosophila* cytokinesis. (1998)
Genes & Dev. 12, 396-410.

Giansanti M.G., Bonaccorsi S. and Gatti M.
The role of anillin in meiotic cytokinesis of *Drosophila* males. (1999)
J. Cell Sci. 112, 2323-2334.

Giansanti M.G., Bonaccorsi S., Bucciarelli E. and Gatti M.
Drosophila male meiosis as a model system fort he study of cytokinesis in animal cells. (2001)
Cell Structure and Function 26, 609-617.

Giansanti M.G., Bonaccorsi S., Kurek R., Farkas R.M., Dimitri P., Fuller M.T. and Gatti M.
The class I PITP Giotto is required for *Drosophila* cytokinesis. (2006)
Curr. Biol. 16, 195-201.

Giansanti M.G., Belloni G. and Gatti M.
Rab11 is required for membrane trafficking and actomyosin ring constriction in meiotic cytokinesis of *Drosophila* males. (2007)
Mol. Biol. Cell 18, 5034-5047.

Giansanti M.G., Bucciarelli E., Bonaccorsi S. and Gatti M.
Drosophila SPD-2 is an essential centriole component required for PCM recruitment and astral-microtubule nucleation. (2008)
Curr. Biol. 18, 303-309.

Giet R. and Glover D.M.
Drosophila aurora B kinase is required for histone H3 phosphorylation and condensin recruitment during chromosome condensation and to organize the central spindle during cytokinesis. (2001)
J. Cell Biol. 152, 669-682.

Gigliotti S., Callaini G., Andone S., Riparbelli M.G., Pernas-Alonso R., Hoffmann G., Graziani F. and Malva C.
Nup154, a New *Drosophila* Gene Essential for Male and Female Gametogenesis Is Related to the *Nup155* Vertebrate Nucleoporin Gene. (1998)
Journal of Cell Biology 142 (5), 1195-1207.

Glotzer M., Murray A.W. and Kirschner M.W.
Cyclin is degraded by the ubiquitin pathway. (1991)
Nature 349(6305): 132-8.

Glover D.M., Leibowitz M.H., McLean D.A. and Parry H.
Mutations in *aurora* prevent centrosome separation leading to the formation of monopolar spindles. (1995)
Cell 81, 95-105.

Gonzalez C., Tavosanis G. and Mollinari C.
Centrosomes and microtubule organization during *Drosophila* development. (1998)
J. Cell Sci. 111, 2697-2706.

Gould K.L., Moreno S., Tonks N.K. and Nurse P.
Complementation of the mitotic activator, p80cdc25, by a human protein-tyrosine phosphatase. (1990)
Science 250(4987): 1573-6.

Hales K.G. and Fuller M.T.
Developmentally regulated mitochondrial fusion mediated by a conserved novel predicted GTPase. (1997)
Cell 90, 121-129.

Hiller M.A., Lin T.Y., Wood C. and Fuller M.T.
Developmental regulation of transcription by a tissue –specific TAF homolog. (2001)
Genes Dev 15, 1021-1030.

Hiller M., Chen X., Pringle M.J., Suchorolski M., Sancak Y., Viswanathan S., Bolival B., Lin T.Y., Marino S. and Fuller M.T.
Testis-specific TAF homologs collaborate to control a tissue-specific transcription program. (2004)
Development 131, 5297-5308.

Hogarth C., Itman C., Jans D.A. and Loveland K.L.
Regulated nucleocytoplasmic transport in spermatogenesis: a driver of cellular differentiation? (2005)
BioEssays 27, 1011-1025.

Huettner A.F.
Continuity of centrioles in *Drosophila melanogaster*. (1933)
Z. Zellforsch. Mikroskop. Anat. 19, 119.

Ichihara K., Shimizu H., Taguchi O., Yamaguchi M. and Inoue Y.H.
A *Drosophila* orthologue of Larp protein family is required for multiple processes in male meiosis. (2007)
Cell Structure and Function 32, 89-100.

Inoue Y.H., Savoian M.S., Suzuki T., Mathè E., Yamamoto M-T. and Glover D.M.
Mutations in *orbit/mast* reveal that the central spindle is comprised of two microtubule populations, those that initiate cleavage and those that propagate furrow ingression. (2004)
J. Cell Biol. 166(1), 49-60.

Jiang J., Benson E., Bausek N., Doggett K. and White-Cooper H.
Tombola, a tesmin/TSO1-family protein, regulates transcriptional activation in the *Drosophila* male germline and physically interacts with Always early. (2007)
Development 134, 1549-1559.

Julian M., Tollon Y., Lajoie-Mazenc I., Moisand A., Marzaguil H., Puget A. and Wright M.
γ-tubulin participates in the formation of the midbody during cytokinesis in mammalian cells. (1993)
J. Cell Sci. 105, 145-156.

Kolthur-Seetharam U., Martianov I. and Davidson I.
Specialization of the general transcriptional machinery in male germ cells. (2008)
Cell Cycle 7 (22), 3493-3498.

Kopytova D.V., Krasnov A.N., Kopantceva M.R., Nabirochkina E.N., Nikolenko J.V., Maksimenko O., Kurshakova M.M., Lebedeva L.A., Yerokhin M.M., Simonova O.B., Korochkin L.I., Tora L., Georgiev P.G. and Georgieva S.G.
Two isoforms of Drosophila TRF2 are involved in embryonic development, premeiotic chromatin condensation, and proper differentiation of germ cells of both sexes. (2006)
Mol & Cell Biol 26 (20), 7492-7505.

Krek W. and Nigg E.A.
Mutations of p34cdc2 phosphorylation sites induce premature mitotic events in HeLa cells: evidence for a double block to p34cdc2 kinase activation in vertebrates. (1991)
EMBO J. 10(11): 3331-41.

Krek W. and Nigg E.A.
Differential phosphorylation of vertebrate p34cdc2 kinase at the G1/S and G2/M transitions of the cell cycle: identification of major phosphorylation sites. (1991)
EMBO J. 10(2): 305-16.

Labbe J.C., Capony J.P., Caput D., Cavadore J.C., Derancourt J., Kaghad M., Lelias J.M., Picard A. and Dorèe M.
MPF from starfish oocytes at first meiotic metaphase is a heterodimer containing one molecule of cdc2 and one molecule of cyclin B. (1989)
EMBO J. 8(10): 3053-8.

Lee J.Y. and Orr-Weaver T.L.
The molecular basis of sister –chromatid cohesion. (2001)
Annu. Rev. Cell Dev. Biol. 17, 753-777.

Li K., Xu E.Y., Cecil J.K., Turner R., Megraw T.L. and Kaufman T.C.
Drosophila centrosomin protein is required for male meiosis and assembly of the flagellar axoneme. (1998)
Journal of Cell Biology 14(2), 455-467.

Li M.G., Serr M., Newman E.A. and Hays T.S.
The *Drosophila* tctex-1 light chain is dispensable for essential cytoplasmic Dynein functions but is required during spermatid differentiation. ((2004)
Mol. Biol. Cell 15, 3005-3014.

Liebrich W.
The effects of cytochalasin B and colchicine on the morphogenesis of mitochondria in Drosophila hydei during meiosis and early spermiogenesis. An in vitro study. (1982)
Cell Tissue Res. 224(1), 161-168.

Lifschytz E. and Meyer G.F.
Characterization of male meiotic-sterile mutations in *Drosophila melanogaster*. The genetic control of meiotic divisions and gametogenesis. (1977)
Chromosoma 64, 371-392.

Lin T.Y., Viswanathan S., Wood C., Wilson P.G., Wolf N. and Fuller M.T.
Coordinate developmental control of the meiotic cell cycle and spermatid differentiation in *Drosophila* males. (1996)
Development 122, 1331-1341.

Lindsley D. and Tokuyasu K.T.
Spermatogenesis. (1980)
In *Genetics and Biology of Drosophila*. 225-294.

Lindsley D. L. and Zimm G.G.
The genome of *Drosophila melanogaster*. (1992)
San Diego, California: Academic Press.

Llamazares S., Moreira A., Tavares A., Girdham C., Spruce B.A., Gonzalez C., Karess R.E., Glover D.M. and Sunkel C.E.
Polo encodes a protein kinase homolog required for mitosis in *Drosophila*. (1991)
Genes Dev. 5, 2153-2165.

Luetjens C.M., Xu E.Y., Rejo Pera R.A., Kamischke A., Nieschlag E. and Gromoll J.
Association of meiotic arrest with lack of BOULE protein expression in infertile men. (2004)
The Journal of Clinical Endocrinology & Metabolism 89(4), 1926-1933.

Maines J.Z. and Wasserman S.A.
Post-transcriptional regulation of the meiotic Cdc25 protein Twine by the Dazl orthologue Boule. (1999)
Nat. Cell Biol. 1, 171-174.

McCollum D.
Cytokinesis: the central spindle takes center stage. (2004)
Curr. Biol. 14, 953-955.

McKee B.D. and Karpen G.H.
Drosophila ribosomal genes function as an X-Y pairing site during male meiosis. (1990)
Cell 61, 61-72.

Metcalf C.E. and Wassarman D.A.
Nucleolar colocalization of TAF1 and testis-specific TAFs during *Drosophila* spermatogenesis. (2007)
Dev Dyn 236, 2836-2843.

Metz C.W.
Observation on spermatogenesis in *Drosophila*. (1926)
Anat 4, 1-28.

Michiels F., Gasch A., Kaltschmidt B. and Renkawitz-Pohl R.
A 14 bp promoter element directs the testis specificity of the *Drosophila* β2-tubulin gene. (1989).
EMBO J. 8(5), 1559-1565.

Mikhaylova L.M., Boutanaev A.M. and Nurminsky D.I.
Transcriptional regulation by Modulo integrates meiosis and spermatid differentiation in male germ line. (2006)
PNAS 103 (32), 11975-11980.

Mishima M., Kaitna S. and Glotzer M.
Central spindle assembly and cytokinesis require a kinesin-like protein/RhoGAP complex with microtubule bundling activity. (2002)
Dev. Cell 2, 41-54.

Monesi V.
Synthetic activities during spermatogenesis in the mouse. (1965)
Exp. Cell. Res. 39, 197-224.

Moore D.P., Miyazaki W.Y., Tomkiel J.E. and Orr-Weaver T.L.
Double or *nothing*: a Drosophila mutation affecting meiotic chromosome segregation in both females and males. (1994)
Genetics 136, 953-964.

Naim V., Imarisio S., Di Cunto F., Gatti M. and Bonaccorsi S.
Drosophila citron kinase is required for the final steps of cytokinesis. (2004)
Mol. Biol. Cell 15, 5053-5063.

Nurse P.
Universal control mechanism regulating onset of M-phase. (1990)
Nature 344(6266): 503-8.

Olivieri, G., Olivieri, A.
Autoradiographic study of nucleic acid synthesis during spermatogenesis in *Drosophila melanogaster*. (1965)
Mutat. Res. 2, 366–380.

Perezgasga L., Jiang J., Bolival B., Hiller Jr M., Benson E., Fuller M.T. and White-Cooper H.
Regulation of transcription of meiotic cell cycle and terminal differentiation genes by the testis-specific Zn-finger protein *matotopetli*.
Development 131, 1691-1702.

Rappaport R.
Experiments concerning the cleavage stimulus in sand dollar eggs. (1961)
J. Exp. Zool. 148, 81-89.

Ratan R., Mason D.A., Sinnot B., Goldfarb D.S. and Fleming R.J.
Drosophila Importin α performs paralog-specific functions essential for gametogenesis. (2008)
Genetics 178, 839-850.

Rathke C., Baarends W.M., Jayaramaiah-Raja1 S., Bartkuhn M., Renkawitz R. and Renkawitz-Pohl R.
Transition from a nucleosome-based to a protamine-based chromatin configuration during spermiogenesis in *Drosophila.* (2007)
Journal of Cell Science. 120 (9), 1689-1700.

Rebollo E. and Gonzalez C.
Visualizing the spindle checkpoint in *Drosophila* spermatocytes. (2000)
EMBO reports 1(1), 65-70.

Rebollo E., Llamazares S., Reina J. and Gonzalez C.
Contribution of noncentrosomal microtubules to spindle assembly in *Drosophila* spermatocytes. (2004)
PLOS Biology 2(1), 54-64.

Riparbelli M.G., Callaini G., Glover D.M. and do Carmo Avides M.
A requirement for the abnormal spindle protein to organise microtubules of the central spindle for cytokinesis in *Drosophila*. (2002)
J. Cell Sci. 115, 913-922.

Rupes I.
Checking cell size in yeast. (2002)
Trends Genet 18, 479-485.

Russell P. and Nurse P.
Schizosaccharomyces pombe and Saccharomyces cerevisiae: a look at yeasts divided. (1986)
Cell 45(6): 781-2.

Sadhu K., Reed S.I., Richardson H. and Russel P.
Human homolog of fission yeast cdc25 mitotic inducer is predominantly expressed in G2. (1990)
Proc. Natl. Acad. Sci. 87, 5139-5143.

Saint R. and Somers W.G.
Animal cell division: a fellowship of the double ring? (2003)
J. Cell Sci. 116, 4277-4281.

Salina D., Bodoor K., Eckley D.M., Schroer T.A., Rattner J.B. and Burke B.
Cytoplasmic dynein as a facilitator of nuclear envelope breakdown. (2002)
Cell 108, 97-107.

Sampaio P., Rebollo E., Varmark H., Sunkel C.E. and Gonzalez C.
Organized microtubule arrays in γ-tubulin-depleted *Drosophila* spermatocytes. (2001)
Curr. Biol. 11, 1788-1793.

Shevchenko A., Wilm M., Vorm O. and Mann M.
Mass spectrometric sequencing of proteins silver-stained polyacrylamide gels. (1996)
Anal. Chem. 68, 850–858.

Sigrist S., Ried G. and Lehner C.F.
Dmcdc2 kinase is required for both meiotic divisions during *Drosophila* spermatogenesis and is activated by the Twine/cdc25 phosphatase. (1995)
Mech. Dev. 53, 247-260.

Somers W.G. and Saint R.
A RhoGEF and Rho family GTPase-activating protein complex links the contractile ring to cortical microtubules at the onset of cytokinesis. (2003)
Dev. Cell 4, 29-39.

Stern B., Ried G., Cegg N.J., Grigliatti T.A. and Lehner C.F.
Genetic analysis of the *Drosophila* cdc2 homolog. (1993)
Development 117, 219-232.

Szafer-Glusman E., Giansanti M.G., Nishihama R., Bolival B., Pringle J., Gatti M. and Fuller M.T.
A role for very-long-chain fatty acids in furrow ingression during cytokinesis in *Drosophila* spermatocytes. (2008)
Curr. Biol. 18, 1426-1431.

Takemori N. and Yamamoto M.-T.
Proteome mapping of the *Drosophila melanogaster* male reproductive system. (2009)
Proteomics 9, 1-10.

Texada M.J., Simonette R.A., Johnson C.B., Deery W.J. and Beckingham K.M.
yuri gagarin is required for actin, tubulin and basal body functions in *Drosophila* spermatogenesis. (2008)
J. Cell Sci. 121, 1926-1936.

Theurkauf W.E. and Hawley R.S.
Meiotic spindle assembly in *Drosophila* females: behaviour of nonexchange chromosomes and the effects of mutations in the *nod* kinesin-like protein. (1992)
J. Cell Biol. 116, 1167-1180.

Tokuyasu K.T.
Dynamics of spermiogenesis in *Drosophila melanogaster* IV. Nuclear transformation. (1974)
J. Ultrastruct. Res. 48, 284-303.

Tokuyasu K.T.
Dynamics of spermiogenesis in *Drosophila melanogaster* V. Head-tail alignment. (1975)
J. Ultrastruct. Res. 50, 117-129.

Tomkiel J.E., Wakimoto B.T. and Briscoe A., Jr.
The *teflon* gene is required for maintenance of autosomal homolog pairing at meiosis I in male *Drosophila melanogaster*. (2001)
Genetics 157, 273-281.

Tsai J., McKee B.
Application of fluorescence in situ hybridization (FISH) in studies of heterochromatin pairing in *Drosophila* male meiosis.
Communication at the Drosophila Conference Chicago 2009.

Vader G., Medema R.H. and Lens S.M.A.
The chromosomal passenger complex: guiding Aurora B through mitosis. (2006)
J. Cell Biol. 173(6), 833-837.

Vazquez J., Belmont A.S. and Sedat J.W.
The dynamics of homologous chromosome pairing during male *Drosophila* meiosis. (2002)
Current Biology 12, 1473-1483.

Vernì F., Somma M.P., Gunsalus K.C., Bonaccorsi S., Belloni G., Goldberg M.L. and Gatti M.
Feo, the Drosophila homologue of PRC1, is required for central spindle formation and cytokinesis. (2004)
Curr. Biol. 14, 1569-1575.

Vogt N., Koch I., Schwarz H., Schnorrer F. and Nusslein-Volhard C.
The γTuRC components Grip75 and Grip128 have an essential microtubule-anchoring function in the *Drosophila* germline. (2006)
Development 133, 3963-3972.

Wakimoto B.T., Lindsley D.L. and Herrera C.
Toward a comprehensive genetic analysis of male fertility in *Drosophila melanogaster*. (2004)
Genetics 167(1), 207-216.

Wei H-C., Rollins J., Fabian L., Hayes M., Polevoy G., Bazinet C. and Brill J.A.
Depletion of plasma membrane PtdIns(4,5)P_2 reveals essential roles for phosphoinositides in flagellar biogenesis. (2008)
J. Cell Sci. 121, 1076-1084.

Wente S.R. and Blobel G.
A temperature-sensitive NUP116 null mutant forms a nuclear envelope seal over the yeasy nuclear pore complex thereby blocking nucleocytoplasmic traffic. (1993)
J. Cell Biol. 123, 275-284.

White-Cooper H., Alphey L. and Glover D.M.
The *cdc25* homologue *twine* is required for only some aspects of the entry into meiosis in *Drosophila*. (1993)
Journal of Cell Science 106, 1035-1044.

White-Cooper H., Schafer M.A., Alphey L.S. and Fuller M.T.
Transcriptional and post-transcriptional control mechanisms coordinate the onset of spermatid differentiation with meiosis I in *Drosophila*. (1998)
Development 125, 125-134.

White-Cooper H.
Molecular mechanisms of gene regulation during *Drosophila* spermatogenesis. (2009)
Reproduction (Epub ahead of print).

Williams B.W., Riedy M.F., Williams E.V., Gatti M. and Goldberg M.L.
The *Drosophila* kinesin-like protein KLP3A is a midbody component required for central spindle assembly and initiation of cytokinesis. (1995)
J. Cell Biol. 129, 709-723.

Wilson P.G., Fuller M.T. and Borisy G.G.
Monastral bipolar spindles: implications for dynamic centrosome organization. (1997)
J. Cell Sci. 110, 451-464.

Wilson P.G., Zheng Y., Oakley C.E., Oakley B.R., Borisy G.G. and Fuller M.T.
Differential expression of two γ-tubulin isoforms during gametogenesis and development in *Drosophila*. (1997)
Dev. Biol. 184, 207-221.

Winkler S., Schwabedissen A., Backasch D., Bokel C. and Seidel C.
Target-selected mutant screen by TILLING in *Drosophila*. (2005)
Genome Res. 15, 718-723.

Wright K.J., Marr II M.T. and Tjian R.
TAF4 nucleates a core subcomplex of TFIID and mediates activated transcription from a TATA-less promoter. (2006)
PNAS 103 (33), 12347-12352.

Xu H., Brill J.A., Hsien J., McBride R., Boulianne G.L. and Trimble W.S.
Syntaxin 5 is required for cytokinesis and spermatid differentiation in *Drosophila*. (2002)
Develop. Biol. 251, 294-306.

Yaffe M.P., Stuurman N. and Vale R.D.
Mitochondrial positioning in fission yeast is driven by association with dynamic microtubules and mitotic spindle poles. (2003)
PNAS 100, 11424-11428.

Yuan X., Miller M. and Belote J.M.
Duplicated proteasome subunit genes in *Drosophila melanogaster* encoding testes-specific isoforms. (1996)
Genetics 144, 147-157.

Yue L., Karr T.L., Nathan D.F., Swift H., Srinivasan S. and Lindquist S.
Genetic analysis of viable Hsp90 alleles reveals a critical role in *Drosophila* spermatogenesis. (1999)
Genetics 151, 1065-1079.

Zeitlin S.G. and Sullivan K.F.
Animal cytokinesis: breaking up is hard to do. (2001)
Curr. Biol. 11, 514-516.